PhD degree in Systems Medicine (curriculum in Oncology)

European School of Molecular Medicine (SEMM),

University of Milan and University of Naples “Federico II”

Settore disciplinare: BIO/11

Epigenetic mechanisms of Polycomb Repressive Complex 1 in intestinal lineage commitment

Annachiara Del Vecchio

Matricola n. R12408

Tutor: Dr. / Prof. Diego Pasini

PhD Coordinator: Prof. Saverio Minucci

Anno accademico 2022-2023

TABLE OF CONTENTS

1. ABSTRACT

Polycomb group proteins are key transcriptional repressive complexes involved in cell fate decisions during development and cell identity maintenance during homeostasis (1).

Polycomb group proteins primarily assemble into two different complexes: Polycomb repressive complex 2 (PRC2) with the catalytic subunit EZH1/2 which can mono, di, and tri- methylase the histone H3 at lysine 27 (H3K27); and Polycomb Repressive Complex 1 (PRC1) with the catalytic subunits RING1A/B, which catalyze the monoubiquitylation of histone H2A at lysine 119 (H2AK119) (1,2). In PRC1, the RING1A/B subunits form a core heterodimer with one of the 6 mutually exclusive PCGF (1-6) proteins, thus creating six subcomplexes (PRC1.1 – PRC1.6). Simply put, PRC1 subcomplexes can be divided into canonical PRC1 (PRC1.2 and PRC1.4) and variant PRC1 (PRC1.1, PRC1.3, PRC1.5 and PRC1.6) (1,2).

Polycomb Repressive Complexes are essential for the transcriptional repression of developmental genes, such as germ-line related genes in embryonic stem cells (ESCs) (3).

During intestinal homeostasis, chromatin modifiers play important roles in maintaining transcriptional signatures of specific cell types. Our group has already demonstrated that RING1A/B are necessary to maintain normal tissue homeostasis by preservation of the WNT/B-catenin activity (4).

However, the contribution of PCGFs in adult intestinal homeostasis is unclear. To address this, we evaluated the role of six different PRC1 subcomplexes in transcriptional repression maintenance in intestinal cells by using several inducible PCGFs knockout mouse models.

Our data suggest that the lack of single PCGF proteins does not alter intestinal homeostasis due to the compensatory effects of PRC1 subcomplexes in chromatin binding and in transcriptional repression maintenance.

In fact, we observed that PRC1.1, PRC1.2 and PRC1.4 share binding sites on chromatin in intestinal cells. The simultaneous depletion of PCGF1, PCGF2, PCGF4 affects not only RING1b binding, but also its activity and H2AK119ub deposition. This leads to a transcriptional de-repression in adult intestinal cells, and so to a disrupted intestinal homeostasis.

Interestingly, we observed that the Tuft cell number increases remarkably following PCGF6-deletion. Tuft or Brush cells are a very rare cell population with chemosensory activity in the intestinal epithelium (5). However, the Tuft cell differentiation program is under investigation.

2. INTRODUCTION

2.1 EPIGENETIC AND POLYCOMB GROUP PROTEIN

2.1.1 CHROMATIN STRUCTURE AND FUNCTION

In molecular biology the term *Epigenetic* indicates "*the mechanisms by which chromatin-associated proteins and post-translational modification of histones regulates transcription"*. The epigenetic studies the heritable characteristic that are associated with DNA accessibility but not associated with DNA sequence (7). Nuclear DNA binds histones and non-histones proteins that compose the two different chromatin type: the heterochromatin and the euchromatin. The euchromatin is more accessible and it is associated to an active transcriptional state. Indeed, the heterochromatin is highly compacted, and it is linked with less permissive transcriptional state (8). The heterochromatin in specific genomic loci, such as centromeres, telomeres, repeated and noncoding regions is highly and permanent condensate and it is called *constitutive heterochromatin*. The other fraction of DNA, called *facultative heterochromatin* present dynamic histone modification that can be easily added or removed, leading to change of chromatin conformation.

The term *chromatin* refers to the complex of DNA and proteins that was first found more than 40 years ago in Eukaryotes cells (9). The unit of chromatin called *nucleosome* is composed by DNA wrapped for 147 bp around the octamer of histone proteins (two tetramers of histone H3, H4 and two dimers of H2A and H2B), stabilized by the presence of histone H1. Nucleosomes are spaced each other from free DNA linker (9).

Histone proteins presents dynamic tails outside of the nucleosome that are subjected to post-translational modification by different classes of epigenetic players (10). Those modification affects DNA – histones and proteins – proteins interactions leading to chromatin remodeling.

Chromatin remodeling, histone variants, DNA modification and histone modification are the four mechanisms of epigenetic control, which control the regulation of DNA accessibility on genomic site, affecting the transcriptional outcome (11). This dynamic organization of the chromatin is possible through spatially dynamic reorganization of nucleosome among the DNA filament by four different

class of proteins. Those epigenetic modifiers are characterized by unique domains and share ATPase domain that is necessary for their activity (12).

The DNA accessibility and the transcription is also regulated by the presence of histone variants that can be incorporated to the nucleosome core. Normal histone proteins are encoded by high copies number genes, absence of intron and 3'PolyA, and their mRNA is characterized by the presence of stem loop very important for their integrity during S phase (13). In fact, normal histone proteins are incorporated to chromatin during DNA replication, however histone variants can be substitute throughout cell cycle (14). The presence of histone variants leads to aberrant chromatin compaction, and the consequent transcriptional process alteration.

Transcriptome landscape could be also changed by DNA covalent modifications, that influence the binding on the DNA to the proteins, especially the transcriptional machinery.

Four different DNA modification have been described: 5-methyl cytosine (5mC), 5-hydroxymethylcytosine (5hmC), 5-formylcytosine (5fC) and 5-carboxylcytosine (15). DNA methylation, which represent the most abundant and important DNA modification, occurs at the 5-position of cytosine residues (5mC) at the CpG dinucleotides, present on the CpG island, mainly at gene promoter (16). DNA methylation is associated with DNA compaction and the consequent transcriptional repression. This DNA modification is catalyzed by DNA-methyltransferases (DNMTs), that can act during replication to maintain the normal methylation patten or can ensures "de novo" methylation deposition (17) (18).

Together with DNA modification, chromatin accessibility and plasticity are modulated also by histone modifications. Histone modifications are post-translational alteration (PTMs) that can influence chromatin architecture and plasticity. These chemical alterations occur at histone tails, in a reversible manner, and control histone-DNA and histone-histone interactions.

The most characterized histone modifications are lysine acetylation, Lysine/Arginine methylation and Serine/Threonine/Tyrosine phosphorylation. Instead, the less abundant histone modifications are: Ubiquitination, Sumoilation, and Succinylation (19). Different histone modifications affect in different manner the DNA accessibility, and so the gene expression.

Modification	Histone	Residue	Effects of transcription
Acetylation	H2A	K5	Activation
	H2B	K5, K12, K15, K20	Activation
	H3	K4, K9, K14, K18,	Activation
	H3	K23, K36,	Activation
	H3	K56	DNA repair, histone deposition
	H4	K5, K8, K16	Activation
	H4	K12	Activation, histone deposition
	H4	K91	Histone deposition
Methylation	H3	K4, K79	Activation
	H3	K9, K27	Repression
	H3	R2, R8, R17, R26	Activation
	H3	K36	Elongation
	H4	R3	Activation
	H4	K20	Repression
Phosphorylation	H2A	S1, T120	Mitosis
	H2AX	S139	DNA repair
	H2B	S14	Apoptosis
	H3	T6	Activation
	H3	T3, S10, T11, S28	Mitosis, DNA repair
	H3	T45	DNA replication
	H4	S1	Mitosis, activation
Ubiquitination	H2A	K119	Repression
	H2B	K120	Elongation
	H3	K23	Maintenance of DNA methylation

K lysine, *R* arginine, *S* serine, *T* threonine

Table 1: summary of PTMs and their effects on transcription

In general, histone modifications control the chromatin compactions and the accessibility of the transcriptional machinery on the DNA, leading to a repressive or active state (21).

Histone modifications are added by specific epigenetic factors called *chromatin writers*, are read from protein called *chromatin readers*, and are removed by protein called *chromatin eraser* (20). Writers, readers and erasers regulates in a reversible and dynamic manner genes expression not only in cellular fate establishment during embryogenesis, but also in cellular identity maintenance in adult tissues. These important processes are strictly preserved but are altered in different human disease.

2.1.2 POLYCOMB GROUP PROTEINS

Among these chromatin regulators Polycomb group proteins (PcG) are the best described repressors in development, differentiation, and cell fate decisions. Polycomb proteins were discovered first in Drosophila Melanogaster, where are implicated in controlling the expression of Homeotic (Hox) genes during development and differentiation (22).

Years later the discovery of PcG proteins, was appreciated also the function of those proteins. In fact, in *Pc* mutant embryo was observed the shift of abdominal segments to the posterioral axis (22) (23). Other group of protein was found to be involved in Hox genes expression regulation, the Trithorax group of proteins (TrxG) (24), (25), (26), (27). Mutation of TrxG proteins affects embryonic segments transformation towards a more anterior type, opposite to the PcG protein mutation (27). In fact, in drosophila Melanogaster the crosstalk between TrxG and PcG proteins is essential for normal body segmentation during development.

PcG proteins are also present in mammalian cells, and are extremely conserved, indicating the important role of those proteins (27).

Based on biochemical differences, PcG proteins were classified in two major complexes: Repressive Complex 1 and 2 (PRC1 and 2) (28). Both complexes are implicated in chromatin compaction and in genes repression by specific catalytic functions. PRC2 deposits mono-, di-, tri-methylation on lysin 27 of histone H3 (H3K27me1/me2/me3), while PRC1 catalyzes the mono-ubiquitination of lysine 119 of histone H2A (H2AK119ub1) (29) (30) (31).

POLYCOMB REPRESSIVE COMPLEX 2

In Drosophila the Polycomb repressive complex 2 is composed by the presence Enhancer of Zeste (Ez), Suppressor of Zeste (Suz), and Extra sex combs (Esc). In mammalian cells PRC2 is composed by EZH1 or EZH2 (homolog of Ez), SUZ12 (homolog of Suz), and EED (Embryonic Ectoderm Development) (homolog of Esc), which together forms the PRC2 core (27) (32) (33).

The catalytic unit of PRC2, EZH1/2 which are mutually exclusive, can mono/, di- and tri- methylase the lysin K27 on the histone H3 through their SET domain (34). Indeed, SUZ12 and EED proteins are necessary to maintain the structure and functionality of the PRC2 complex (31) (35).

PRC2 core is associated with other ancillary subunits, that are extremally important for the binding of the complex on chromatin but are not necessary for PRC2 catalytic activity.

However, the histone chaperone RbAp48/46 (retinoblastoma associated proteins 48/46), is required for methylation deposition by PRC2 in vivo (36). JARID2 is involved in PRC2 recruitment on DNA by recognizing CpGs islands (37). AEBP2 enhance KTM activity in vitro, and the three Polycomb-like proteins (PCLs), PHF1, MTF2, PHF19 which recognize and binds H3K36me3 mark through their TUDOR domain, leading silencing initiation of active genes (38).

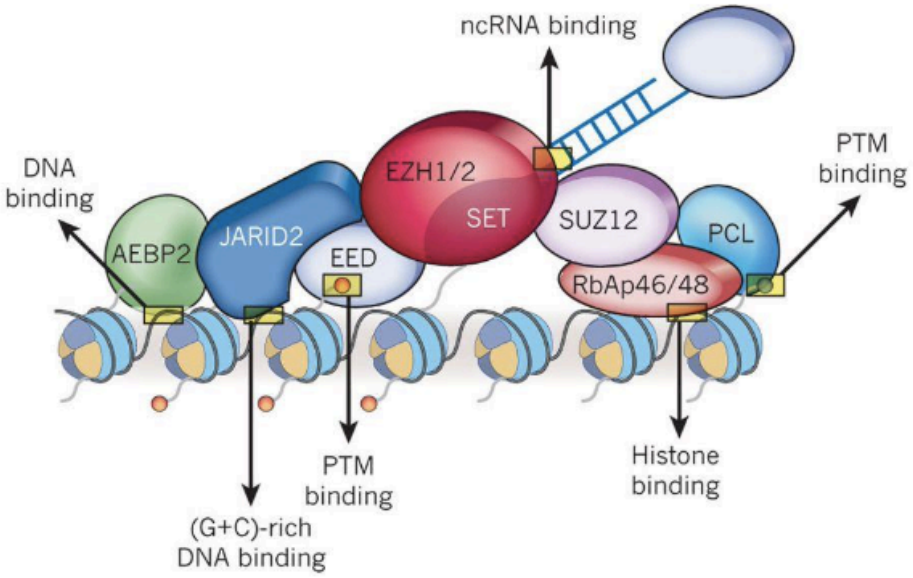

Figure 1: Schematic representation of PRC2

PRC2 components and their putative interaction with chromatin structure (Margueron and Reinberg 2011)

EZH1 and EZH2 proteins are not redundant. In fact, EZH1is associated with mono-methylase on active genomic regions, while EZH2 is associate more with di-, and tri – methylation deposition on repressive genomic regions (36). EZH1 and EZH2 shows also different catalytic activity ability; EZH2 shows 20-fold higher capacity in methylation, compared to EZH1 (39). Moreover, EZH2 can fully compensate the absences of his paralog, but EZH1 can only complement the absence of EZH2 in H3K27me (40). EZH1 knock out mice are viable, fertile and present unaltered phenotype, while EZH2 loss leads very early embryonic lethality (40).

PRC2 mark level enhance a positive feedback loop of PRC2 activity through the EED protein which recognize H3K27me3 by its WD40 domain (41).

Histone methylation influence the chromatin compaction and modulated the accessibility of TFs and the transcriptional machinery (42) (43). Histone methylation have different effect, depending on the methylation type, that can lead to both transcriptional activation and repression (44). In fact, the tri-methylation of K27 on H3 is present in CpG-rich promoter of silenced genes, di-methylation of K27 on H3 is associated with extended silenced genomic regions, while H3K27me1 is deposit on full body of active genes (45).

The methylation patterns on the chromatin identify a regulatory effect on genes expression. In Embryionic stem cells (ESCs) the combination of H3K4me3 deposited by the COMPASS complex and the concomitant presence of H3K27me3 deposited by PRC2 is present on the bivalent genes, specially related to development (46), This double modification leads to both activation and repression possibility, necessary to switch the chromatin status needed during the differentiation (47) (48). However, this characteristic disappear in differentiated cells, retaining only one status, depending of the specific gene and the specific tissue (49).

POLYCOMB PRESSIVE COMPLEX 1

Polycomb repressive complex 1 (PRC1) in Drosophila Melanogaster is composed by Polycomb (Pc), Polyhomeotic (Ph), Posterior sex combs (Psc) and Sex comb extra (Sce, also known as dRING) (27). In mammalian cells PRC1 complex present an architecture much more complicated. It is

composed by E3 ligase RING1a/b (Really Intresting New Gene 1a and 1b), mutually exclusive, which catalyze the monoubiquitynation on lysin 119 of the histone H2A of the histone core, and at least one of three Polyhomeotic-like protein (PHC1, PHC2 and PHC3, Ph homolog) (27).

PRC1 can be divided in "*Canonical PRC1*", or "*Variant PRC1*", depending on the presence of CBX subunit (Chromobox, Pc homolog), or RYBP subunits. CBX and RYBP proteins are mutally exclusive, and they influence in different way the recruitment of the PRC1 complex to chromatin. Moreover, in mammalian cells five different CBX protein exit (CBX2,4,6,7,8), and RYBP replace with YAF2 protein (27), (1).

In mammalian cells different CBX proteins can be present in *canonical PRC1* (CBX2,4,6,7,8) which are mutually exclusive, and their presence is regulated during differentiation process. CBX7 is more abundant in Esc, indeed CBX2 and CBX4 are more abundant in fully differentiated cell (50) (51). Canonical PRC1, through the chromobox domain of CBX subunits, recognize and bind H3K27me3 mark deposited by PRC2, where they cooperate in chromatin compaction and gene silencing (28).

From chromatin binding investigation of PRC1 and PRC2 complexes, turns out that the majority of RING1b binding sites overlap with CBX proteins, but partially overlap with H3K27me3 (8) (52) (53). Moreover, in absence of the H3K27me3 mark, the global H2AK119ub1 level remains unaltered, suggesting that PRC1 activity does not need PRC2 activity.

Together with RING1a/b, in *non-canonical* (or variant) PRC1, is present RYBP subunit (Ring and YY1 binding protein) or YAF2 (YY1 Associated factor 2), which lack the presence of subunit that identify H3K27me3 mark, meaning that they recruitment on chromatin is independent from PRC2 activity (54).

Both in Canonical PRC1, and in Non-Canonical PRC1, the E3 ligase RING1b is associated with PCGF proteins. PRC1 can form 6 biochemically distinct subcomplexes depending on the different and mutually exclusive PCGF protein (PCGF1 to PCGF6) that bind to the RING1A/B protein. Importantly, PCGF proteins are not only mutually exclusive, but in the case of close paralog pairs PCGF3/5 or PCGF2/4 share redundant functions (1). PCGF2 (Mel18), and PCGF4 (Bmi1) in presence with CBX, forms the *canonical* PRC1, instead PCGF1, PCGF3, PCGF5 and PCGF6 are

present in *non-canonical* PRC1 (1). However, different group found that a small part of PCGF2, and PCGF4 can also bind RYBP.

PRC1.1 contains the PCGF1 (or NSPC1) and represent the homolog of dRAF in Drosophila. In PRC1.1, an important subunit is KDM2B protein, a H3K36 demethylase, that drives the complex on CpG rich genome loci (55) (56) (57).

PCGF3 and PCGF5, in PRC1.3 and PRC1.5 complex respectively, are redundant and bind the same interactors. In particular, PCGF5 and PCGF3 bounds AUTS2, together with FBRS and FBRSL1 (1) (57). Very interesting, our group found that PCGF3 interacts with the transcription factor USF1, and it is necessary for PRC1.3 chromatin interaction (2).

PCGF6 or MBLR present in PRC1.6 is associated with different proteins: E2F6,MGA, MAX,DP1,L3MBTL2 and DP1. The subunit E2F6 mediates the binding of the PRC1.6 complex on DNA, and MGA mediates the recruitment on T-box sequence (1) (8).

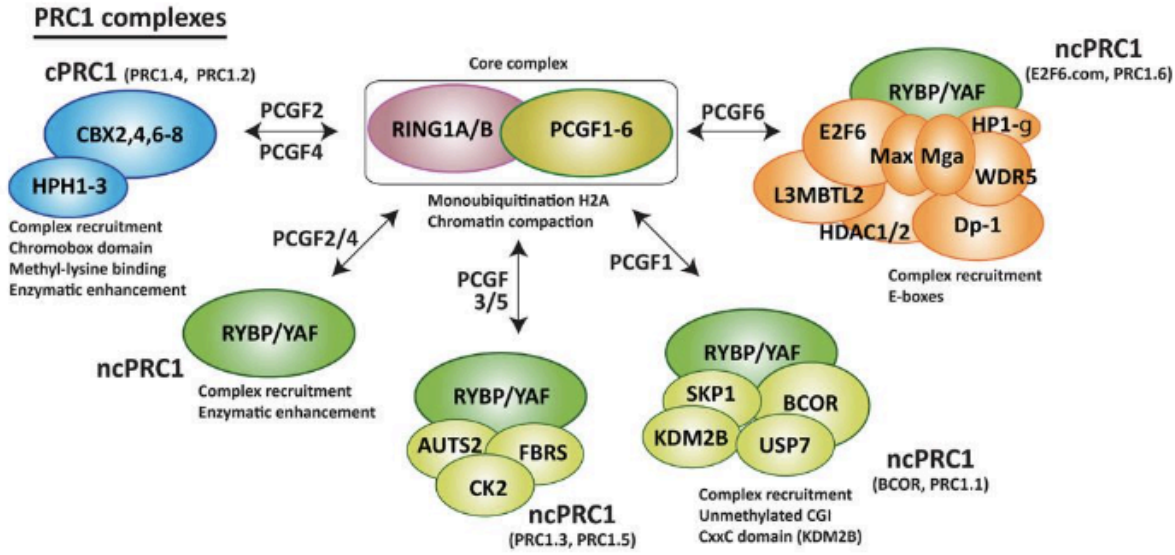

Figure 2: Schematic representation of PRC1

The illustration represents the six PRC1 subcomplexes, with the core complex and the different ancillary subunits. (Adapted from Aranda,Mas et al. 2015).

All those complexes are implicated in monoubiquitination deposits and gene repression, through the E3 ligase Ring1a/b (58). Importantly, histone ubiquitination is a reversable modification, that can be easily removed by specific deubiquitinating enzymes (DUBs). Specifically, Polycomb protein BAP1 is the H2A-specific histone DUB, and its absence increment H2AK119ub1 levels on PRC1 targets (59).

2.1.3 POLYCOMB BIOLOGY AND MECHANISM

Embryonic stem cells (ESc) derive from blastocyst and are an excellent tool to study the epigenetic control of Polycomb proteins. In fact, Polycomb proteins are high expressed in ESc and they are bound preferentially at CpG-rich promoters of development and differentiation genes, which are repressed (32) (52). Overall, the chromatin in ESc presents an open conformation with high level of activating histone marks and low level of DNA methylation (60). This open chromatin architecture is gradually lost during differentiation, with accumulation of H3K27me3 mark, and the concomitant acquisition of closed status (60).

In mammal PcGs bind non methylated CpG rich promoters (61). The speculated classic mechanism of Polycomb complexes recruitment on chromatin predicts two-step mechanism: first PRC2 recognize CpG rich sequence and mediates the methylation of lysin 27 on the histone H3. H3K27me3 is recognize by CBX subunits of the Canonical PRC1, that monoubiquitinate the lysin 119 on the histone H2A through Ring1a/b catalytic units. This cooperation between PRC1 and PRC2 complexes leads to a chromatin compaction and transcriptional repression. However, this mechanism remain valid only for canonical PRC1.

Given that PRC1 and PRC2 catalytic core do not bind directly the DNA, other alternative recruitment mechanism have been investigated. BCOR (BCL6 Co-repressor), a component of PRC1.1 is able to recruit the complex on target genes (27), and KDM2B demethylase allow the binding on H3K36 metylated (56), (62), (63). Moreover, it has been demonstrated that MGA, E2F7 and L3MBTL2 are

able to recruit the PRC1.6 on chromatin (2), (64). AUTS2, a component of PRC1.5 has been reported to lead the binding of PCGF5 on DNA. Last, how group has demonstrated USF1 is able to let PCGF3 bind the DNA on specific E-box motifs (2).

The component of PRC2, JARID2, thanks to its AT-rich interaction domain (ARID) and a Zn-finger domain, leads to recruitment on the chromatin of the complex However, recent studies have demonstrated, that lack of Jarid2 do not affect completely PRC2 binding and function, suggesting that other mechanism can regulates PRC2 chromatin recruitment (34) (37) (49).

Polycomb biology remain not clear. In fact, from new data turned out that canonical PRC1 complexes can be found also in active chromatin, displaying differences from classic Polycomb biology (65) (66) (67). Moreover, the majority of the information about Polycomb group protein biology arise from studied on Embryonic stem cells, and less is known about PcG roles in adult tissue.

Knock out mice for PRC2 core subunits died in post-implantation stage, since those proteins are indispensable for early embryogenesis *in vivo* (35) (68). Deletion of *Jarid2* affects neural tube formation (at 15.5 dpc), and deletion of *Pcl2* (mtf2) affects the normal left-right symmetry in chicken, but is not necessary in mouse embryogenesis (70) (71).

Ezh2 loss does not affect adult hematopoietic stem cells but impairs embryonic hematopoietic stem cell renewal. By contrast, and in accordance with the different level of EZH1 and EZH2 protein, in adult loss of EZH1 impairs the hematopoietic stem cells self-renewal, by controlling the expression of *Ink4a/Arf* locus, which is known to be involve in cell cycle regulation (35).

Different is for PRC1 complex. Ring1a knock out mice are viable and fertile, however, depletion of Ring1b leads the arrest of gastrulation and so embryonic lethality (72). As expected, ESCs lacking Ring1b, the H2AK119ub levels were reduced (73). Importantly, depletion of both Ring1a/b severely affects ESCs self-renewal in vitro (74).

In contrast with depletion of the catalytic units RING1a/b, depletion of single different PCGFs protein affects ESC differentiation but not self-renewal. PCGF1 loss induce de- repression of stem cell

markers during ESC differentiation but does not alter colony formation in vitro (75). PCGF1 is also indispensable for HoxA gene promoter repression in hematopoietic stem cell (76).

PCGF2 (Mel18) and PCGF4 (Bmi1) are the most investigated PCGF proteins. Depletion of PCGF2 or PCGF4 affect anterior-posterior segmentation of skeleton, while the depletion of both proteins cause mouse death at 9.5 dpc (77) (78) (79). PCGF4 or BMI1 is necessary to maintain the normal stem cell self-renewal thought inhibition the Ink4a/Arf locus, that encodes for two important cell cycle inhibitors, p16 and p19 (80). Both canonical PRC1 subcomplexes are involved in cancer biology. In fact it is know that Mel18 can acts as a tumor suppressor via downregulation of BMI1 which acts as oncogene in cancer (81).

PCGF3/5 are dispensable for ESC self-renewal but are necessary to maintain the repression of mesodermal marker (82). Moreover, our group have demonstrated that loss of PCGF3/5 in ESC, decrease the H2AK119ub1 at intergenic regions, but not on promoters, probably for the dynamic activity of this two PRC1 subcomplexes (1) (2).

Overall PCGF6 loss affect viability and fertility in mice. Embryo lethality was observed at blastocyst and post-implantation stages (74). Depletion of PCGF6, as depletion of MAX, in ESC reactivates the expression of germ and meiosis related genes (74).

In adult tissue Polycomb protein maintain some roles, but achieve also specific functions.

In adult intestinal homeostasis, PRC2 and PRC1 plays different important roles. Depletion of PRC1 in intestinal stem cells (ISCs) causes in a Ink4a?arf independent manner, loss of cellular identity and the self-renewal capacity, leading to the exhaustion of stem cell comportment, important for normal tissue homeostasis (4). PRC2 loss does not affect ISC compartment, but alterets the balance between secretory and absorptive cell population in adult intestine (83).

2.1.4 CELLULAR IDENTITY

As I mentioned above, Polycomb group protein are important complex that maintain cellular identity. Cellular identity is not only important for organism development, and for tissues integrity in adult, but is also important for homeostasis preservation and pathological events prevention.

During cellular identity establishment during embryogenesis, and cellular identity during organs homeostasis different regulatory mechanism and elements, such epigenetic players, coordinate and regulates specific transcriptional pathways.

Among them, Polycomb group proteins, display an important regulatory role, through DNA accessibility for RNA Pol machinery on specific genes, which are associated with development. This mechanism leads to ensure the correct cell genetical identity (84).

Recently has be demonstrated that, epigenetic players, such Polycomb proteins in different way in adulthood and development.

In adult tissues, adult stem cells have the important and fundamental role to replace the damaged or died cells during homeostasis or tissue repair (85). Those processes are tightly regulated, where cells retain a specific epigenetic footprint and a specific transcriptional profile. Alteration of those peculiarity are found in different pathology, such cancer. In fact, in cancer epigenetic mechanism is affected at different levels, reaching almost 40% of total altered protein in tumors (86).

2.2 INTESTINE

2.2.1 INTESTINAL ARCHITECTURE AND PATHWAYS

Intestine is one of the most large and extended epithelium of the body, and plays two functions: nutrients uptake and protection against the microenvironment.

The intestine is divided in small, that include Duodenum, Jejunum and Ileum, and large intestine that include the colon. The architecture of intestinal tissue is organized in crypts-villus units. The crypts of Lieberkühn are present at the bottom, while villi are protrusion that spread from the surface. The length of villi decrees among small intestine and large intestine.

The intestine is a very plastic organ with renewal time of 4-5 days. The tissue turnover is maintained by a pool of proliferation intestinal stem cells (ISCs), positive for R-spondin receptor LGR5, that are present on the bottom of the crypts of Lieberkühn (95). During tissue homeostasis ISCs are able to generate the proliferating transient amplifying progenitor cells (TA), which gradually differentiate in all the intestinal cells type.

The intestinal epithelium is composed by different cell types. Intestinal crypts are the niches for ISC and TA cells, which are undifferentiated cells. Instead differentiated cells, which are present among the villi, and can be also divided in absorptive and secretory cells. Absorptive *Enterocytes* cells are the most abundant, and are necessary for nutrients uptake; *Goblet cells*, are able to produce mucins necessary for intestinal lumen formation and function (105); the *Enteroendocrine* cells that release important hormones (106); The taste-chemosensory *Tuft cells* a very rare cell population among intestine, that are involve in Type 2 immune response during pathogen inflammation (107). The intestinal crypts are the nich not only for ISCs but also for differentiated *Paneth cells*. These cells have a protective function by producing defensins and lysozyme (108). Conversely to other differentiated cells, Paneth cells do not migrate through the crypt-villi axis but remain in the crypts niche for 7-8 day (109) (110). Here, Paneth cells are interspersed with ISCs and contribute to their function. In fact, Paneth cells produce WNT ligand and Epidermal growth factor (EGF) providing the important substance for ISC (94) (111).

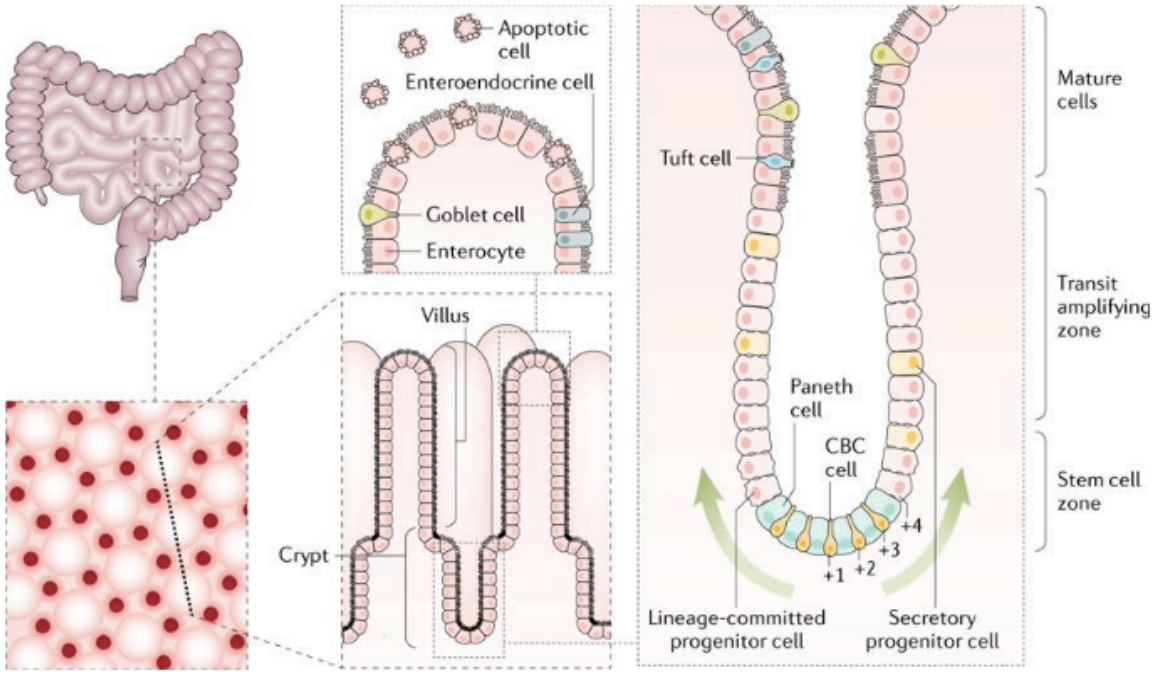

Figure 3: Schematic representation intestine

Figure representing intestinal tissue structure (Gehart and Clevers 2019),

Intestinal stem cells (ISCs), also known as Crypts base columnar cells (CBCs) present high rate proliferation with cell cycle of 24 hours, generating other ISCs or transit amplifying (TA) progeny that differentiated in all the intestinal cell types. TA cells, located in the middle of the crypts divided every 14-16 hours and migrate upward while differentiating during homeostasis (95).

In adult intestine two different stem population are present: the CBCs and the so called +4 cells, that are positioned at +4 position from crypt base, and are able to dedifferentiate into a multipotent state and participate to intestinal homeostasis.

The discovery of CBCs stemness was achieved thanks to the identification of Lgr5 (Leucine-rich repeat-containing G- protein coupled Receptor 5) as effective marker for CBCs intestinal stem cells, and thanks to the generation of the mouse model Lgr5-CreERT2-Rosa26-LoxSTOPLox-LacZ by Barker (95). Different works demonstrated that loss of LGR5 expressing cells form intestine, CBCs

are depleted from the epithelium and the homeostasis in compromise. However, after CBCs loss, LGR5 expressing cells reappears and reconstitute and participate in tissue regeneration (113).

Intestinal homeostasis is maintained thanks to specific pathways. The most important pathways that are involved in intestinal stem renewal and differentiation are: Wingless integration site (WNT), Bone Morphogenetic Protein (BMP), NOTCH and Epidermal Growth Factor (EGF) pathways.

WNT signaling pathway accurse between Paneth cell and ISCs. Paneth cells are the main source for glycoprotein WNT ligand, instead ISCs present the Frizzled receptor. WNT ligand binds the N-terminal region of Frizzled (Fz) receptor on ISCs cell, and this activate the signal transmission. In intestine, canonical WNT, pathway causes the accumulation of B-catenin in the cytoplasm and the translocation in to the nucleus. Here, the coactivator B-catenin and the of TCF/LEF family proteins, forms a complex that is a major player for transcription of gene specific for stemness and ISCs proliferation, such cyclin D1 and c-myc, which control the G1-S phase in cell cycle (114).

Inhibition of WNT signaling leads to ISCs loss and affect intestinal homeostasis. LGR5 receptor present on ISCs is involved in the potentiation of WNT signaling. In fact, LGR5 bind the R-spondin ligand, and this leads to a downregulation of the activity of RNF43 and ZNRF, which are Fz specific E3 ubiquitin ligases. The blocking of RNF43 and ZNRF impairs WNT signaling (115). The WNT signaling pathway follow a gradient that is higher into the crypt base and less present thought the villi. This is due the fact that proliferation is maintain in crypts and not in villi, in which other pathway such NOTCH and BMP pathways regulates cellular differentiation.

The gradient of BMP pathway is opposed to the WNT pathway, and restrict the stemness propriety among crypts-villi, by negatively regulating stem cell identity. BMP pathway is part of TGF-B family, in which the activation started with the binding of BMP ligand to BMPRI or ALK2-6 receptor. This binding leads to a cascade of phosphorylation events, that causes the activation and the translocation in to the nucleus of the transcription factor SMAD (116). In the intestinal crypts, niches for ISCs, the inhibition of BMP signaling by the presence Noggin and Gremlin 1-2, is crucial for homeostasis regulation (117).

NOTCH signaling is also important for the intestinal homeostasis. Binding of the ligand DLL1, 3, 4 and Jagged1, 2, and the receptor (NOTCH1-4), induces the activation of gamma-secretase which is able to cleavage Notch receptor and to release its intracellular domain (NCID) into the nucleus. Here, NCDI forms a dimer with RBPJ, which recruit MALM1-4 leading to the transcriptional activation. NOTCH signaling cascade is associated with proliferation and differentiation depending on the context. In intestine, NOTCH signaling is played between Paneth cells which release the DLL ligand, and ISCs which present Notch receptor. The impairment of Notch pathway, in small intestine, leads ISCs and TA cell to differentiate toward the secretory lineage, compromising the absorptive lineage differentiation (111) (118). In fact, one important NCDI target is HES1, which is expressed in cycling cells and is essential for ISC and TA maintenance (120).
Blocking of NOTCH signaling or Hes1 depletion leads the upregulation of ATOH1 transcription factor, that is directly involved in regulation of intestinal secretory lineage.

Another important pathway in intestine homeostasis is the EGF-ERBB pathway. The activation of this cascade is possible due the binding of 13 different ligand with four different EGF receptor (ERBB1, ERBB2-4). Phospho-activated receptors are then involved in GTPase/ MAPK cascade activation. In intestine, EGF pathway is involved in cellular proliferation and stemness preservation (119).

2.2.2 ROLE OF POLYCOMB PROTEINS IN INTESTINAL HOMEOSTASIS

The intestinal homeostasis is a very regulated process in which signaling pathway and epigenetic machinery plays in concomitance to permit cellular identity establishment and maintenance. Polycomb group protein PRC2 and PRC1 have been found to regulates gene expression among crypts-villi during intestinal homeostasis. The transcriptome profiles of differentiated intestinal cells and ISCs are completely different, due to the presence of different histone markers among their chromatin. PRC2 in more active in differentiated cell, where genes associated with stemness such

Myc, Ascl2 and Lgr5 are repressed (122). Depletion of PRC2 from intestine causes loss of stem cells and dysregulation of genes involved in WNT signaling (123). There are differences in genes expression regulated from Polycomb protein also among the differentiated cells. In absorptive cells, Atoh1 promoter is strictly repressed with high level of H3K27me3 deposits from PRC2. In fact, EED loss from intestine leads to description of H3k27me3, the activation of Atoh1 expression and the consequent Goblet cell differentiation and accumulation (83). PRC2 activity is also associated with intestinal regeneration after irradiation, while prevent LGR5+ cells senescence by repressing the Ink4a/Arf locus (83).

PRC1 activity is also associated with intestinal homeostasis. It has been reported that catalytic unit Ring1a/b is required for intestinal stem cell self-renewal. Depletion of PRC1 activity from intestinal cells leads to a massive deregulation of gene expression, which cause the reactivation of non-lineage specific genes (4). The activation of other transcription factor upon PRC1 loss, interfere with B-catenin transcriptional activity, leading to the ablation of ISCs in a INK4a/Arf independent manner. These founding identify PRC1 complex fundamental for intestinal stem cell identity during homeostasis.

However, knowledges about different PRC1 subcomplexes in transcriptional regulation in intestine are still needed.

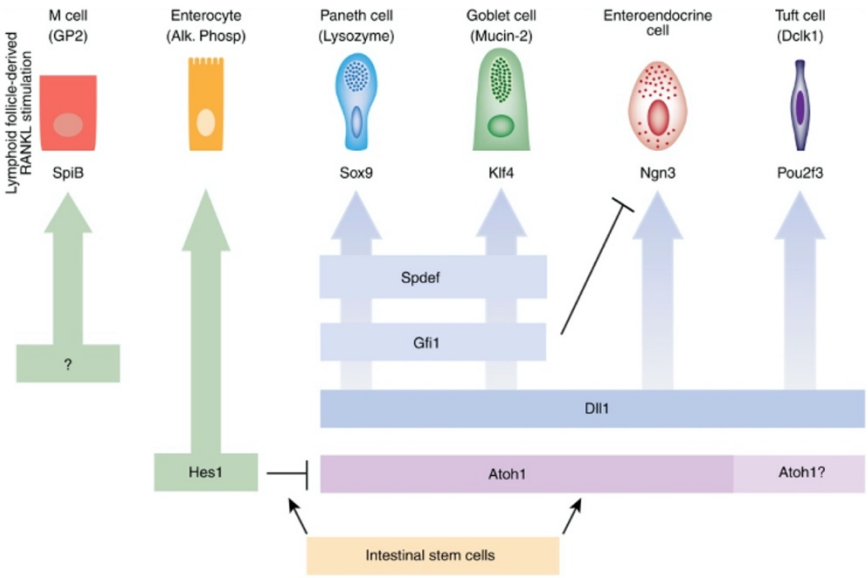

Figure 4: Schematic representation intestinal cells differentiation pathways

2.3 2.3 POLYCOMB REPRESSIVE COMPLEX 1.6 AND INTESTINAL TUFT CELLS

2.2.3 PCGF6 PROTEIN IN EMBRIONIC STEM CELL AND TUMORIGENESIS

PCGF6 protein, also known as MBLR, was first discovered ad a unit in a multiprotein complex together with E2F6, RING1a/b, DP1, L3MBTL2, CBX3, G9A, YAF2, MAX and MGA (124). The component of PRC1.6 are specific for this complex: MGA/MAX are implicated in DNA recognition and binding, while L3MBTL2 for histone identification.

MGA (MAX gene-associated protein) is formed by T-box domain and bHLH domain, which represent the DNA-binding domains. MGA binds MAX, and this heterodimeric complex recognize E-boxes on DNA. Instead, E2F6 binds the transcription factor DP1 or DP2, which recognize E2F6 specific sequence (64) (103). L3MBTL2 interact with histone H3 and H4 tails, thanks to four different MBT domains (8) (103). Chromatin association studies demonstrated that Pcgf6, Mga and L3mbtl2 colocalize genome-wide in mouse ESCs, and that their loading on chromatin is absolutely dependent

of PRC1.6 complex integrity (103). However, binding of PRC1.6 subunits are lost in Mga depleted cells, meaning that the integrity of the complex and the co-presence of Mga, L3mbtl2, E2f6 and Pcgf6 is necessary for PRC1.6 chromatin association (64). Despite this cooperation in PRC1.6 recruitment on DNA, L3mbtl2 and E2f6 recruit PCGF6-containeng PRC1 to different set of genes, associated with different biological process (64).

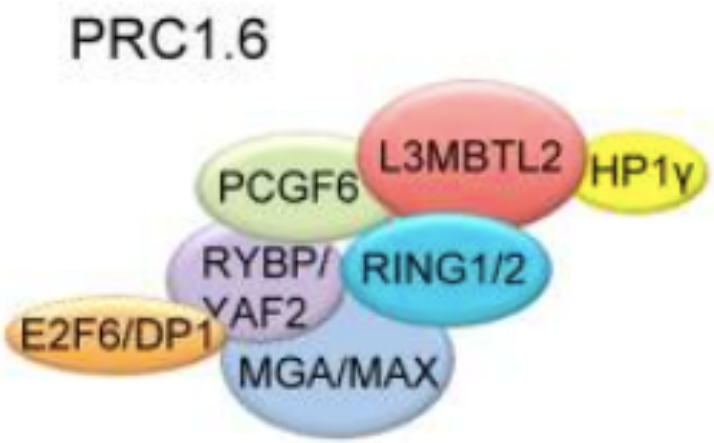

Figure 5: schematic representation of PRC1.6 complex.
(Adapted from. Stielow, B., et al.)

PCGF6 is the higly expressed PCGF protein in undifferentiated embryonic stem cells, and PRC1.6 is the major PRC1 subcomplex in ESCs (134) (135).

PRC1.6 has been investigated in embryonic stem cells in which its function is to repress germline genes and to maintain ESC cellular identity (102) (125). The specification of germline genes is repressed in ESC and in somatic cell, and the deregulation of this could lead to oncogenic transformation. Whereas, in germ cells, germline genes need to be express, and lack of the expression of these genes lead to the impairment of fertility (106). In fact, mutant mice with depletion of *Pcgf6* gene, exhibited compromised fertility, and the consequent partial embryonic lethality. For the survived mice, depletion of *Pcgf6* cause the de-repression of genes associated with meiosis and

germ cells (128). It has been shown that PCGF6 could repress the germ cell related genes, not via H2AK119ub deposition, but by recruitment of G9a/Glp and Hdac1/2 with transcriptional silencing proprieties by H3K9 methylation (128). In vitro, depletion of Pcgf6 reduced cellular growth, lead to aberrant ES cell morphology, and tendency to differentiation into the endoderm lineage in embryoid bodies (2) (125). In ESCs it has been demonstrated that PCGF6, L3MBTL2 and MGA co-localize on promoters of meiosis-specific genes. Specifically, depletion of Pcgf6 or L3mbtl2, or Mga from ESCs leads to upregulation also of mesodermal genes (135).

In ESc the recruitment of PCGF6 on chromatin is independent from H3K27me3 deposition by PRC2. Moreover, in ESc lacking Pcgf6, the H2AK119ub level is not affected on Pcgf6 targets. Then, different studies, are suggesting that PCGF6 could have a Ring1a/b independent mechanism. Moreover, it has been shown that Pcgf6 is required to maintain ESC cellular identity by modulating the expression of Oct4, Sox2, Klf4 and Nanog in both human and murine cells (133).

Pcgf6-cointaned PRC1 may act as a repressor and activator, depending on its recruitment on chromatin. Different work demonstrated that PCGF6 can bind both active chromatin region in which is present H3K4me3, H3K27ac histone marker, and repressive region, in which is present H3K27me3 histone marker. This, suggest a bivalent function for PRC1.6 complex in ESCs (1) (2) (134).

The recruitment of PRC1.6 on chromatin depends on presence a cooperation among the different subunits. In fact, loss of Pcgf6, L3mbtl2, Max and Mga is associated with the activation of the expression of germline gene (129, 130, 102, 131, 132). Importantly, the recruitment on chromatin of PRC1.6 is independent from RING1A/B presence, suggesting an alternative function for PCGF6 not related with Polycomb activities (2).

Very interestingly, it has been shown that PCGF6 can also bind a group of super-enhancer (SE) regions, leading the boost of expression of upstream pluripotency genes (136). Additionally, PCGF6 was found to be involved in the interaction not only of promoter-promoter, but also for the interaction of enhancer-promoter, in which share the binding with different pluripotency factors, including OSN (136) (137).

The role of PCGF6 in adult cell has been investigated in last few years. It has been shown that PCGF6 present a tumor suppressor activity in a Mga and PRC1.6 independent manner (138). MGA and MAX are component of PRC1.6 and binds the DNA thanks to recognition of E-box CACGTG. As I mentioned above, in ESCs loss of Mga lead to detachment of L3MBLT2, E2F6 and PCGF6 from chromatin, instead, depletion of Pcgf6 caused the dissociation of PRC1.6 and RYBP, but not of MAX and L3MBTL2 (1) (2). Different studies have reported the possible role of Mga/Max dimer as a tumor suppressor. For example, loss of function of MAX has been related with some types of neuroendocrine tumor (139). Moreover, in small-cell lung cancer (SCLC), different mutation can occur independently, such loss of function of MAX, MGA or MYC amplification (140). In other contest, it has been demonstrated that loss of MGA, in a Myc - dependent tumorigenesis, accelerated tumor formation, and lead to PRC1.6, E2F and MYC/MAX target genes upregulation (141). MGA loss of function and the consequent MYC activation, or MYC overexpression are associated with Leukemia and lymphoid malignancies (142) (143). It has been founded that PCGF6 plays as a tumor suppressor in Myc - associated lymphomagenesis but showed no tumor suppressor propriety in Eu-myc mice (138). Also in this contest, PCGF6 was associated with both active chromatin region, distinguished by the presence of H3K4me3, H3K4me1, and H3K27ac histone marks, and repressive chromatin region distinguished by the presence of H3K27me3 and H2AK119Ub histone marks (138) (144). The tumor suppressor activity of PCGF6 in Myc - associated lymphomagenesis was found to be not linked to Mga and PRC1.6 activity, arising the hypothesis of the possible alterative PCGF6 activities in tumors, and not only (138).

2.2.4 INTESTINAL TUFT CELLS POPULATION

Among secretory intestinal cell types, Tuft cells, also named as brush, microvillous or multivesicular cells, are the less abundant in intestine. Tuft cells represent only the 2% of the entire intestinal trat, with chemosensory proprieties (145). Tuft cells can be found in the crypts and also among intestinal villi, and the majority express Dclk1 marker. Intestinal Tuft cell present morphology appears with small microvilli toward the lumen, cup like shape with nucleus at the basal portion and numerous vesicles at apical portion (146) (Figure 1.5).

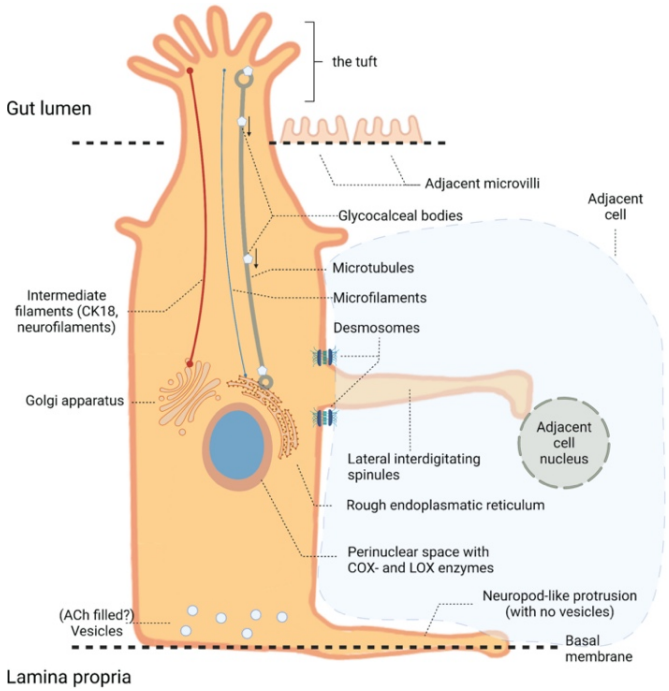

Figure 6: schematic representation of Tuft cell morhology
(Adapted from Westphalen et al.,Long-lived intestinal tuft cells serve as colon cancer-initiating cells)

This cells, appears first in the distal stomach only at embryonic days E16.5, and into other digestive organs at 3 weeks after birth (147). Moreover, Tuft cells have been found also in pancreas, respiratory tract and submandibular glands. Tuft cells have a specific signature that was first discovered by Besancon and colleagues by sorting Trpm5 positive Tuft cell. As Tuft cells marker

they found *Ac- tub, Dcamkl-1, Gfi1b, Chat, Trpm5, Ptgs1, Ptgs2, Il-25, Il-17, Dclk1 and Pou2f3.* Moreover, those cells are not proliferative, and are quiescent among the intestinal epithelium (145). The knowledge about intestinal brush cell differentiation is controversial. Some groups have demonstrated that Dclk1-expressing cells differentiation is Atoh1 dependent, like the other secretory intestinal cells (149). However, in contrast with this founding, other group reported the presence of Tuft cells even after Atoh1 depletion (150). In all those scenarios, Tuft cell originated always from Lgr5+ ISC during homeostasis.

Motsumoto and colleagues discovered a crucial role for the transcription factor Pou2f3 in intestinal brush cell differentiation. By taking advantage of the use of mouse model lacking of the expression of Skn-1a/Pou2f3, they found that this transcription factor acts as master regulator for intestinal Tuft cell differentiation (151). Moreover, it has been found that the transcription factor Pou2f3 is involved in Trpm5-expressing cells, such chemosensory cell in oropharyngeal epithelium, and salivary cells in respiratory epithelium (152). Interesting, the role of Pou2f3 in Tuft cell differentiation was also observed in small cell lung cancer subtype (6). Pou2f3 is a transcription factor able to bind specific sequence on DNA (ATTTGCAT) and regulated the expression of different genes. Skn-1a a POU homeodomain transcription factor was first discovered in chemosensory cells for sweet, umami and bitter taste cells (153).

Tuft cell has been reported to play important role in immune response in intestine (154) (155) (156). Different studies have been identified the Tuft cells as important sentinels against intestinal parasites infection in intestine, by activation of type 2 immunity response (154). Type 2 immune response in intestine include the presence of tissue resident group 2 innate lymphoid cells (ILC2) in lamina propria and the secretion of type 2 cytokines, such IL4 and IL13. Tuft cells was found to be indispensable for this immune response. In fact, under the parasite infections, Tuft cells number increase, and they present high expression of IL4Ra, and IL25 production (155) (156). Importantly, IL4Ra signaling cascade is sufficient to Tuft cell hyperplasia and activation (155) (Figure 1.6).

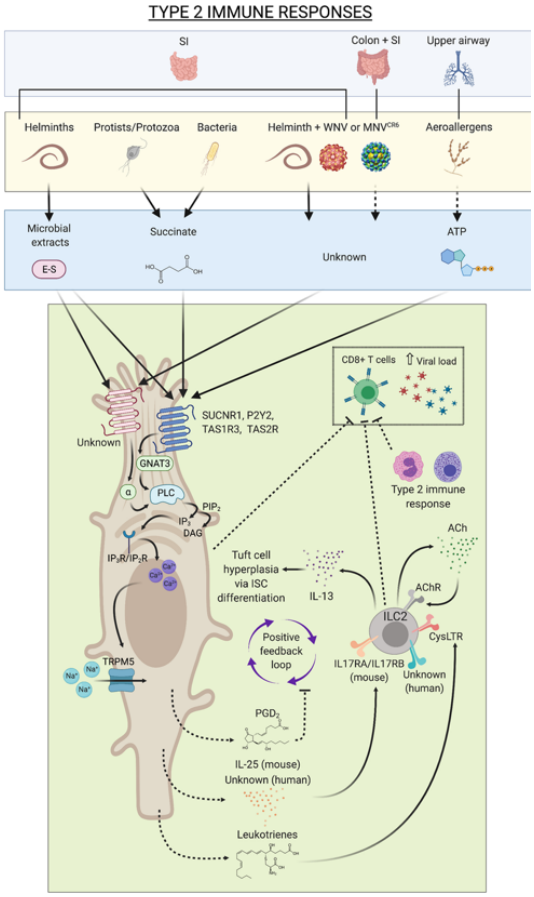

Figure 7: schematic representation of Tuft cell type 2 immune response propriety.
(Adapted from: Madison S. Strine et al., Tuft cells are key mediators of interkingdom interactions at mucosal barrier surfaces)

The presence of parasite, such Helminths, induce Tuft cells to express IL25, which sustain ILC2 cells recruitment in lamina propria, where they secrete IL13. This, acts on intestinal progenitor cells to differentiate in Tuft cells, leading to a hyperplasia state (156). Additionally, it has been shown that the secretion of Succinate metabolite by parasites is sufficient to promote Tuft cells activation and lead the activation of the signaling cascade between IL25 secretion and ILC2 cell activation (157) (158). In fact, it has been found that intestinal Tuft cell express Succinate receptor (SUCNR1), validating the role of this cells in immune response, and the protection role against Helminth infection.

Moreover, Tuft cells are necessary for tissue regeneration after inflammation and injury (159). These cells play important role also in different intestinal diseases, such ulcerative colitis (UC) and Crohn's disease (CD) (159).

Thus, it is important to take in mind that intestinal Tuft cells may rap resent potential therapeutic purpose in gastrointestinal pathologies.

3. PROJECTS AIM

Polycomb group proteins are necessary to establish (in stem cells) and to maintain (in adult cells) cellular identity. Polycomb group proteins play different roles in intestinal homeostasis. To establish a correct cellular identity profile, a specific transcriptional program is necessary. Polycomb group proteins are important players in chromatin remodeling that influence the transcriptional landscape in both stem and adult cells.

During intestinal homeostasis, intestinal stem cells (ISC) are able to differentiate and to generate all different intestinal cell types. It is widely known that the PRC1 complexes are indispensable for transcriptional repression in this process. Mice lacking both Ring1a/b catalytic subunits show impaired intestinal stem cell self-renewal and differentiation leading to an aberrant homeostatic event.

However, the role of different PRC1 subcomplexes in intestinal homeostasis remain unknown. The aim of this work is to characterize the PRC1 subcomplexes in chromatin remodeling and the contribution of different PCGF proteins in transcriptional repression maintenance in adult intestinal cells.

4. RESULTS

4.1 Single PCGF proteins are dispensable for intestinal homeostasis

It is known that Polycomb Repressive complex 1 is an important regulator in cellular lineage identity for embryonic stem cells (27). Very recently we characterize the fundamental role of PRC1 in adult intestine and in Intestinal stem cells (ISC) cellular identity. We demonstrate that the catalytic unit of PRC1, Ring1a/b, is indispensable to maintain cellular transcriptome profile, and to preserve the normal intestinal architecture (4). In fact, PRC1 acts as a repressor for non-lineage-specific transcription factor that alters B-catenin/Tcf transcriptional activity and Wnt pathway necessary for ISC self-renewal (4). However, the role of different PRC1 subcomplexes in adult intestinal homeostasis remain unclear. PRC1 is composed by four different biochemically subcomplexes, depending on which PCGF (PCGF1-6) protein is assembled to the catalytic unit Ring1a/b (1). PCGF2 and PCGF4, as PCGF3 and PCGF5, are redundant, and they are considered only one subcomplex.

To understand the difference in transcriptional repression maintenance in adult intestinal cells by different PCGF proteins, we took advantage of the use of inducible mouse models with the Cre recombinase system which leads the depletion of transgenic allele flanked with loxp sites (89). In particular, we used an *AhCRE* inducible mouse model, in which the Cre recombinase is under the cytochrome P450 promoter element and allows the recombination in all the intestinal cell types upon Beta-Naphtoflavone administration (87). The *VillinCREert2,* where the Cre recombinase translocate into the nucleus of all intestinal cell types after tamoxifen administration, was also used (88). We also used the mouse model *LGR5-GFP-ires-CreERT2/Rosa26Lox-stop-Lox LacZ,* in which the Cre recombinase and a GFP reporter are activated only in ISC after tamoxifen administration and expresses a LacZ reporter gene used as a tracer for stem cells and their progeny.

To characterize the role of PCGFs function, mouse models carrying the Cre recombinase were crossed in our laboratory with mouse models in which PCGF alleles were flanked by Loxp sites (Figure 4.1.1).

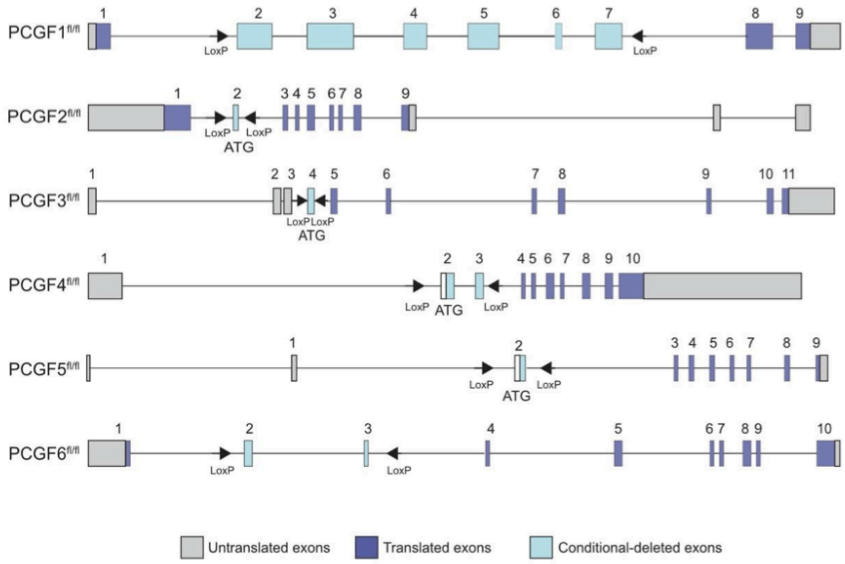

Figure 4.1.1: Schematic representation of PCGFs alleles for conditional Knock out mouse models

To have a better overview, we assessed the PCGFs expression among the intestinal cell types. We used antibodies against murine PCGFs produced in our laboratory and primers designed specifically on exon-exon junction for each PCGFs. Proteins and mRNA were extracted from Villi and Crypts of wildtype intestine to compare the expression levels among undifferentiated and differentiated cells. In intestinal Villi, PCGF1 and PCGF5 seem to be the most abundant, while PCGF2, PCGF3, PCGF4 and PCGF6 are more expressed in intestinal crypts (Figure 4.1.2 A, B).

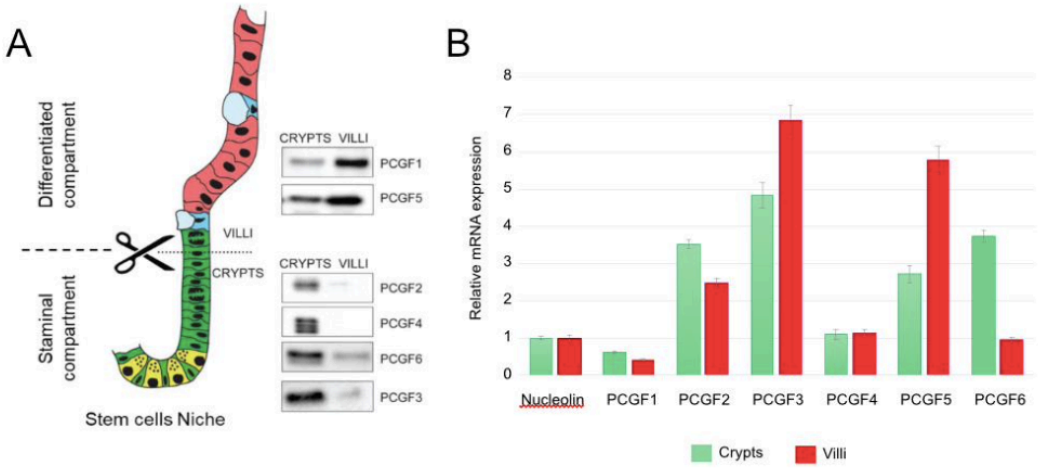

Figure 4.1.2: Differences of PCGFs expression among intestinal Villi and Crypts

A. Western Blot of protein relative levels of PCGFs proteins

B. RT-qPCR of mRNA levels of PCGF proteins

The differences in PCGFs expression levels may account for the specific and peculiar roles of PRC1 subcomplexes in adult intestine.

Thus, we first investigated the role of single PCGFs, in *AhCRE* mice as a control, and *AhCRE;PCGF1*$^{flox/flox}$, *AhCRE;PCGF6*$^{flox/flox,}$ *AhCRE;PCGF3/5*$^{flox/flox}$, and *in VillinCREert2;PCGF2/4*$^{flox/flox}$. *PCGF3/5*-KO and *PCGF2/4*-KO were considered as single knockouts due to the redundancy of those proteins.

To evaluate if the absence of single PCGFs altered the normal intestinal homeostasis, mice were intraperitoneally injected for four consecutive days with either beta-naphthoflavone (*AhCRE*) or tamoxifen (*VillinCREert2*) and intestines were harvested 15 days after the first injection. By performing histopathological analysis of intestinal sections obtained from *AhCRE*, *AhCRE;PCGF1*-KO, *AhCRE;PCGF3/5*-KO, *AhCRE;PCGF6*-KO, *VillinCREert2* and, *VillinCREert2;PCGF2/4*-KO, I found that the depletion of single PCGFs did not affect intestinal homeostasis (Figure 4.1.3). In fact, the duodenum of KO mice did not show any significant alteration of intestinal architecture and morphogenesis, in contrast to what we observed in absence of the catalytic subunit Ring1a/b (4).

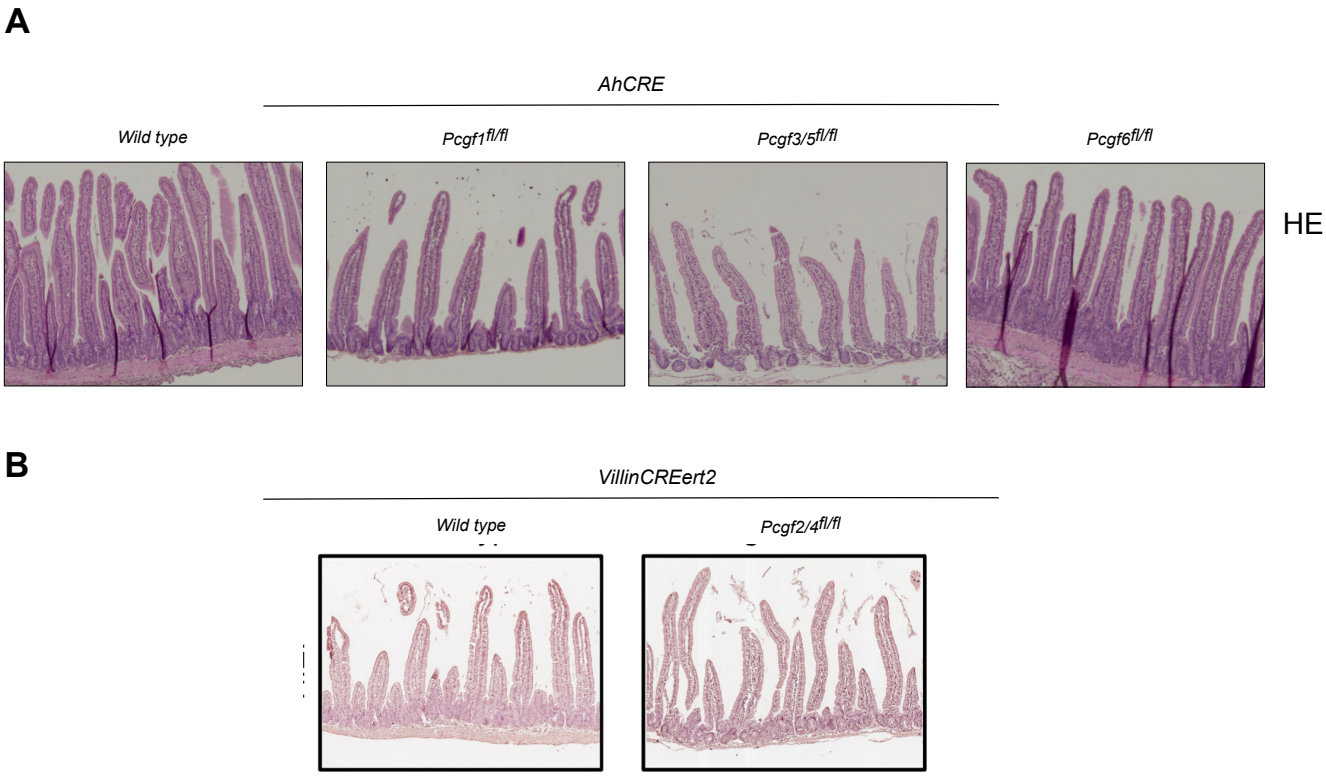

Figure 4.1.3: Hematoxylin and Eosin of duodenum sections from different conditional KOs

A. HE of intestinal sections from AhCRE Ctrl and AhCRE PCGF1, PCGF3/5, PCGF6 KOs
B. HE of intestinal sections from VillinCREert2 Ctrl and VillinCREert2 PCG2/4 KO.

After 15 days from the first tamoxifen injection, which lead to the depletion of each single PCGF from all the intestinal cell types, differentiation was not perturbed either. In fact, when we performed immunohistochemistry analysis on sections from duodenum using intestinal cell markers, such as chromogranin A for enteroendocrine cells, lysozyme for Paneth cells or Alcian blue for goblet cells, we did not observe any alteration in KO sections compare to WT intestinal sections (Figure 4.1.3 C,D).

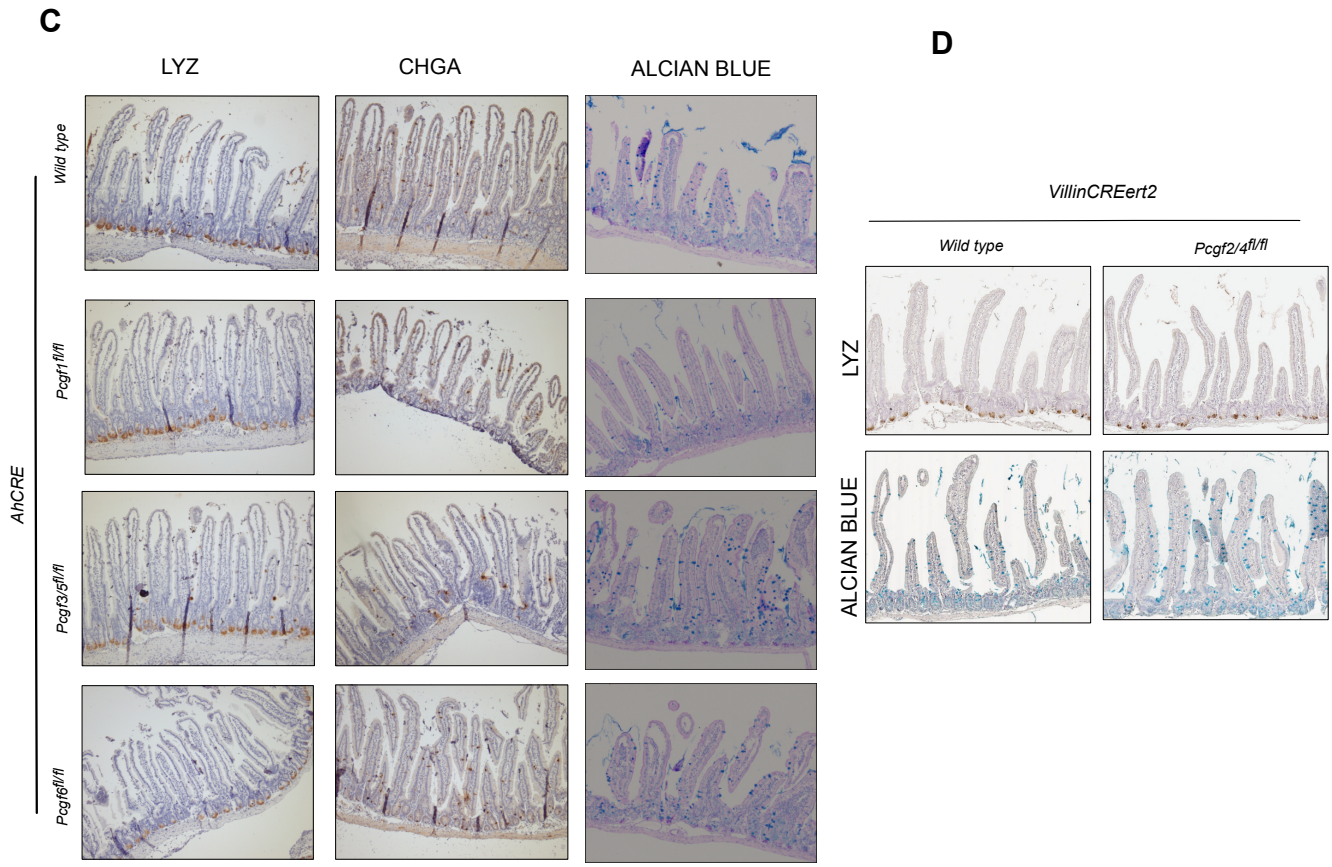

Figure 4.1.3: immunohistochemistry of intestinal section derived from wild type and KO mice at 15 days

- **C.** IHC for Lysozyme, Chromogranin A and Alcian Blue in AhCre wild type and AhCre PCGF1, PCGF3/5 and PCGF6 KOs
- **D.** IHC for Lysozyme, and Alcian Blue in VillinCREert2 wild type and VillinCREert2 PCGF2/4 KO

Taken together, these data suggested that single PCGF proteins are dispensable for adult intestinal homeostasis, and that the absence of PRC1.1, PRC1.2/4, PRC1.6 or PRC1.3/5 does not have the same catastrophic effect on intestinal architecture as the absence of the catalytic subunit RING1a/b (4).

The intestine is a very plastic organ with a complete self-renewal of 2-5 days (94) (95). During organ homeostasis and also during regeneration after injury, ISC also called Crypt base columnar (CBCs) cells, are able to differentiate in all the intestinal cell types and to maintain the ISC population (90), (91). LGR5 positive intestinal stem cells proliferate every 24 hours, generating or other LGR5+ ISC,

or the transient amplifying (TA) progeny that localize in the middle-bottom of the crypts. Those cells in 16-20 hours differentiate and migrate gradually upward on the villi (95).

To investigate if the depletion of single PCGF proteins could alter the number of proliferative cells, we performed immunohistochemistry analysis of intestinal sections. Staining for the proliferation marker Ki67 did not show any difference between AhCre and AhCre PCGF1, PCGF3/5, PCGF6 KOs, nor between VillinCREert2 and VillinCREert2 PCGF2/4 KO (Figure 4.1.4). These data suggested that PCGF1, PCGF2/4, PCGF3/5 and PCGF6 are dispensable for the proliferative niche preservation.

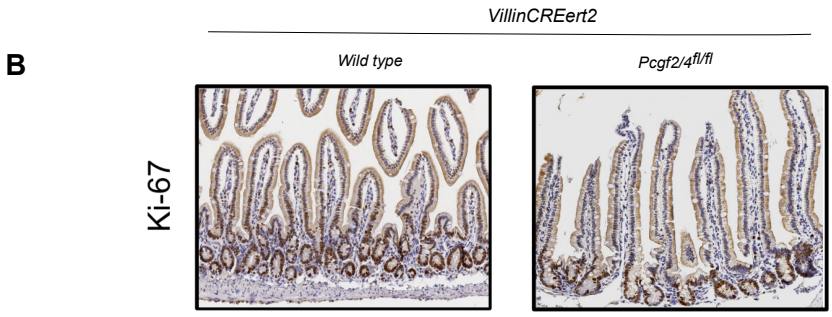

Figure 4.1.4: immunohistochemistry of intestinal section derived from wild type and KO mice at 15 days

A. IHC for Ki67 of AhCre wild type and AhCre PCGF1, PCGF3/5 and PCGF6 KOs sections
B. IHC for Ki67 VillinCREert2 wild type and VillinCREert2 PCGF2/4 KO

Moreover, to better assess the role of single PCGFs in proliferative intestinal stem cell and the capacity of these cells to repopulate the crypts/villi, we performed a lineage tracing experiment. For this experiment, we used the *LGR5-GFP-ires-CreERT2/Rosa26Lox-stop-Lox LacZ* mouse model, in which the Cre recombination occurs in LGR5-positive stem cells and the Rosa26 LSL transgene allows the tracing of the LGR5+ derived progeny with a beta-galactosidase reaction.

Upon activation of Cre and depletion of Stop cassette, LGR5+ ISC will express Beta-Galactosidase which hydrolyses X-Gal substrate into galactose and 5,5'-dibromo-4,4'-dichloro- indigo, which providing a visual assay for lacZ activity by the characteristic blue color. Single *PCGF*-KO mice were sacrificed at 7 days as an early time-point, and at 15 days as a late time-point. Beta-Gal reaction

was performed on fixed samples after the first tamoxifen injection (Figure 4.1.5). Intestinal sections from mice lacking single PCGFs did not show any difference in LacZ staining, which indicates that LGR5+ ISC KOs for PCGF1, PCGF2/4, PCGF3/5 and PCGF6 were able to repopulate the intestinal crypts and to regenerate all the crypts/villi axes.

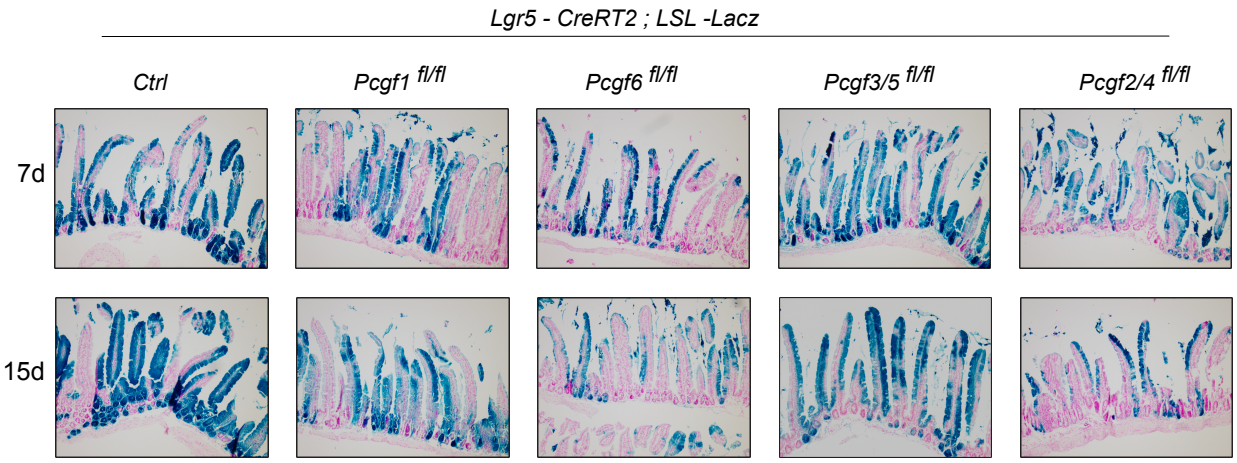

Figure 4.1.5: Beta-Galactosidase reaction on intestinal sections from LGR5-GFP-ires-CreERT2/Rosa26Lox-stop-Lox LacZ wild type and KOs mice.
Panel of LacZ staining at 7 days (top) and 15 days (bottom) in LGR5-GFP-ires-CreERT2/Rosa26Lox-stop-Lox LacZ and LGR5-GFP-ires-CreERT2/Rosa26Lox-stop-Lox LacZ PCGF1, PCGF3/5, PCGF6 and PCGF2/4 KOs

4.2 Single PCGFs are dispensable for PRC1 activity in intestinal cells

Polycomb repressive complex 1 has been divided in two major classes: Canonical PRC1 and Non-Canonical or Variant PRC1 (1). Canonical PRC1, together with Ring1a/b contains the CBX proteins, which recognize H3K27me3 histone marker deposited by Polycomb repressive complex 2, and PCGF2 or PCGF4. Variant PRC1 is composed by RYBP or YAF2 together with Ring1a/b catalytic core, and the recruitment on chromatin is independent of PRC2 activity. Moreover, Variant PRC1 is composed by the presence of PCGF1, PCG3, PCGF5 or PCGF6. Those six different subcomplexes are able to deposit H2Ak119ub1 histone modification and to control the chromatin compaction, and

the consequent DNA accessibility. To investigate the ability of different PRC1 subcomplexes to regulate adult intestinal cell fate decision and maintenance through transcriptional repression, we performed chromatin immunoprecipitation followed by sequencing analysis using intestinal crypts of wildtype and PCGF1, PCGF3/5, PCGF6 and PCGF2/4 KOs.

First, we performed ChIP-seq analysis for H2AK119ub1 in different single KOs in order to verify the activity of the PRC1 whole complex after removing PCGF1, PCGF2/4, PCGF3/5 or PCGF6 in intestinal cells. The number of peaks was different in each KO.

However, the H2AK119ub1 global levels were not significantly changed after removing single PCGFs (Figure 4.2.1 A). In intestinal cells depleted of PCGF1, PCGF2/4 or PCGF6, the levels of H2AK119ub across RING1b targets, including both promoter regions and intergenic regions, were the same compared to the levels found in wildtype cells (Figure 4.2.1 B).

These data suggested that PRC1.1, PRC1.2/4, PCGF3/5 and PRC1.6 are dispensable for PRC1 global activity. In fact, in absence of PCGF1, PCGF2/4, PCGF3/5 and PCGF6, we did not observe altered H2AK119ub1 deposition.

A

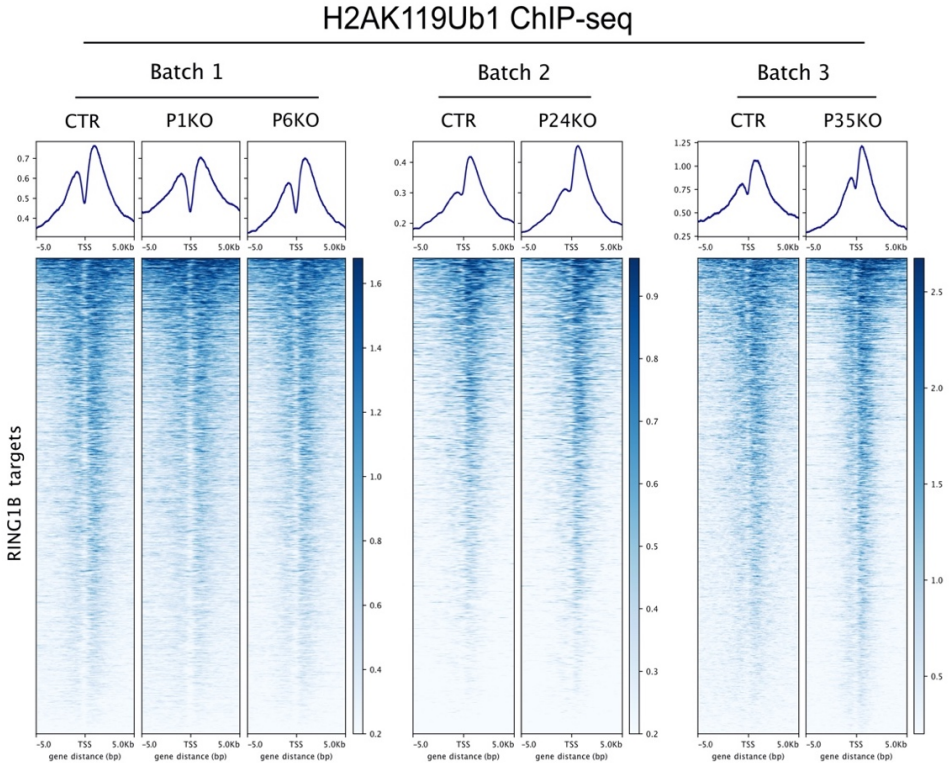

B

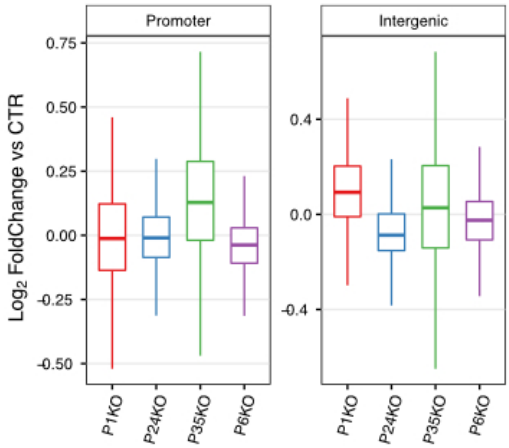

Figure 4.2.1: Chromatin immunoprecipitation following by sequencing for H2Ak119ub1 across Ring1b peaks for wild type intestinal cells and PCGF single KOs.

- **A.** Heatmaps of H2AK119ub1 ChIP levels on Ring1b targets
- **B.** Boxplot of quantitative H2AK119ub1 ChIP levels on Ring1b targets

Interestingly, when we looked at genome-wide levels, we found that the H2AK119ub1 signal was decreased in intestinal cells lacking PCGF3/5, but not in other KO cells (Figure 4.2.2 A, B).

A

B

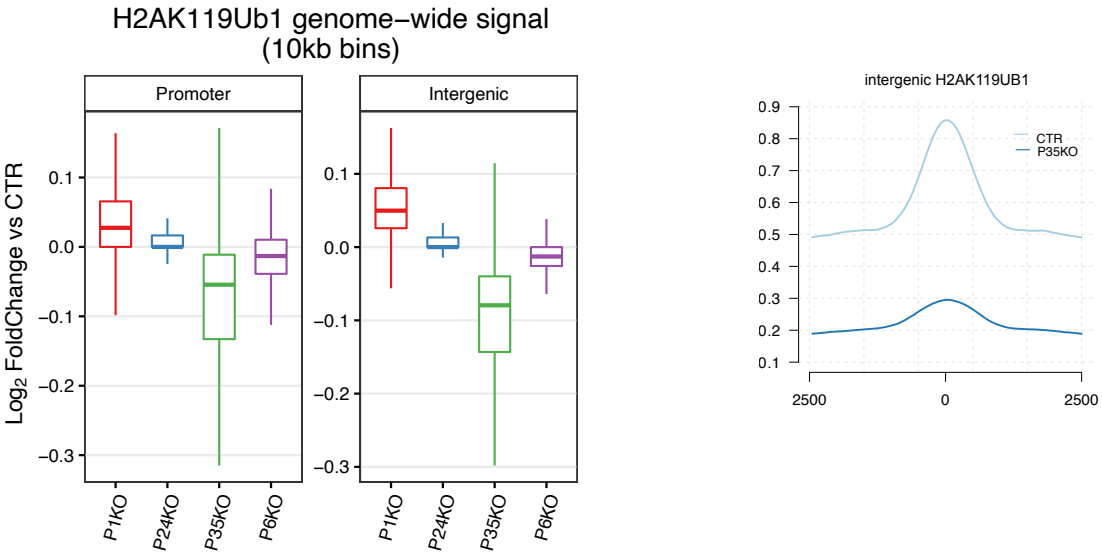

Figure 4.2.2: Chromatin immunoprecipitation following by sequencing for H2Ak119ub1 genome-wide for wild type intestinal cells and PCGF single KOs.

- **A.** Boxplot of H2AK119ub1 genome-wide signal at promoter (left) and intergenic (right) regions
- **B.** Intergenic H2Ak119ub signal

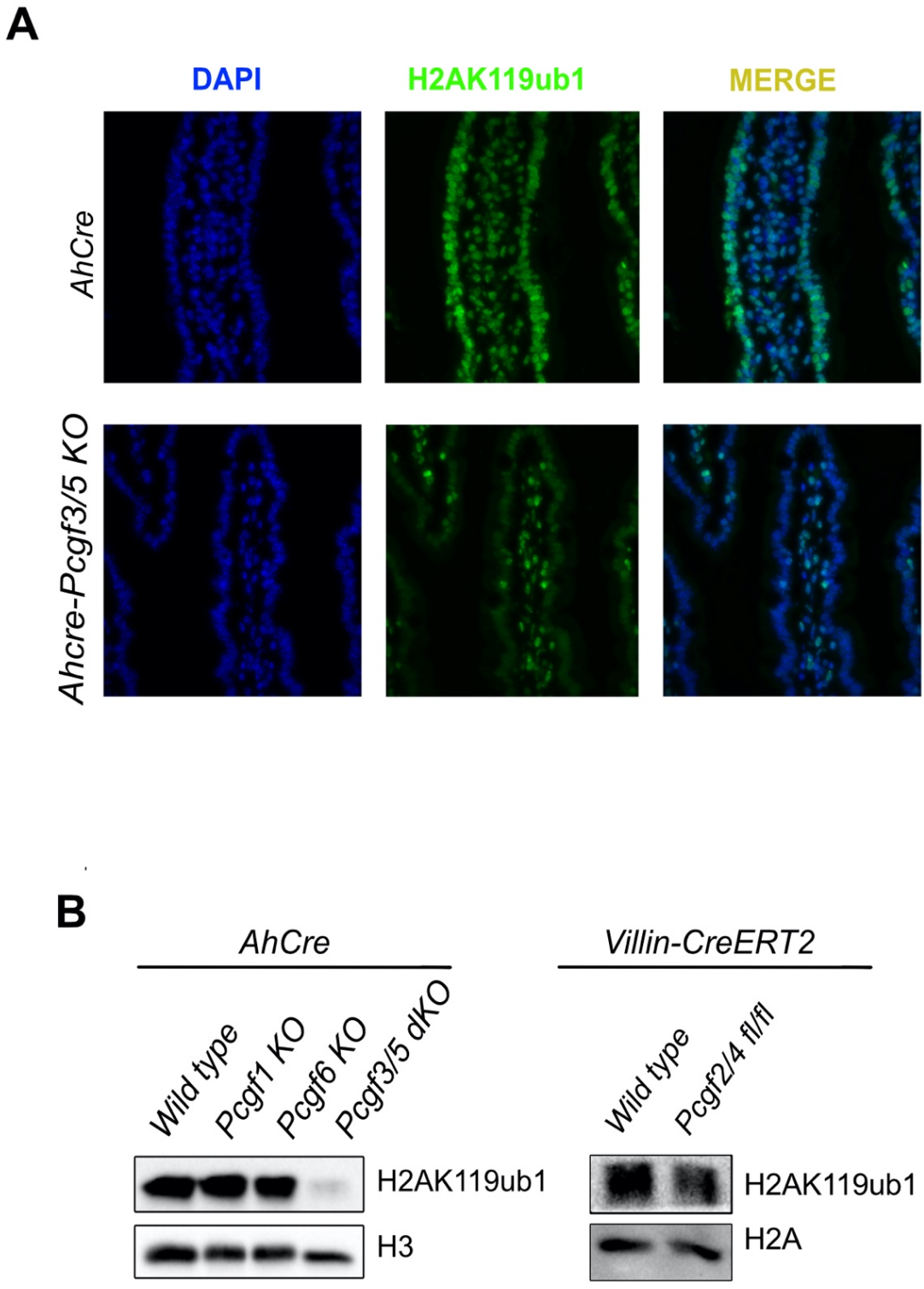

Figure 4.2.3: Chromatin immunoprecipitation following by sequencing for H2Ak119ub1 genome-wide for wild type intestinal cells and PCGF single KOs.

A. Boxplot of H2AK119ub1 genome-wide signal at promoter (left) and intergenic (right) regions
B. Intergenic H2Ak119ub signal

Then, we decided to look at the binding of Ring1b in the absence of single PCGF proteins. we performed chromatin immunoprecipitation in intestinal cells from wildtype and single PCGF-KO mice using a homemade antibody against RING1B. We analyzed the RING1B ChIP-seq signal intensity at +/- 5 Kb across Ring1b targets. We observed the same RING1B enrichment in wildtype, *PCGF1*-KO, *PCGF3/5*-KO, and *PCGF6*-KO. However, the intensity of RING1B signal in *PCGF2/4*-KO was extremely decreased (Figure 4.2.3). These data suggested that PCGF2 and PCGF4 retain the majority of RING1B proteins on chromatin. However, given the unchanged H2Aub1 levels in *PCGF2/4*-KO, we speculated that there might be an enzymatic compensation of single PRC1 subcomplexes in intestinal crypts. This was also observed in our laboratory in embryonic stem cells (2).

A

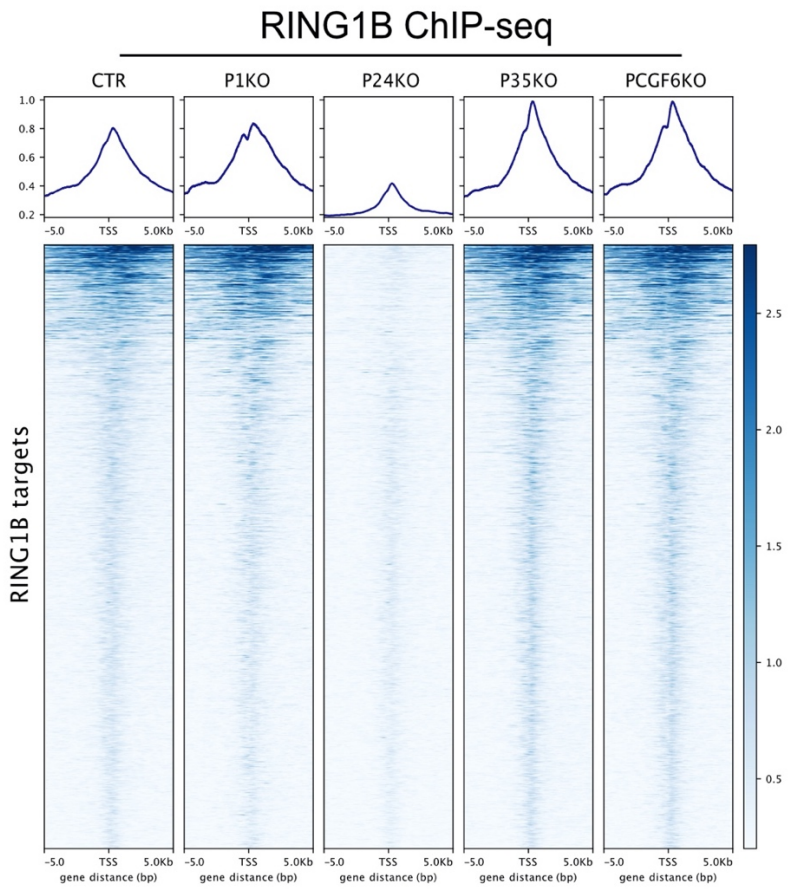

B

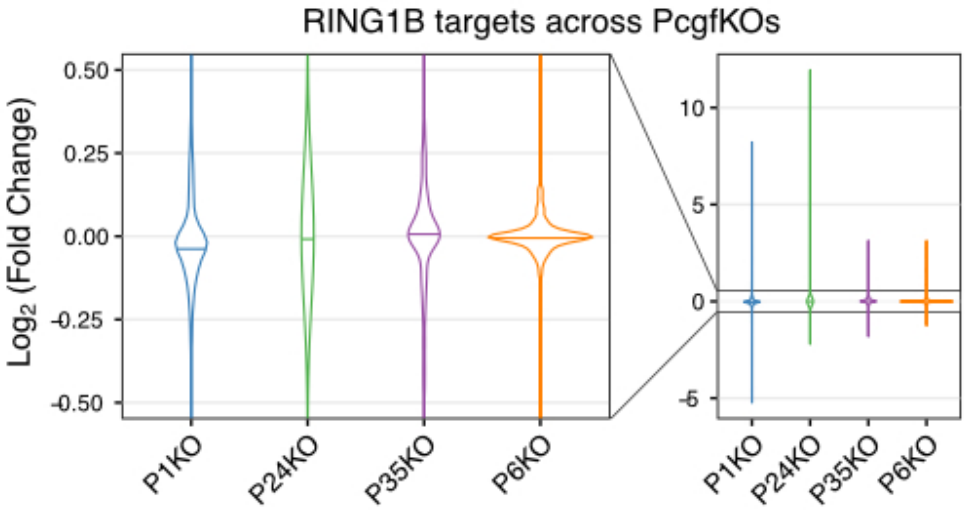

Figure 4.2.4: Chromatin immunoprecipitation following by sequencing for H2Ak119ub1 across Ring1b targets for wild type intestinal cells and PCGF single KOs.

A. Heatmap representing normalized Ring1b CHIP-seq intensity of +/- 5Kb from TSS of Ring1b target genes in intestinal Crypts
B. Boxplot of quantification Ring1b ChIp-seq intensity of Ring1b target genes

Next, we examined the role of distinct PRC1 subcomplexes on PRC2 recruitment to chromatin. We quantified H3K27me3 deposition upon depletion of single PCGFs from intestinal crypts. PCGF1, PCGF6 and PCGF3/5 loss had no effects on PRC2 recruitment and activity at RING1B-associated loci. On the other hand, the absence of PCGF2 and PCGF4 lead to a partial H3K27me3 histone marker reduction (Figure 4.2.5).

A

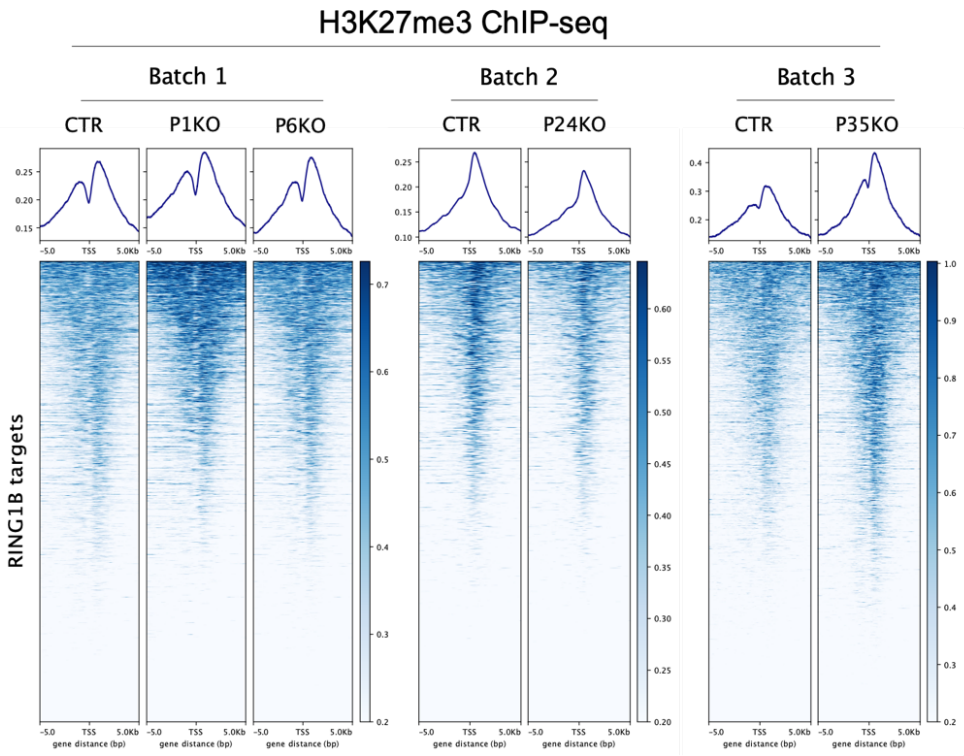

B

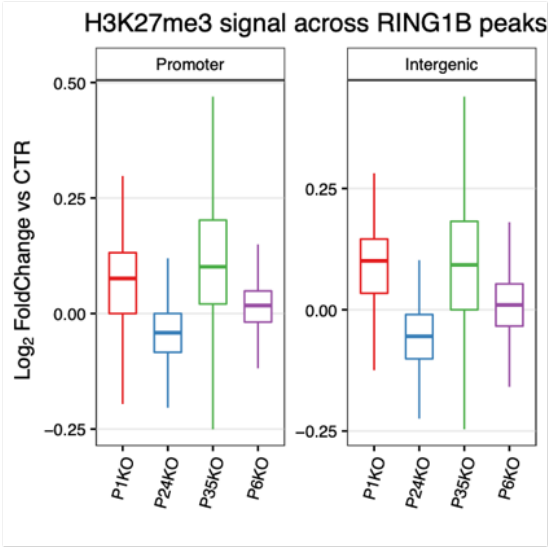

Figure 4.2.5: Chromatin immunoprecipitation following by sequencing for H3K27me3 genome-wide for wild type intestinal cells and PCGF single KOs.

- **A.** Heatmap representing normalized H3K27me3 CHIP-seq intensity of +/- 5Kb from TSS of Ring1b target genes in intestinal Crypts
- **B.** Boxplot of quantification H3K27me3 ChIp-seq intensity of Ring1b target genes

Together, these results revealed a compensatory effect of PCGF proteins on H2AK119ub1 deposition, and that PCGF2 and PCGF4 retain RING1B on chromatin.

4.3 PCGF loss does not affect PRC1-associated transcriptional repression

It is well established that PRC1 is associated with transcriptional repression (8) (27). Moreover, in ES cells we demonstrated that PCGF2 is always correlated with classic Polycomb profile associated with transcriptional repression. But in contrast we found that PCGF6 unique targets show a permissive transcriptional profile, and that PCGF3 targets a active transcriptional state (2). However, nothing is known about the role in transcription regulation of PCGFs in adult intestinal cells.

To understand the role of PCGFs in the regulation of transcription in adult intestinal cells, we assayed the transcriptional properties of each PRC1 subcomplex by performing RNA sequencing. To evaluate the alteration in absence of different PRC1 subcomplexes, we compared the transcriptomic profile of single PCGF-KOs with the Ring1a/b-dKO transcriptomic profile. In intestinal cells depleted of the PRC1 catalytic subunit, the transcriptional repression was completely lost. In fact, up to 800 genes were upregulated in Ring1a/b dKO cells compared to wildtype cells. However, in intestinal cells where PCGF1, PCGF2/4 or PCGF6 expression was lost, we did not observe significant changes in transcriptome repression. In fact, we found 131 upregulated genes in *PCGF1*-KO, 37 in *PCGF2/4*-KO, and 162 in *PCGF6*-KO (Figure 4.3.1.).

A

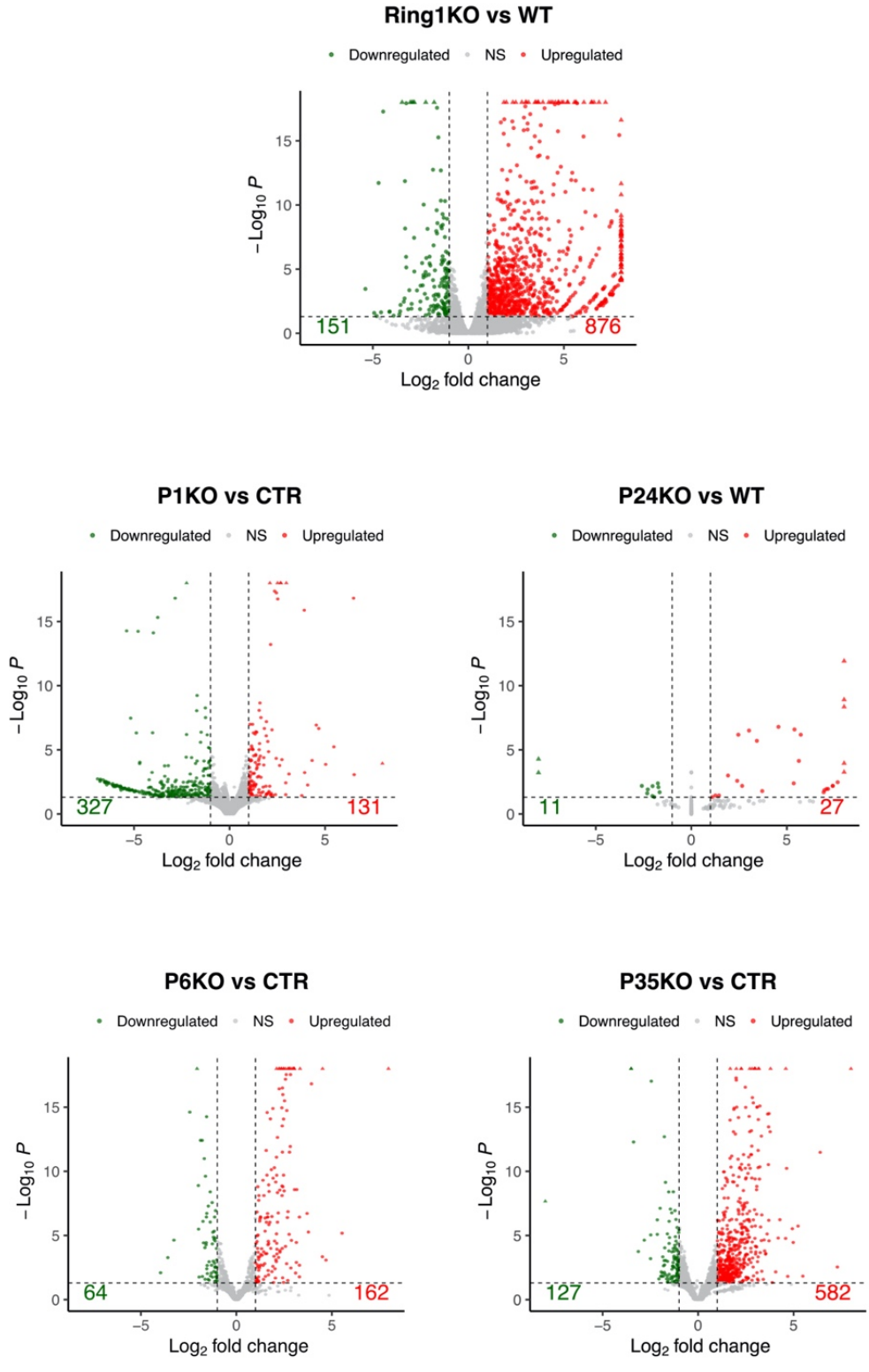
Ring1KO vs WT
Downregulated
NS
Upregulated
−Log10 P
Log2 fold change
151
876
P1KO vs CTR
327
131
P24KO vs WT
11
27
P6KO vs CTR
64
162
P35KO vs CTR
127
582

B

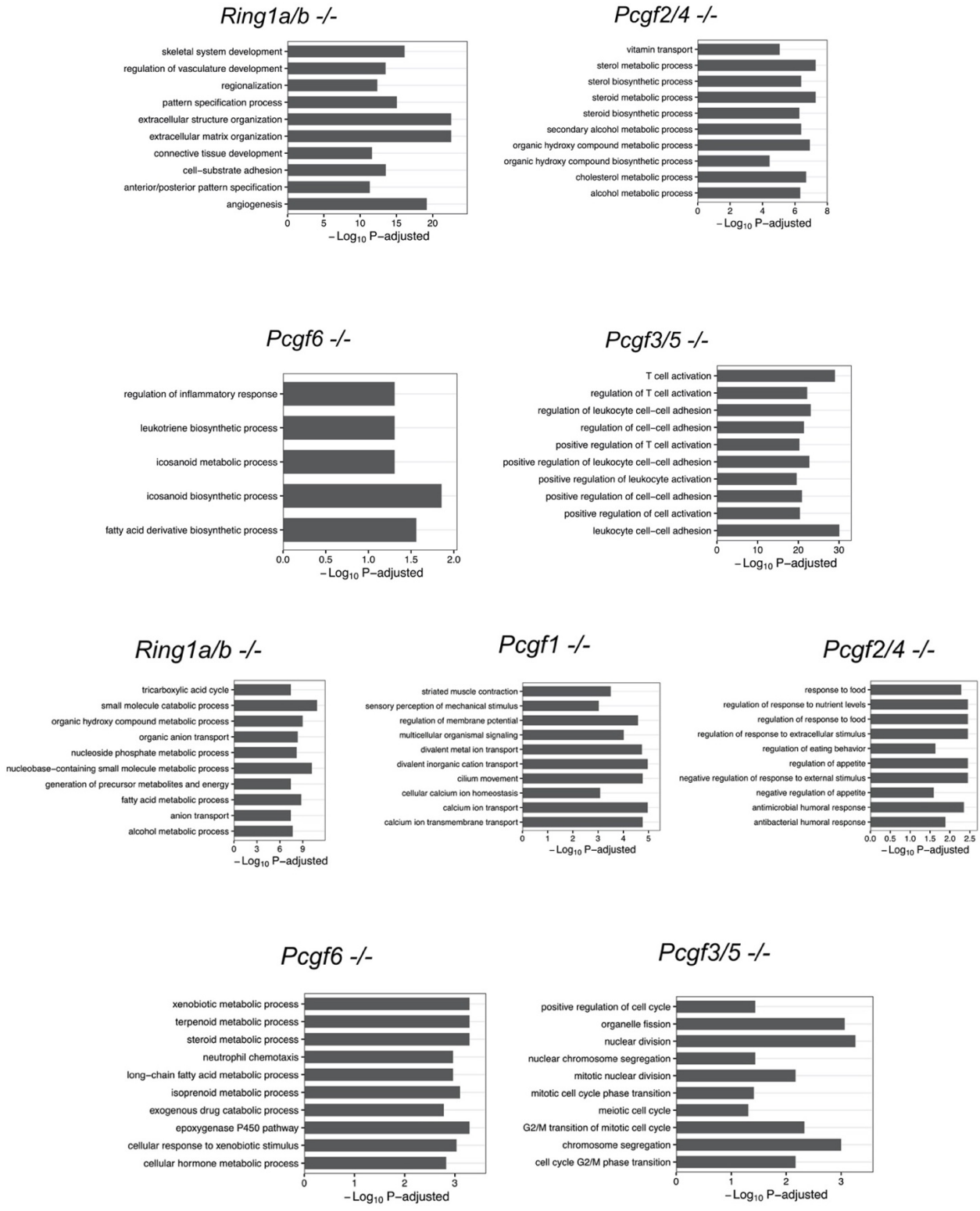

Figure 4.3.1: Transcriptome profile of adult intestinal cells derived from single Knock out mice

- **A.** Volcano blot of de-regulated genes in Ring1a/b dKO, PCGF1 KO, PCFF2/4 KO, PCGF3/5 KO and PCGF6 compared to wild type
- **B.** Gene ontology enrichment analysis of upregulated genes (top) and downregulated genes (bottom)

The percentage of de-regulated genes in single KOs was very low compared to Ring1a/b dKO, suggesting that PCGF1, PCGF2/4, PCGF3/5 and PCGF6 are not involved in global transcriptional

control (Figure 4.3.2). Moreover, even though a significant number of upregulated genes was found in RNA-seq analysis of *PCGF3/5*-KO intestinal cells, gene ontology analysis revealed that there was no enrichment for any Polycomb-associated signature, suggesting that the moderate transcriptional activation was a secondary effect of PCGF3/5 loss (Figure 4.3.1.).

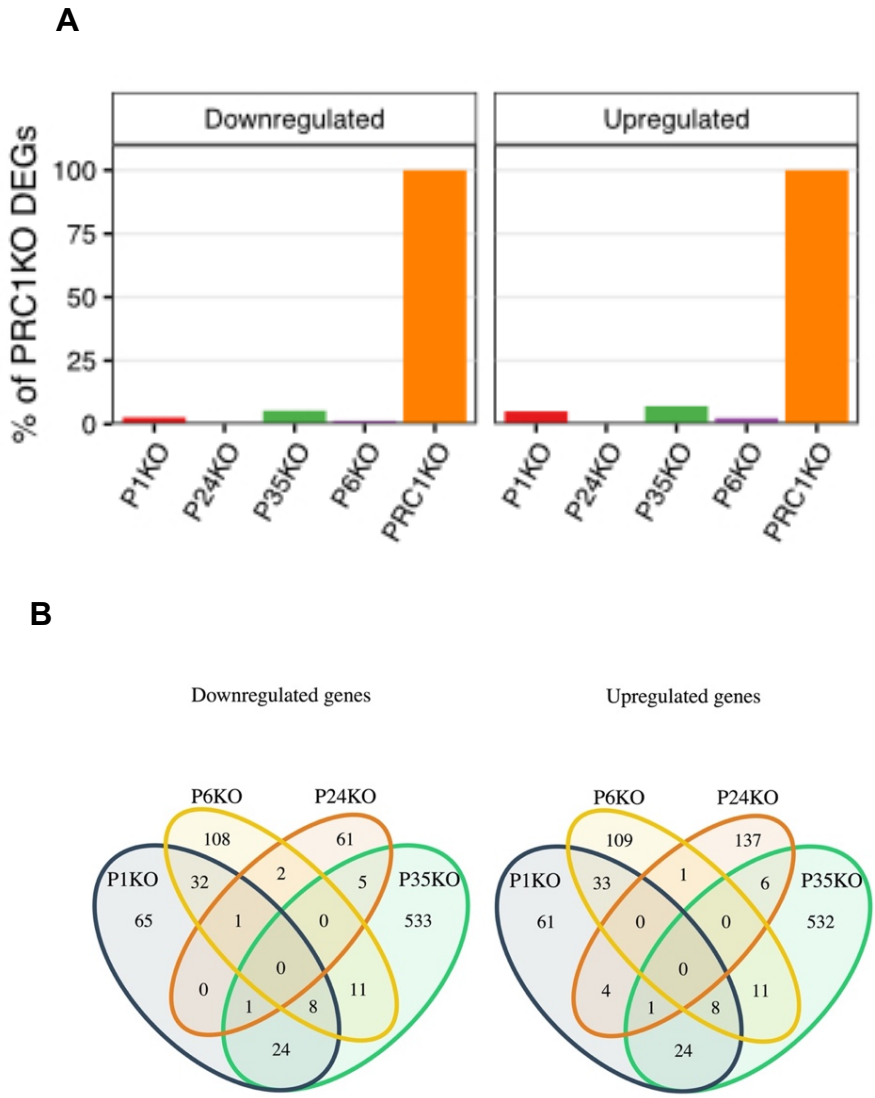

Figure 4.3.2: Transcriptome profile of adult intestinal cells derived from single Knock out mice show different overlap

- **A.** Column graph showing percentage of de-regulated genes in single PCGF KO and Ring1b KO in adult intestinal cells
- **B.** Overlap of downregulated genes found in different PCGF single KOs (left) and upregulated gene (right)

Moreover, the transcriptomic profile of each PCGF-KO was specific, given the absence of overlap in upregulated and downregulated genes (4.3.2 B). These data indicated that PRC1.1, PRC1.2/4, PRC1.3/5 and PRC1.6 are dispensable for transcriptional repression in adult intestinal cells

4.4 PRC1 subcomplexes regulate specific clusters of target genes

Our group and others have already demonstrated that PCGF proteins have a compensatory effect in H2AK119ub1 histone marker deposition and in transcriptional repression (2).

To assess whether PRC1 subcomplexes had compensatory features in the adult intestine, we mapped the chromatin binding of PCGF1, PCGF2, PCGF3, PCGF4 and PCGF6 using intestinal epithelium of wildtype mice. To do that, we performed ChIP-sequencing analysis using specific antibodies against PCGFs produced in our laboratory. Then, we analyzed PRC1 binding by RING1b ChIP- seq, as well as PRC1 activity by H2AK119ub1 ChIP- seq. Moreover, we also checked PRC2 binding and activity, by SUZ12 and H3K27me3 ChIP-seq analysis respectively.

We found differences between Canonical PRC1 and non-canonical PRC1 subcomplexes, in terms of peak length and total number of target genes. In fact, PCGF1 with 1700 target genes, and PCGF6 with more than 4000, where the PCGF proteins with highest number of target genes. While PCGF4 shown to bind 600 target genes, PCGF2 shown to bind to 350 target genes, and PCGF3 shown less than 100 target genes (Figure 4.4.1 C). PCGF3 showed a lower number of target genes (64) and sharper peak length (116-300 bp), probably due to its chromatin binding specificity, while the other non-canonical PCGFs showed broader peaks (500 -1500 bp) and different number of target genes (Figure 4.4.1 A, B). This very low number of target genes found with ChIP-seq analysis for PCGF3 and PCGF5 may be due to the dynamic nature of these proteins and their unstable binding to chromatin.

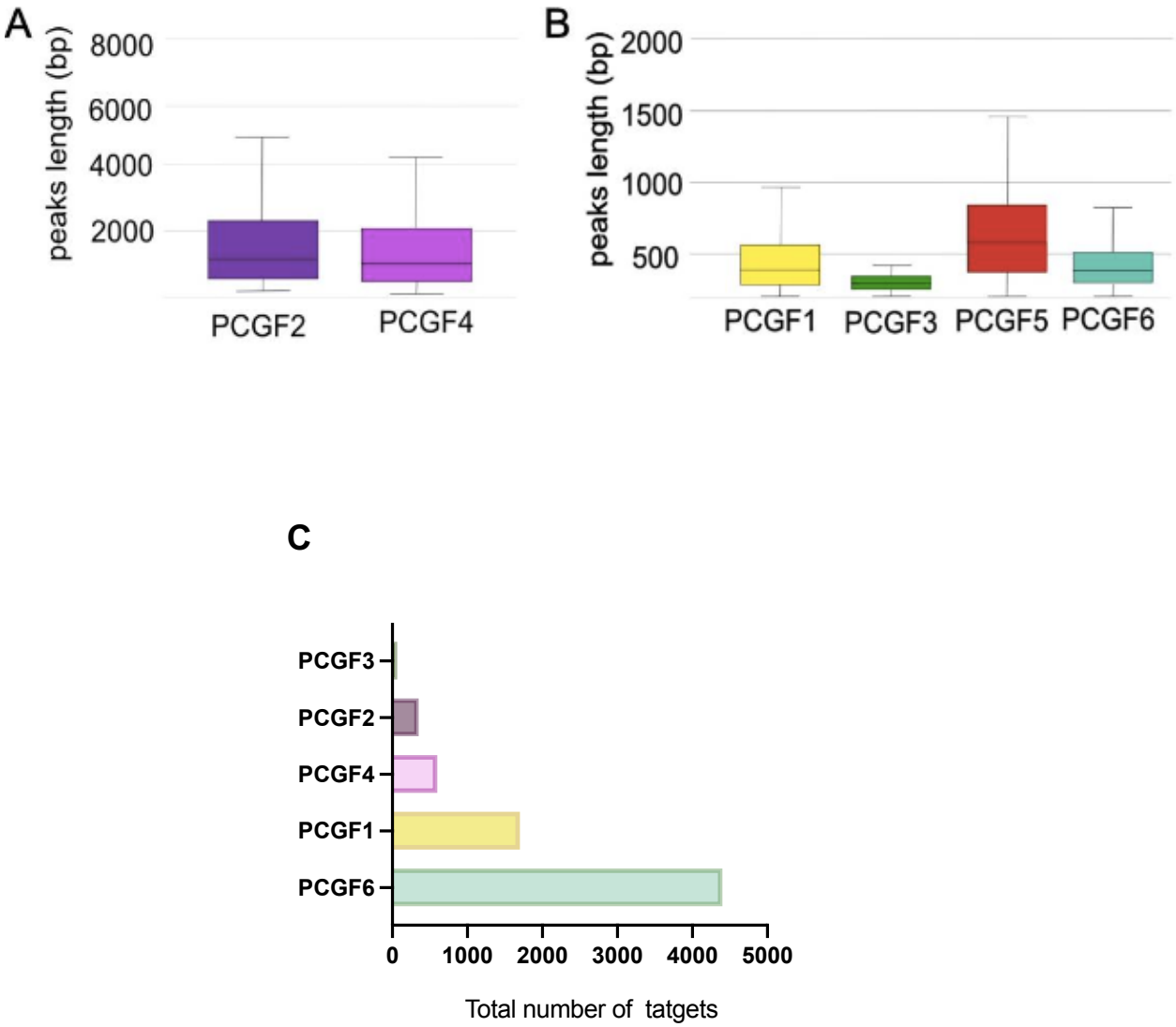

Figure 4.4.1: Boxplot showing peaks length and number for different PCGFs chromatin binding
A. Peaks length for PCGF2 and PCGF4
B. Peaks length for PCGF1, PCGF3, PCGF5 and PCGF5
C. Total Number of single PCGFs target genes

In intestinal cells PCGF2 and PCGF4 shared not only a similar number, but also the same sets of target genes. In fact, as it had been observed in ESc, PRC1.2 and PRC1.4 localized on classic Polycomb-related genes, such as ZIC and HOX genes (Figure 4.4.2).

Interestingly, we found that non-canonical PCGFs, in particular PCGF6 localized on different sets of target genes, which were not related to classical Polycomb-associated genes (4.4.2).

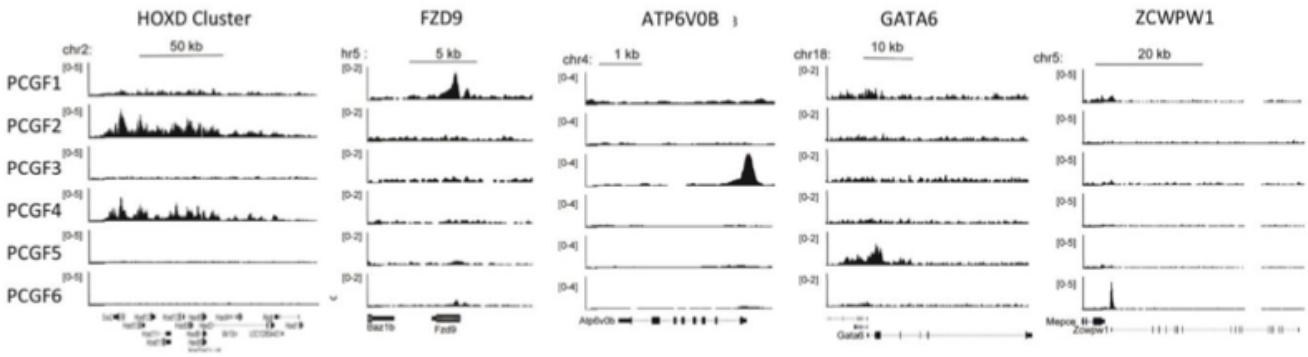

Figure 4.4.2: PCGFs chromatin localization in wild type intestinal cells / cluster targets genes

In line with what we observed in ESc, all PCGFs were preferentially associated to promoter regions and CpG island (2). However, we found that PCGF6, show not only the highest number of target genes, but was mostly associated at distal regions (56%), and negative CpGi. (Figure 4.4.3 A, B). (This will be better characterized in the chapter 4.3 on the role of PCGF6 in Tuft cells differentiation.)

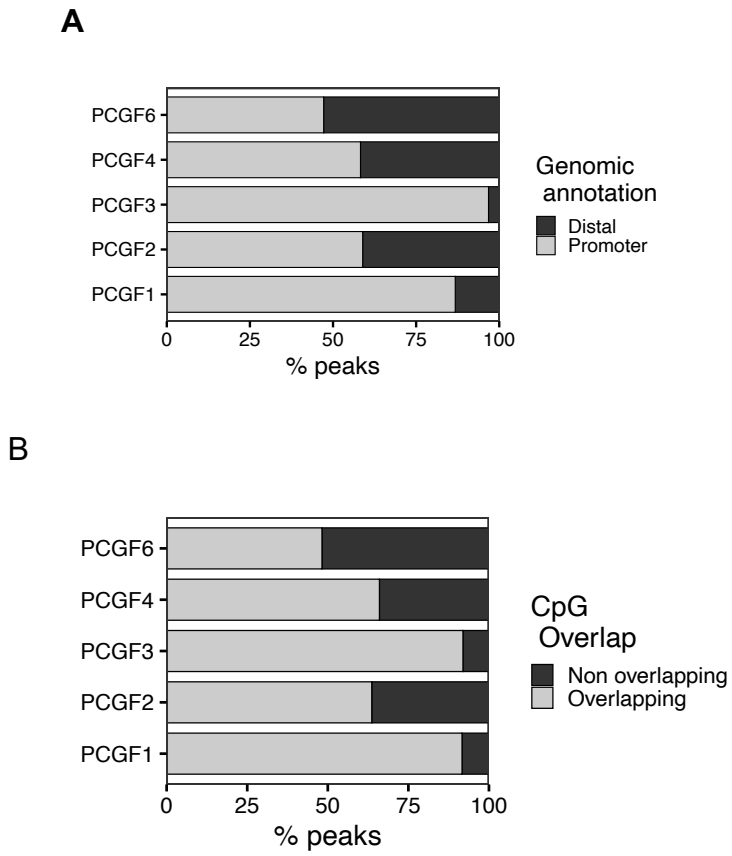

Figure 4.4.3: PCGFs genomic association on promoter/intergenic region (A) and on CpG rich island (B)

All this information that we collected regarding chromatin association of PRC1 subcomplexes suggests different roles of PCGF proteins in chromatin compaction and transcriptional repression in adult intestinal cells.

We had already demonstrated that PCGF proteins could co-occupy the same genomic regions in ESc (2). Additionally, we found that PCGFs compensate each other in transcriptional repression In ESc(2). As such, we decided to dissect the hypothetic compensation of PCGFs also in adult intestinal cells. We analyzed deeper ChIP-sequencing data of each PCGF protein (Figure 4.4.4)

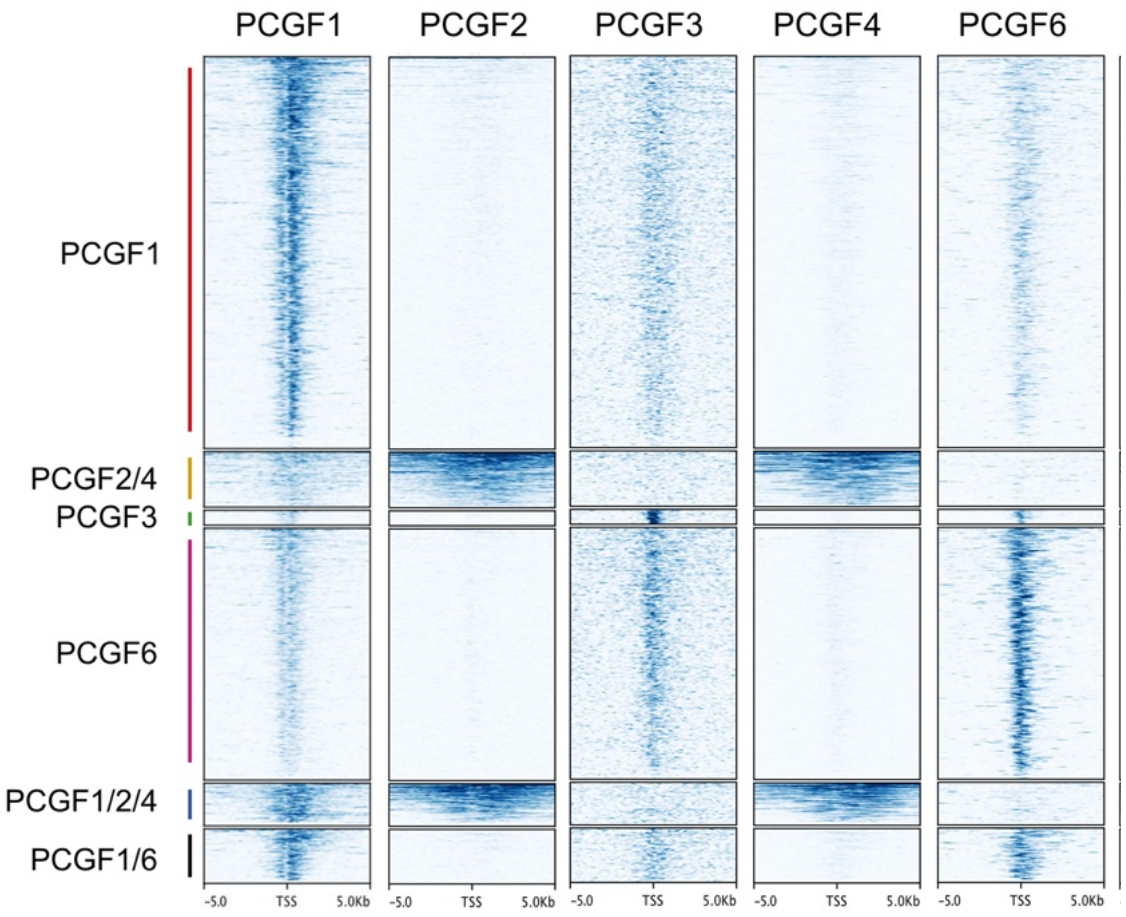

Figure 4.4.4: Heatmaps representing ChIP-seq normalized PCGF1, PCGF2, PCGF3, PCGF4, PCGF6 ChIP-seq intensity of +/- 5Kb from TSS of specific and common PCGFs target genes

By overlapping specific targets of different PCGFs, we observed that PCGF proteins localized with high specificity on the genome. We found that PCGF1 and PCGF6 presented a good number of

unique target genes among all PCGFs. PCGF6 binds 3691 unique targets among 4835 total target genes, and PCGF1 binds 773 unique targets among 1700 total target genes. We also found a partial co-occupancy between PCGF1 and PCGF6 (552 target genes). As expected, PCGF2 and PCGF4 displayed a high number of shared genome loci association, consistent with their redundant properties. Very Interestingly, we also found that canonical PCGF2 and PCGF4 presented a substantial overlap with non-canonical PCGF1 (Figure 4.4.5 A).

Then, we performed a motif enrichment analysis on binding sites of PCGFs and found that PCGF6 recognized CTCF consensus sequence, E-box binding sites, such as that for the c-Myc oncogene, and T-box sequences, bound by MGA, which is also part of the PRC1.6 subcomplex. Instead, PCGF3 preferentially bound BHLH motifs, which are similar to the c-Myc E-box and are known to be directly bound by USF1, as we had already described in ESc (2). (Figure 4.4.5 B).

A

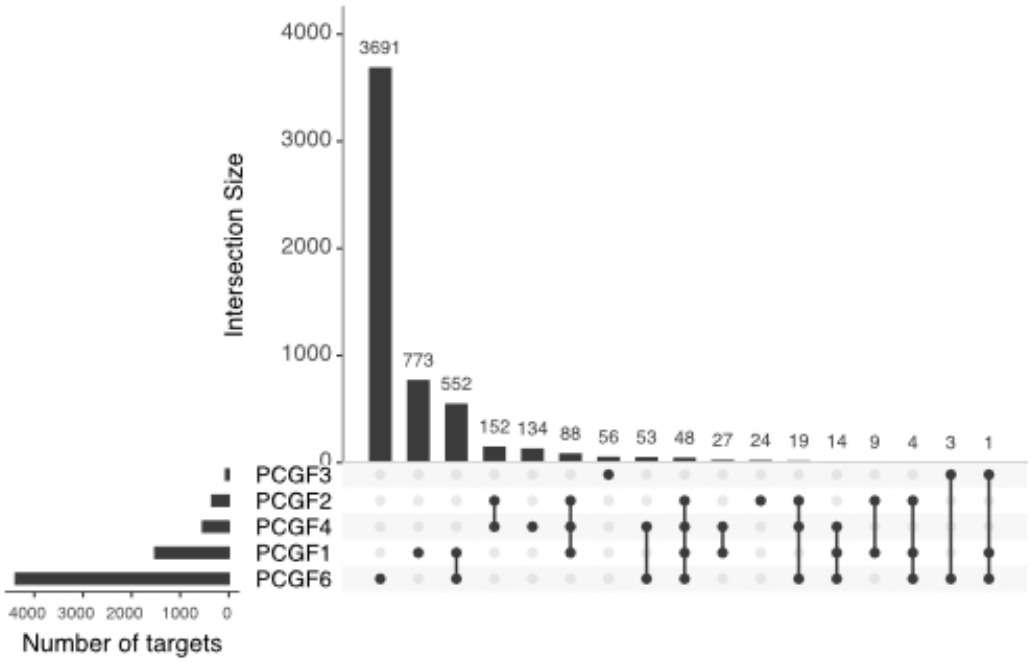

B

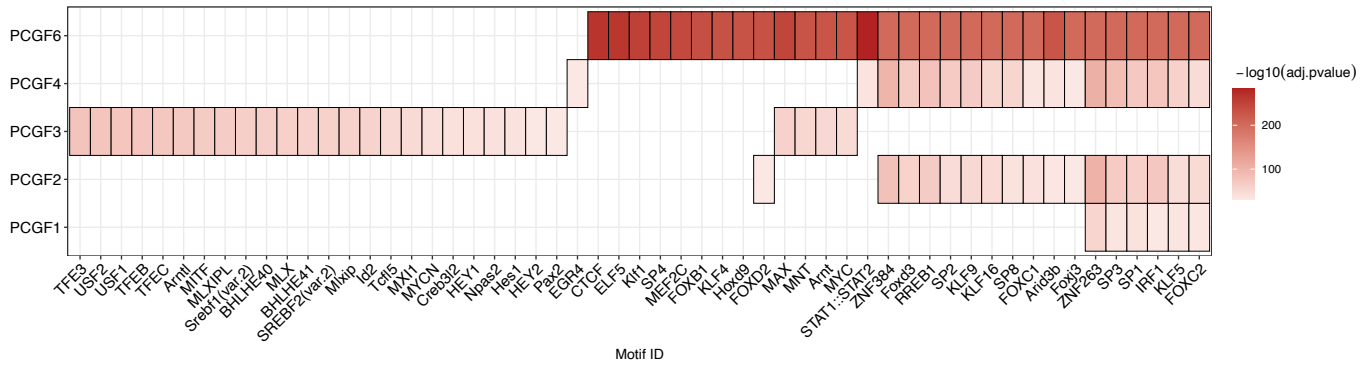

Figure 4.4.5: PCGFs bindings unique and common target genes on chromatin in adult intestinal cells.
A. Column graph representing unique and common PCGFs target genes among
B. Motif enrichment analysis of PCGFs binding sites

Then, we determined the presence of PRC1 and PRC2 catalytic subunits on PCGF binding sites by looking at the overlap between PCGFs - RING1b and PCGFs - SUZ12. Moreover, we also looked at the H2AK119ub and H3K27me3 deposition at PCGF-bound regions (Figure 4.4.6). In intestinal cells RING1B and H2AK119ub were abundant at PCGF2 and PCGF4 target genes, as was observed in ESc (2). Moreover, in intestinal cells, SUZ12 was found to be most abundant at PCGF2 and PCGF4 target genes, compare to other PCGFs, and so was the enrichment of and H3K27me3 histone marks. Additionally, we found that RING1b was present on 60% of PCGF1 target genes, where there were also abundant of H2AK119ub, compared to other variant PCGFs (Figure 4.4.6). in line with specificity of PCGF6, we found that PRC1 and PRC2 catalytic subunits bound less than 30% of PCGF6-associated loci, validating the PCGF6 role independent from PRC1 (Figure 4.4.6).

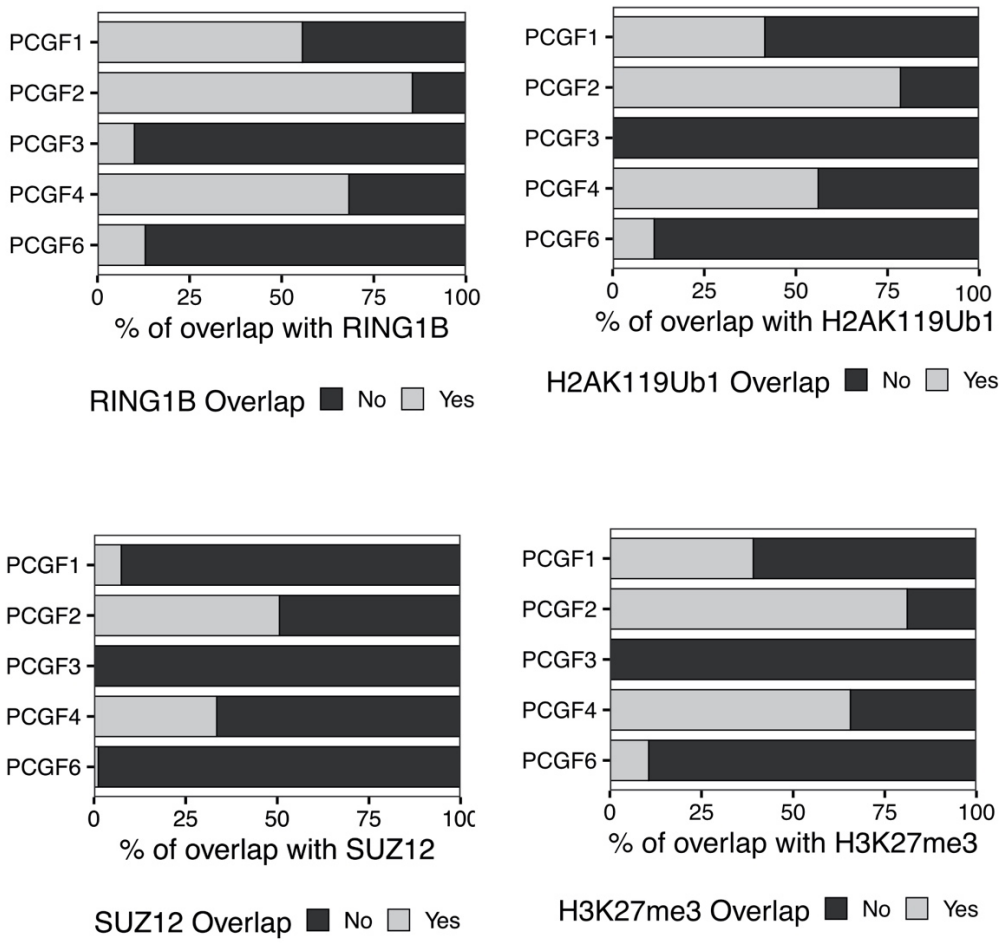

Figure 4.4.6: PCGF proteins show different binding with PRC1 and PRC2 target genes

A. Column graph representing overlap between PCGF targets genes and Ring1b target genes
B. Column graph representing overlap between PCGF targets genes and H2Aub1 target genes
C. Column graph representing overlap between PCGF targets genes and SUZ12 target genes
D. Column graph representing overlap between PCGF targets genes and H3K27me3 target gene

To define the clusters of genes regulated by different PCGFs, we performed gene ontology analysis (Figure 4.4.7). PRC1.2 and PRC1.4 preferentially bound genes involved in cell identity decision, cell identity maintenance and cellular differentiation. In line with their large overlap, PCGF1 targets were also enriched in genes associated with development and differentiation processes, which supports the hypothesis of cooperation of PCGF1, PCGF2, PCGF4 in adult intestinal cells.

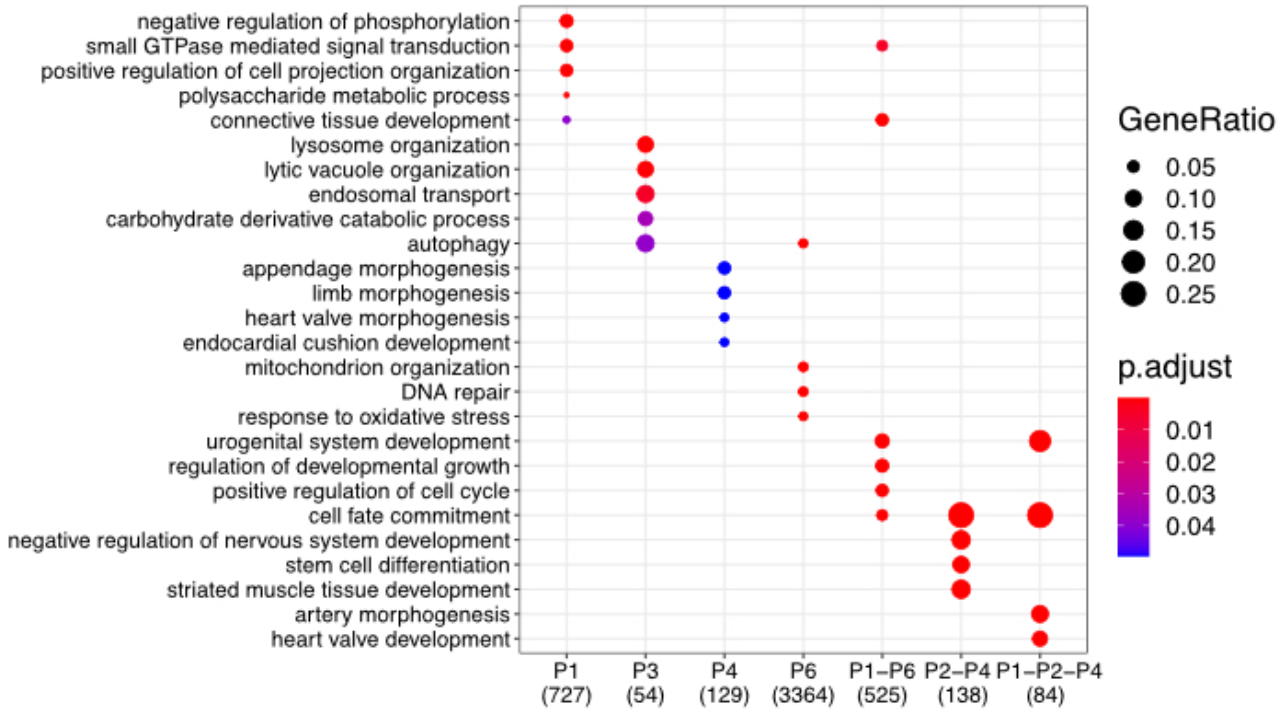

Figure 4.4.7: Gene ontology enrichment analysis of PCGFs unique and common targets genes

On the other hand, non-canonical PRC1 subcomplexes were associated with pathways related to cellular metabolism and trafficking (4.4.7).

Then, we investigated the role of PRC1 subcomplexes in transcriptional regulation by looking at whether PCGF proteins were associated with active or repressed chromatin regions. We compared ChIP-seq and RNA-seq data obtained from intestinal crypts from wildtype mice (Figure 4.4.8). In line with what was previously observed in ESc, PCGF3 and PCGF6, and to some extent PCGF1, were associated with active genes. In contrast, PCGF2 was associated with repressed genes, while PCGF4 with more permissive genes. However, PCGF1, PCGF2 and PCGF4 common targets were globally associated with silenced genes, suggesting that PCGF2 is the most important player in gene repression and chromatin compaction in adult intestinal cells (Figure 4.4.8).

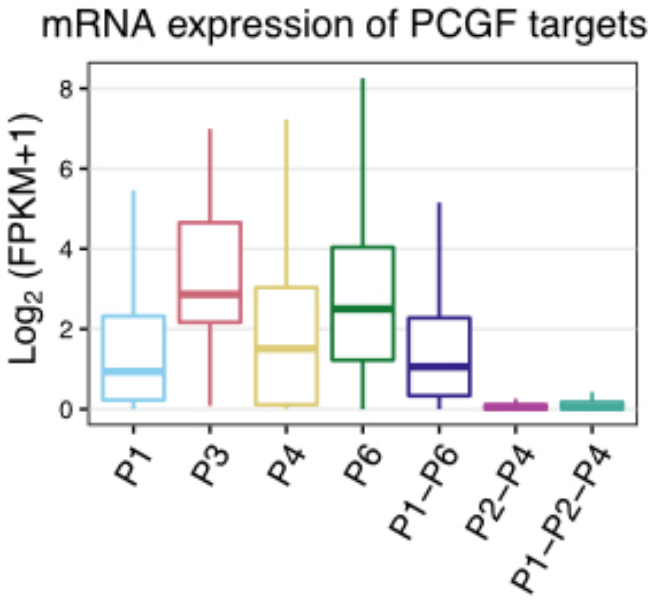

Figure 4.4.8: column graph representing mRNA expression of PCGFs unique and common target genes

All these data collected from wildtype and from single PCGF-KO intestinal cells suggested that PRC1.1, PRC1.2/4, PRC1.3/5 and PRC1.6 are dispensable for intestinal homeostasis. During cellular differentiation and cellular identity maintenance in the adult intestine, singular PCGF1, PCGF2/4, PCGF3/5 and PCGF6 are not required for chromatin compaction and transcriptional repression, maybe due to compensatory effects. In fact, data collected from ChIP-seq analysis indicated that some PCGFs, such as PCGF1, PCGF2 and PCGF4 might cooperate in the regulation of PRC1 activity and H2AK119ub1 deposition.

4.5 PCGF1, PCGF2, PCGF4 are indispensable for intestinal cell self-renewal and cellular identity

Given the findings outlined above, we generated a triple knockout mouse for PCGF1 and PCGF2/4 using the LGR5-GFP-ires-CreERT2/Rosa26Lox-stop-Lox LacZ strain and the VillinCREert2 strains to study the role of those PRC1 subcomplexes in ISCs and in differentiated cells, respectively. Moreover, to assess the role of non-canonical PRC1 in adult intestine, we also generated a quadruple knockout mouse for PCGF1/3/5/6 in the LGR5-GFP-ires-CreERT2/Rosa26Lox-stop-Lox LacZ mouse strain and started the breeding using the VillinCREert2 mouse model. We started to analyze the role of PCGF1/2/4 and PCGF1/3/5/6 in stem cell self-renewal by performing lineage tracing analysis with LacZ staining in LGR5-GFP-ires-CreERT2/Rosa26Lox-stop-Lox LacZ mice. Moreover, the experiment was also performed in Ring1a/b dKO mice, which were used as a positive control. It is important to clarify that the expression of *LGR5-GFP-ires-CreERT2/Rosa26Lox-stop-Lox LacZ* transgene is not homogenous among crypts and villi. It is known that the inactivation of the construct in ISC may occur, causing the heterogeneity of LacZ staining (Gehart and Clevers 2019).

To characterize the role of PCGF1/2/4 and PCGF1/3/5/6 during intestinal homeostasis, mice were sacrificed at 7, 15 and 30 days after tamoxifen administration. With this first experiment we confirmed the important role of the catalytic subunit RING1a/b in ISC maintenance and in tissue regeneration (4). Moreover, intestines derived from LGR5-PCGF1/3/5/6 qKO were normally stained for LacZ lineage tracing, suggesting that the combined depletion of PCGF1, PCGF3/5 and PCGF6 was not sufficient to phenocopy the absence of all PRC1 complexes observed upon depletion of RING1A/B. However, the loss of PCGF1, PCGF2 and PCGF4 together compromised the self-renewal of ISCs and the normal intestinal homeostasis. In fact, lineage tracing performed at 7 days from tamoxifen injections suggested a partial loss of Lacz-positive cells in Ring1a/b (as it had already been demonstrated) as well as in LGR5-PCGF1/2/4-KO, while LGR5-PCGF1/3/5/6 were normally stained compared to the control (Figure 4.5.1). In addition, at 30 days from tamoxifen injections, LGR5-PCGF1/3/5/6-KO-derived progeny were found in crypts and villi, while they were completely absent in LGR5-PCGF1/2/4-KO (Figure 4.5.1, Figure 4.5.2).

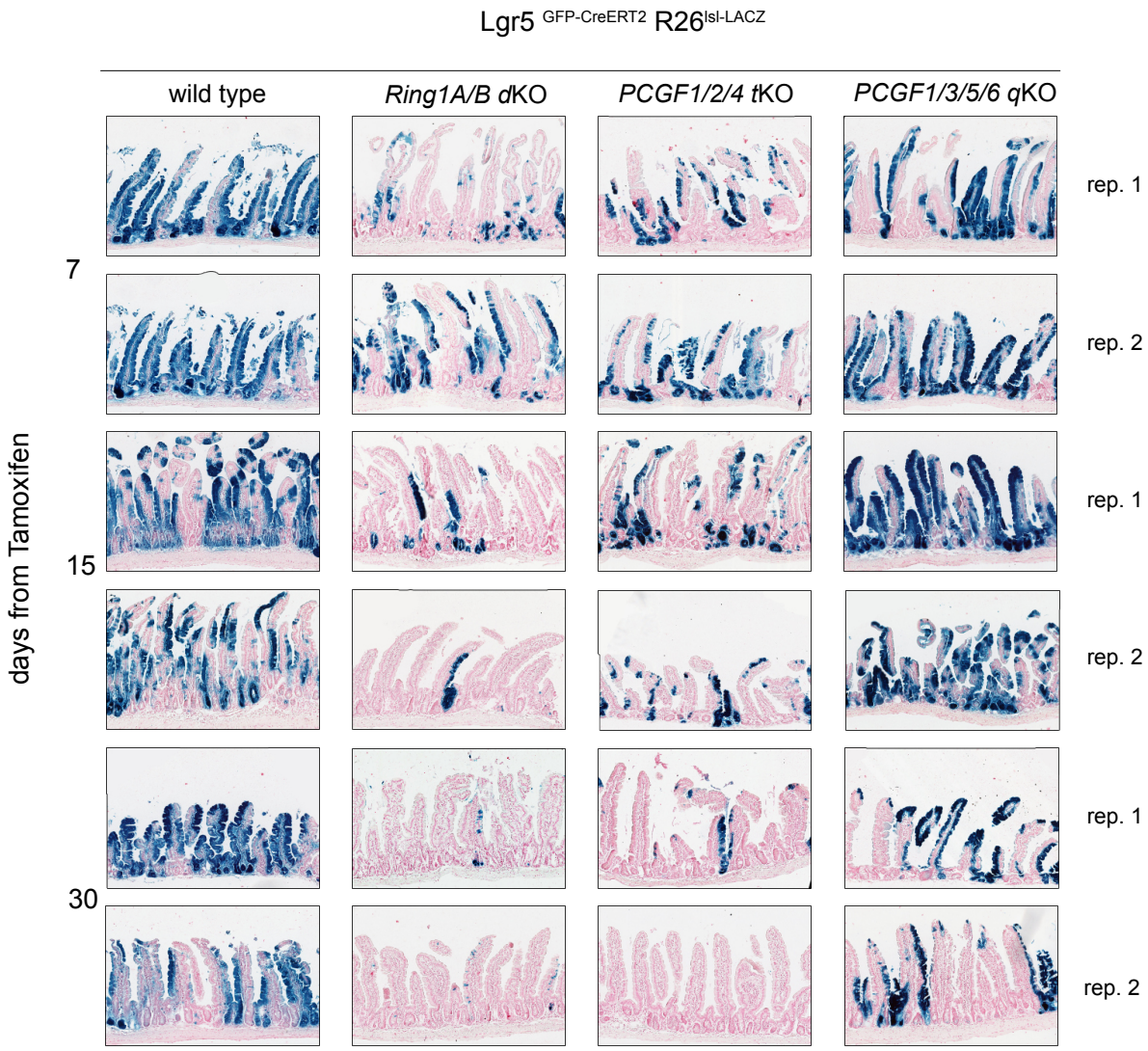

Figure 4.5.1 Lineage tracing analyses of LGR5-GFP-ires-CreERT2 /Rosa26Lox-stop-Lox LacZ at 7, 15 and 30 dpi. Lineage tracing analyses of Ring1a/b dKO, PCGF1/2/4 tKO and PCGF1/3/5/6 qKO, showing the effects of depletion of these subcomplexes on ISC self-renewal and differentiation.

However, mice lacking Ring1a/b and PCGF1/2/4 were viable thanks to the heterogeneity of the LGR5+ construct expression, which leads the intestine regeneration though the wildtype and counter selected ISC.

These data suggest that of PCGF1 and PCGF2/4 are necessary for ISC self-renewal and confirmed our hypothesis of PRC1.1, PRC1.2 and PRC1.4 compensation in adult intestine.

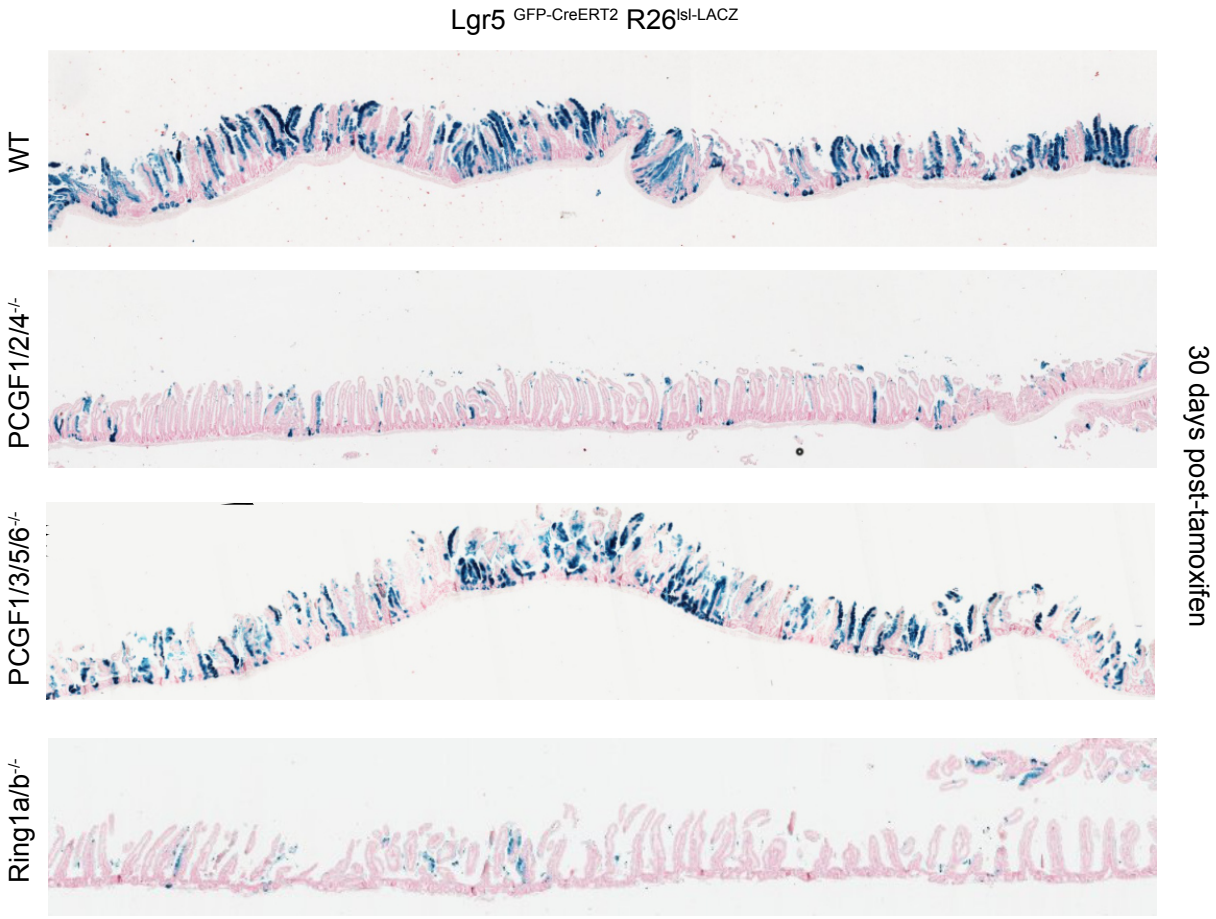

Figure 4.5.2 Lineage tracing analyses of LGR5-GFP-ires-CreERT2 /Rosa26Lox-stop-Lox LacZ at 30 dpi. Lineage tracing analyses of Ring1a/b dKO, PCGF1/2/4 tKO and PCGF1/3/5/6 qKO, showing the effects of depletion of these subcomplexes on ISC self-renewal and differentiation.

This was also confirmed looking at the LGR5-GFP+ intestinal stem cells numbers. In fact, in freshly prepared intestinal sections, the number of GFP-positive cells (i.e. LGR5+ cells) was strongly decreased in PCGF1/2/4 tKO, as well as in Ring1a/b dKO (Figure 4.5.3 A, B).

A

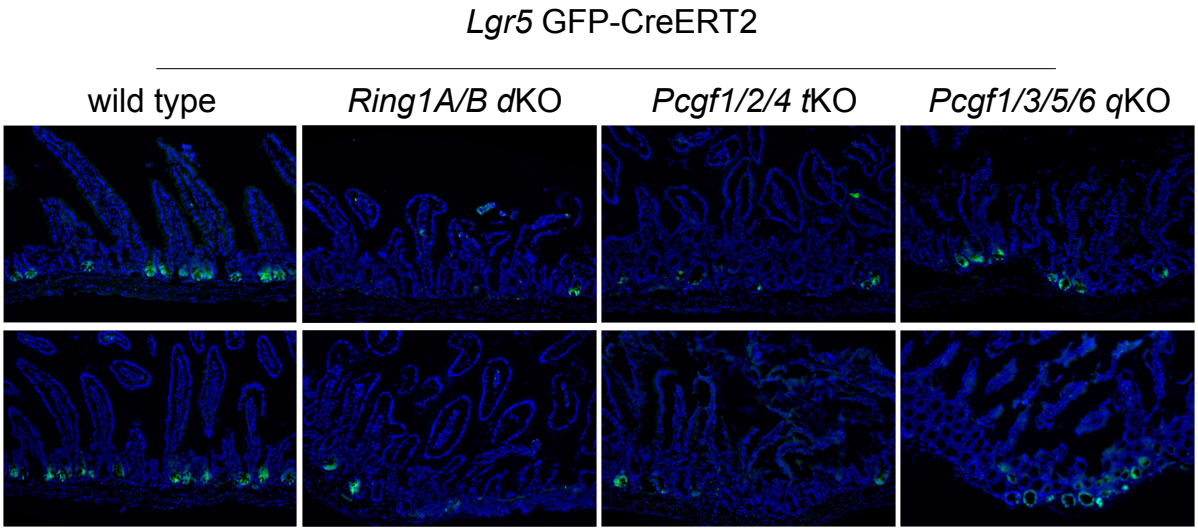

B

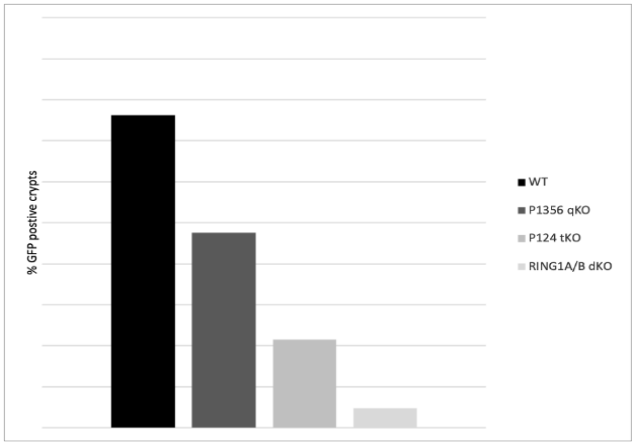

Figure 4.5.3 GFP signal in LGR5-GFP-ires-CreERT2 /Rosa26Lox-stop-Lox LacZ at 30 dpi.

A. Intestinal section stained for DAPI (nuclei) and GFP (LGR5 + ISC)
B. Quantification of percentage of LGR5-GFP+ ISC wild type, Ring1a/b KO, PCGF1/2/4 KO and PCGF1/3/5/6 KO mice

Then, to better characterize the cooperation between PCGF1 and PCGF2/4 in all intestinal cell types, we generated VIllinCREert2-PCGF1/2/4 tKO. First, we observed the general intestinal morphology and architectures of wildtype mice and of mice lacking PCGF1, PCGF2 and PCGF4. Intestines from

VillinCREert2 PCGF1/2/4 KO mice were shorter and thinner compared to intestines from wildtype mice (Figure 4.5.4 A). By histological analysis, we observed that the architecture of small intestine of mice lacking PCGF1/2/4 was compromised. Intestinal sections derived from PCGF1/2/4-deficient mice showed degenerating crypts starting from 7 days post tamoxifen administration. These shrinked crypts stained negatively for Ki67, thus confirming the alteration of the proliferation rate in PCGF1/2/4-KO (Figure 4.5.4 B).

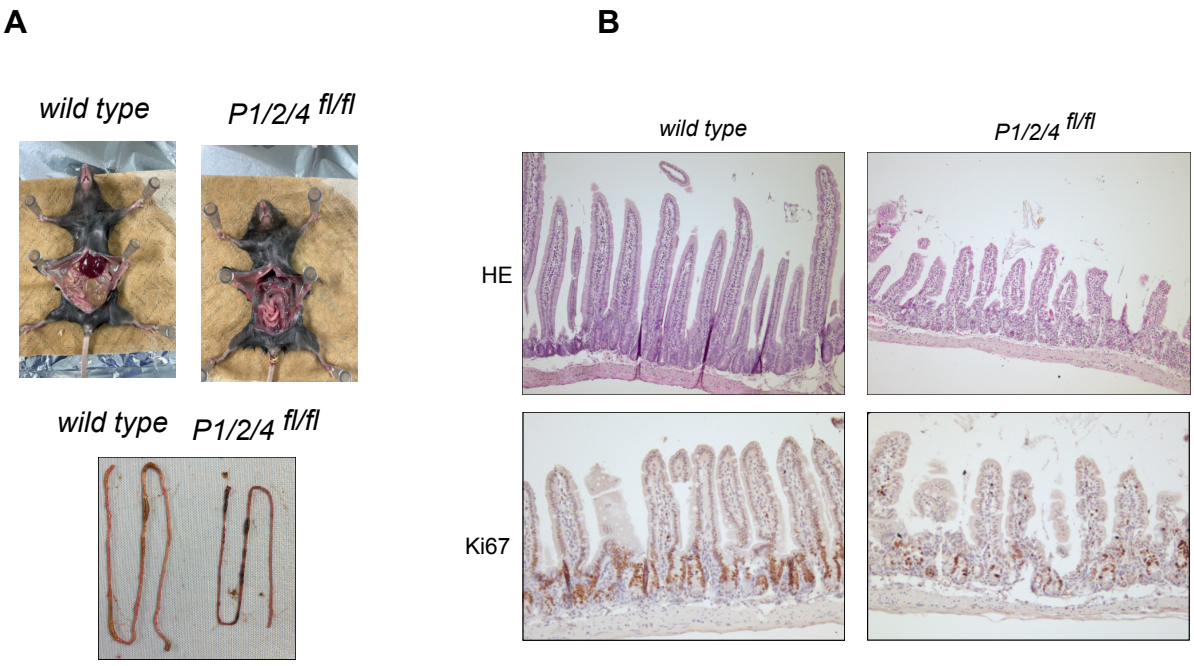

Figure 4.5.4: VillinCREert2 mouse model. PCGF1/2/4 depletion alters intestinal architecture

A. Pictures of intestine of wild type and KO mice
B. Histology analysis of wild type and PCGF1/2/4 KO intestinal section. Hematoxylin and Eosin (up) and Immunohistochemistry for Ki67 (bottom)

Moreover, we observed a decreased deposition of H2Aub upon loss of PCGF1/2/4 activity. These results were confirmed by immunofluorescence analysis showing that H2AK119ub1 was normally

deposited in crypt and villi, and that the inactivation of PRC1.1, PRC1.2 and PRC1.4 together strongly impaired not only its deposition but also the number of proliferative cells (Figure 4.5.5).

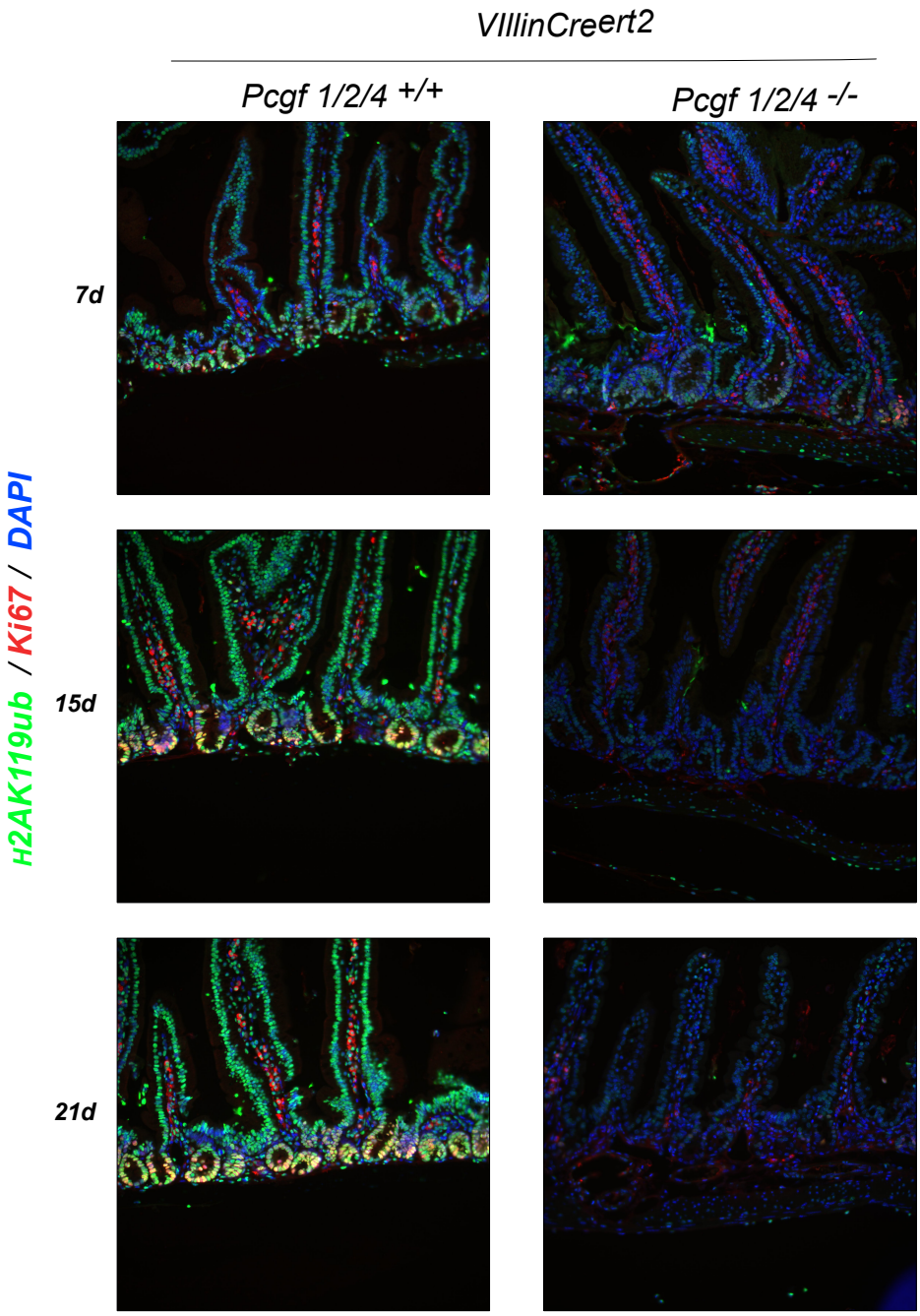

Figure 4.5.5 Immunofluorescence staining for H2AK119Ub1 level (green) and Ki67 (red) in VillinCREert2 wild type and PCGF1/2/4 KO at different time points.

As I mentioned before, the pool of cycling intestinal stem cell (ISC), present in the crypt bottom, maintain the high turnover of intestine epithelium (90), (95). These LGR5+ intestinal stem cell, first generate proliferating transient amplifying progenitor, which during homeostasis migrate from crypts to villi, and differentiate in absorptive and secretory intestinal cells (96), (97), (98). Among crypts-villi axis, the absorptive enterocyte is the most abundant cell type, follow by secretory Goblet cells, enteroendocrine cells, Paneth cells and Tuft cells. Paneth cells are the only secretory cell localized at the bottom of the crypts where they sustain LGR5+ ISC (90), (95). The differentiation of intestinal stem cells in secretory or absorptive cell types is mainly controlled by two important transcription factors, ATOH1 and HES1 respectively, which are regulated by NOTCH pathway (99), (100), (101). During differentiation, ATOH1 and HES1 controls the expression of specific master regulator for intestinal cell signature.

Maintaining transcription repression during differentiation is an important mechanism for cellular identity establishment and maintaining.

Given the ability of PRC1.1, PRC1.2 and PRC1.4 in controlling ISCs proliferation and self-renewal, we decided to investigate also the role of these subcomplexes in intestinal cell differentiation.

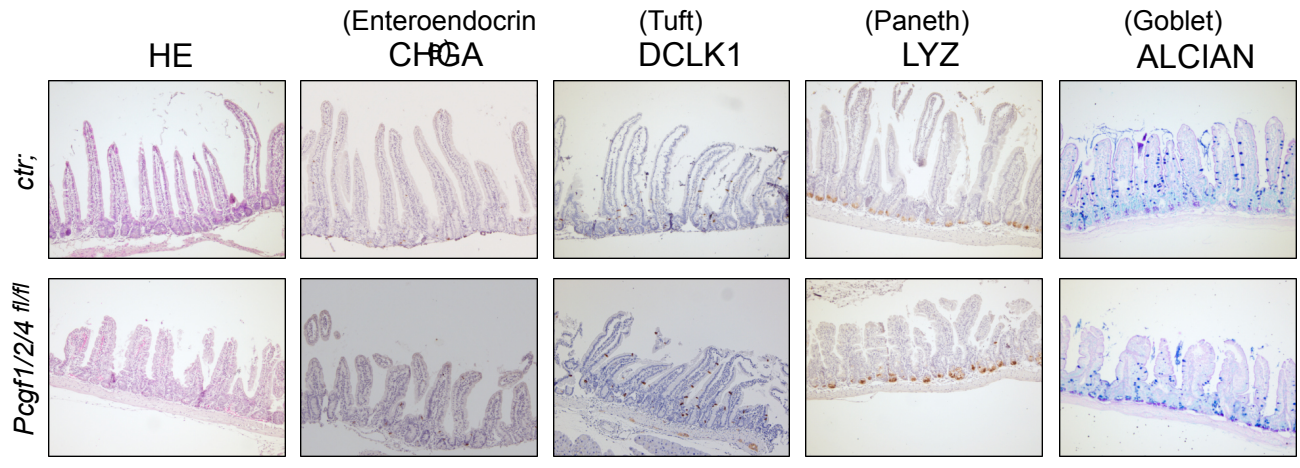

Figure 4.5.6 immunoistochemistry staining for CHGA (enteroendocrine), DCLK1 (Tuft), Lyzozyme (Paneth) and Alcian Blue (Goblet) in VillinCREert2 wild type and PCGF1/2/4 KO.

To do that, we performed immunohistochemistry analysis for specific markers for different intestinal cell types, in VillinCREert2 wildtype and VillinCREert2 PCGF1/2/4-KO intestinal sections. Immunohistochemistry analysis for Chromogranin A (Enteroendocrine cells), Dclk1 (Tuft cells), Lysozyme (Paneth cells) and Alcian Blue staining (Goblet cells) showed no differences in cellular differentiation upon depletion of PCGF1/2/4 in the whole intestine. All the intestinal secretory cell types were present in equal number and morphology (Figure 4.5.6). These results suggested that PRC1.1, PRC1.2 and PRC1.4 are not necessary in secretory cellular identity establishment and maintenance during homeostasis. However, when we looked at the differentiation rate of absorptive cells by performing Alkaline phosphate staining for enterocytes, we observed a complete abrogation of those cell types (Figure 4.5.7).

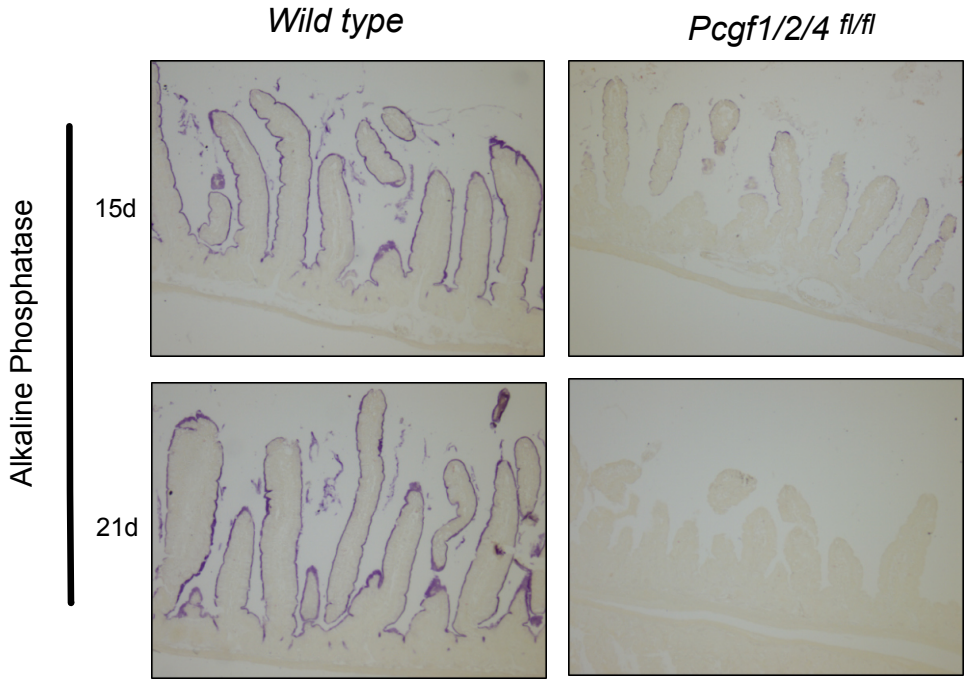

Figure 4.5.7: Alkaline phosphatase staining for enterocytes in VillinCREert2 and VillinCREert2 PCGF1/2/4 KO at 15 and 21 days.

Together, these data pointed to the important role of PCGF1, PCGF2 and PCGF4 in LGR5+ ISC self-renewal and in secretory lineage differentiation. Moreover, it is now clear that more than one subcomplex is involved in cellular identity maintenance.

To determine the molecular mechanism behind the regulation of PRC1.1, PRC1.2 and PRC1.4 in intestinal regeneration during homeostasis, we decided to investigate the contribution of those PRC1 subcomplexes in chromatin compaction and transcriptional regulation.

4.6 Loss of PRC1.1, PRC1.2 and PRC1.4 resulted in total RING1b chromatin displacement, loss of H2AK119ub1 and strong transcriptional reactivation

To elucidate the role of PCGF1, PCGF2 and PCGF4 proteins in intestinal homeostasis we decided to evaluate the PRC1 global activity by performing a chromatin immunoprecipitation for the H2AK119ub1 histone marker in intestinal crypts derived from wildtype and PCGF1/2/4 tKO.

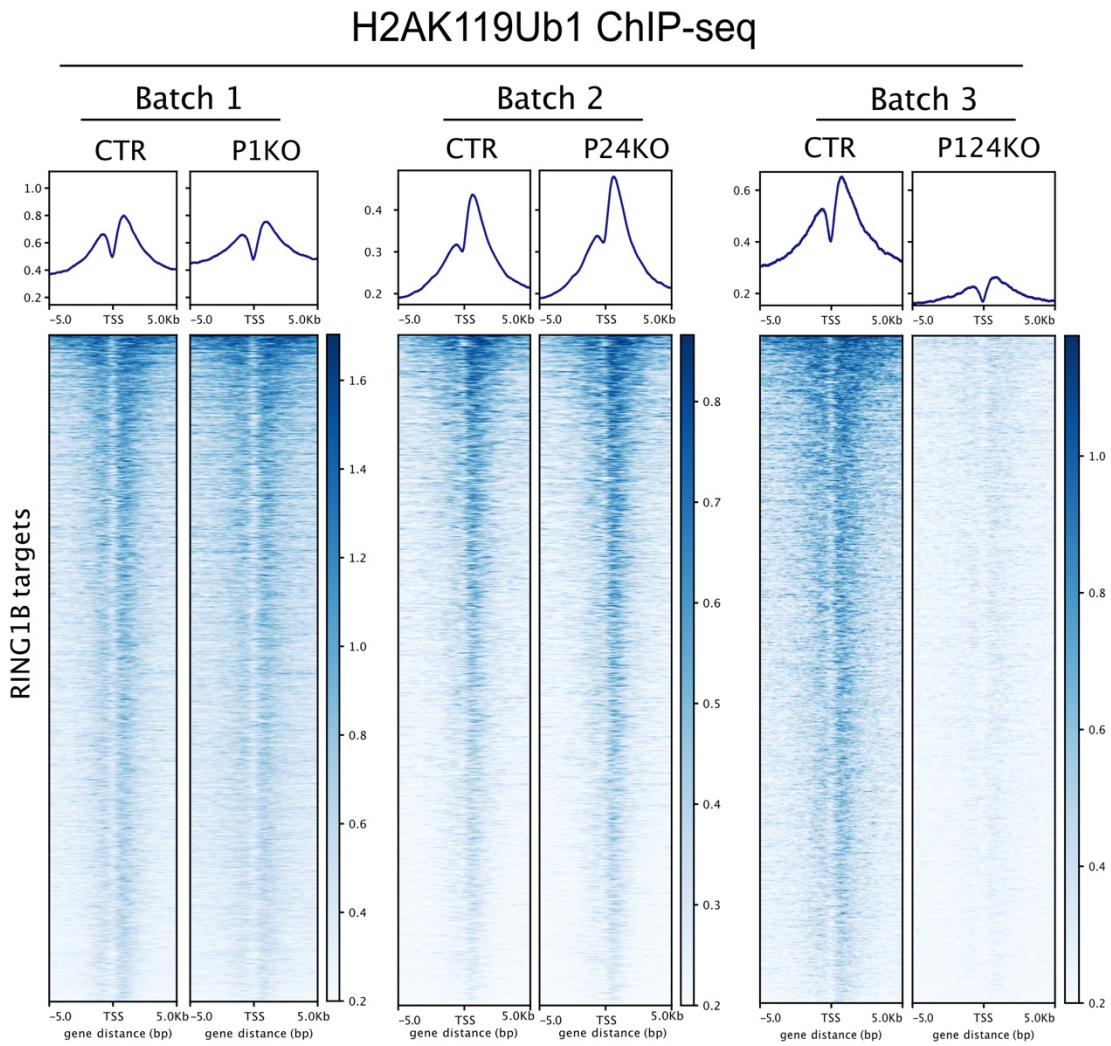

Figure 4.6.1: Heatmap representing normalized H2AK119ub1 CHIP-seq intensity of +/- 5Kb from TSS of Ring1b target genes in intestinal Crypts from PCGF1, PCGF2/4 and PCGF1/2/4 KO.

From ChIP-seq analysis we confirmed that PCGF1 and PCGF2/4 alone, did not alter the H2AK119ub1 on Ring1b sites. However, interestingly we found that in absence of PCGF1, PCGF2 and PCGF4 together, PRC1 activity was completely compromised and the deposition of the H2AK119ub histone marker was abrogated (Figure 4.6.1).

Following this finding we speculated that the PCGF1/2/4 module preserves H2AK119ub1 deposition in intestinal crypts.

Next, we quantified the binding of RING1b at Ring1b sites in the PCGF1/2/4 tKO, and we compared it with binding of Ring1b in PCGF1-KO and PCGF2/4-KO. By ChIPseq analysis, we confirmed

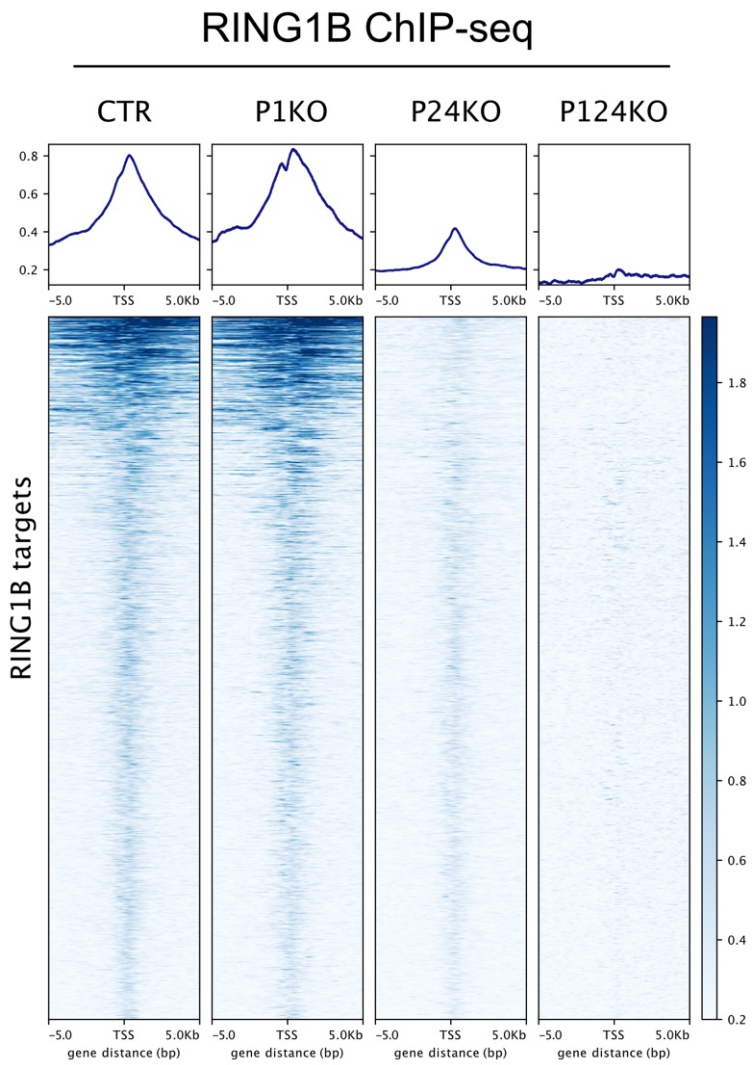

Figure 4.6.2: Heatmap representing normalized H2AK119ub1 CHIP-seq intensity of +/- 5Kb from TSS of Ring1b target genes in intestinal Crypts from PCGF1, PCGF2/4 and PCGF1/2/4 KO.

that the association of RING1b in PCGF1-KO was stable, and that it was partially lost in PCGF2/4. However, RING1b binding was completely lost upon depletion of PCGF1 and PCGF2/4 together, suggesting full compensation between PRC1.1, PRC1.2 and PRC1.4 in chromatin remodeling and transcriptional repression in adult somatic cells (Figure 4.6.2).

Moreover, by looking at H3K27me3 deposition on Ring1b site, we found that PRC2 activity was partially compromised by the loss of PCGF2/4 and this was more evident upon depletion of PCGF1 and PCGF2/4 (Figure 4.6.3). All these data pointed to the important role of PCGF1 together with PCGF2/4 in chromatin remodeling, by controlling PRC1 activity and partially PRC2 activity.

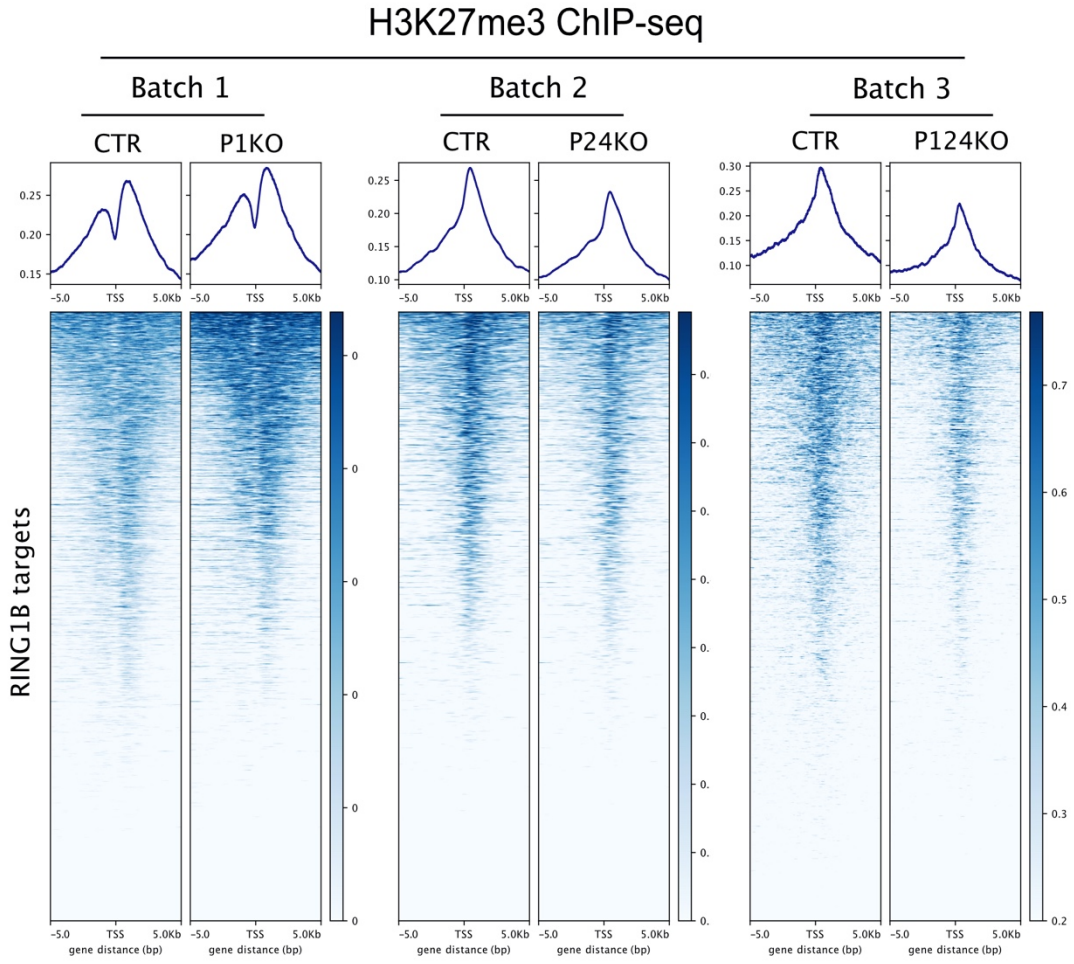

Figure 4.6.3: Heatmap representing normalized H3K27me3 CHIP-seq intensity of +/- 5Kb from TSS of Ring1b target genes in intestinal Crypts from PCGF1, PCGF2/4 and PCGF1/2/4 KO.

We next assayed the transcriptional control of PCG1/2/4 cooperation in intestinal cells by RNA sequencing analysis, and by comparing those results with results already obtained in RING1a/b-KO, PCG1-KO, and PCGF2-KO. Principal component analysis (PCA) from transcriptional profiles, showed that the transcriptome from VillinCREert2 PCGF1/2/4 tKO cells was largely altered compared to control, or Ring1a/b KO, PCGF1 KO, and PCGF2/4 KO (Figure 4.6.4). In intestinal cells lacking PCGF1/2/4 there was a massive upregulation of genes compared to controls.

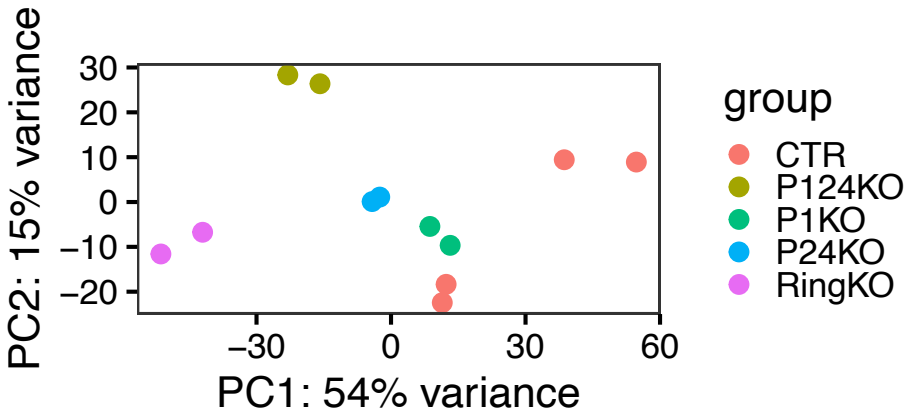

Figure 4.6.4: Principal component analysis of transcriptome profiles of Ring1a/b KO, PCGF1 KO, PCGF2/4 KO and PCGF1/2/4 KO intestinal cells at 15 days prost tamoxifen administration

We found 665 downregulated genes, probably due to a secondary effect, and 1052 upregulated genes (Figure 4.6.5). The observation of the absence of transcriptional de - repression in VillinCREert2 PCGF1, and in VillinCREert2 PCGF2/4, together with the observation of the total transcriptional de - repression in VillinCREert2 PCGF1/2/4 KO, confirmed the full compensation of PCGF1 in PCGF2/4 KO.

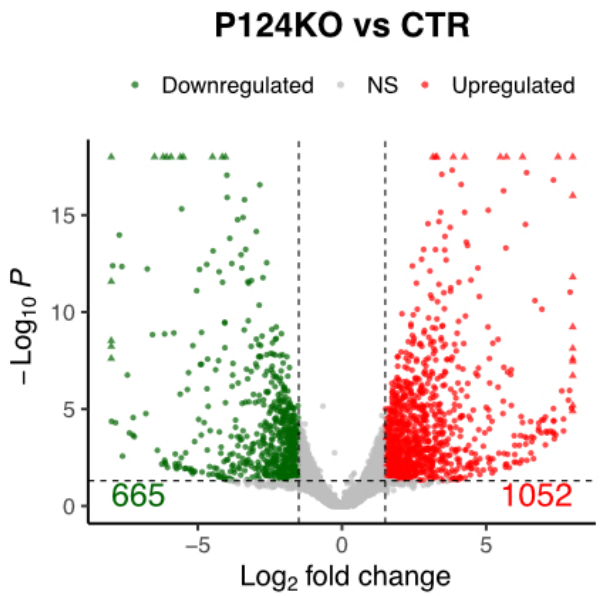

Figure 4.6.5: Volcano blot of deregulated genes In VillinCREert2 PCGF1/2/4 tKO derived intestinal cells. In green downregulated genes, in red upregulated genes.

Gene ontology analysis of deregulated genes showed enrichment of pathways correlated with various developmental processes, and cell cycle, highlighting the important role of PRC1.1, PRC1.2 and PRC1.4 in establishment of cellular identity and maintenance, as well as normal cellular self-renewal rate during homeostasis (Figure 4.6.6.).

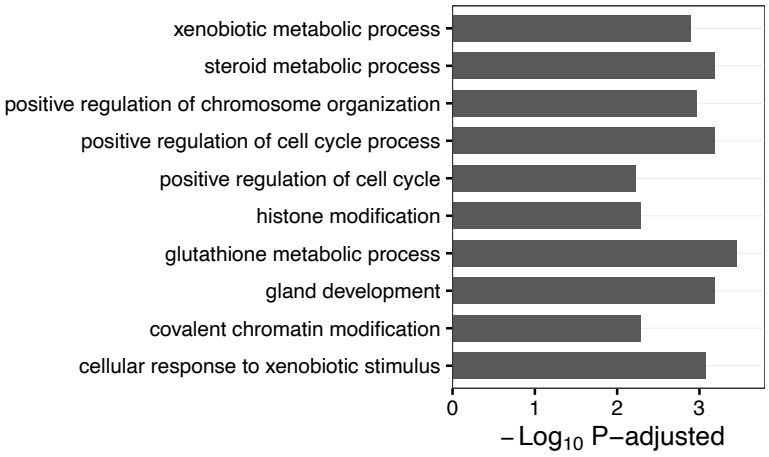

Figure 4.6.6: Gene ontology analysis of deregulated genes in PCGF 1/2/4 KO adult intestinal cells.

Then we crossed data from RNAseq and ChIPseq analysis derived from intestinal cells of RING1b KO, PCGF1 KO, PCGF2/4 KO and PCGF1/2/4 KO. We first looked at the expression level of RING1b target genes in PCGF1/2/4 tKO intestinal cells, PCGF1 and PCGF2/4 KO. We confirmed that the loss of PCG1, and PCGF2/4 alone was not sufficient to reactivate the expression of RING1b target genes, but that the concomitant removal of PCGF1, PCGF2 and PCGF4 lead to reactivation of almost all PRC1-associated genes. (Figure 4.6.7).

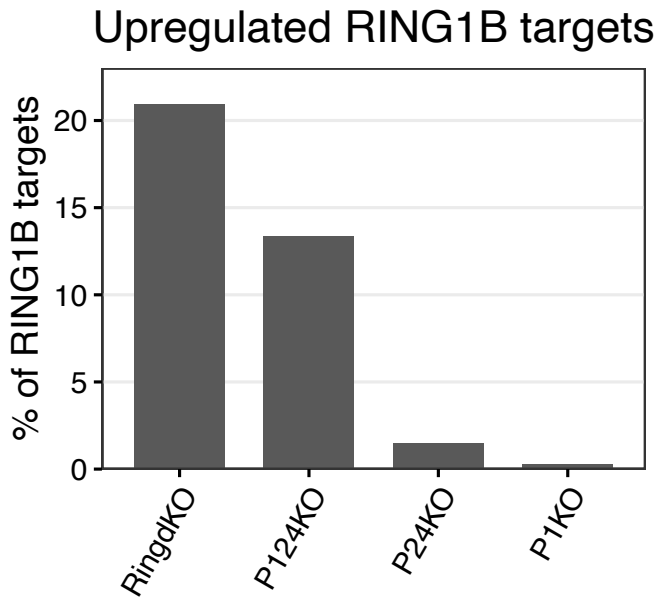

Figure 4.6.7: Column plot of percentage expression of RING1b associated genes in RING1b KO, PCGF1 KO, PCGF2/4 KO and PCGF1/2/4 KO

The expression of target genes of PCGF3, PCGF4 and PCGF6, was unchanged in intestinal cells lacking Ring1b, PCGF1, PCGF2/4 and PCGF1/2/4. Instead, the expression of common target genes of PCGF2 and PCGF4, was completely unaffected in PCGF2/4 KO, but it was reactivated upon depletion of PCGF1/2/4. Moreover, loci that were bound by PCGF1, PCGF2 and PCGF4, were associated with transcriptional derepression only upon depletion of PCGF1 in combination with PCGF2/4, which was very similar to the derepression observed in RING1a/b KO (Figure 4.6.8).

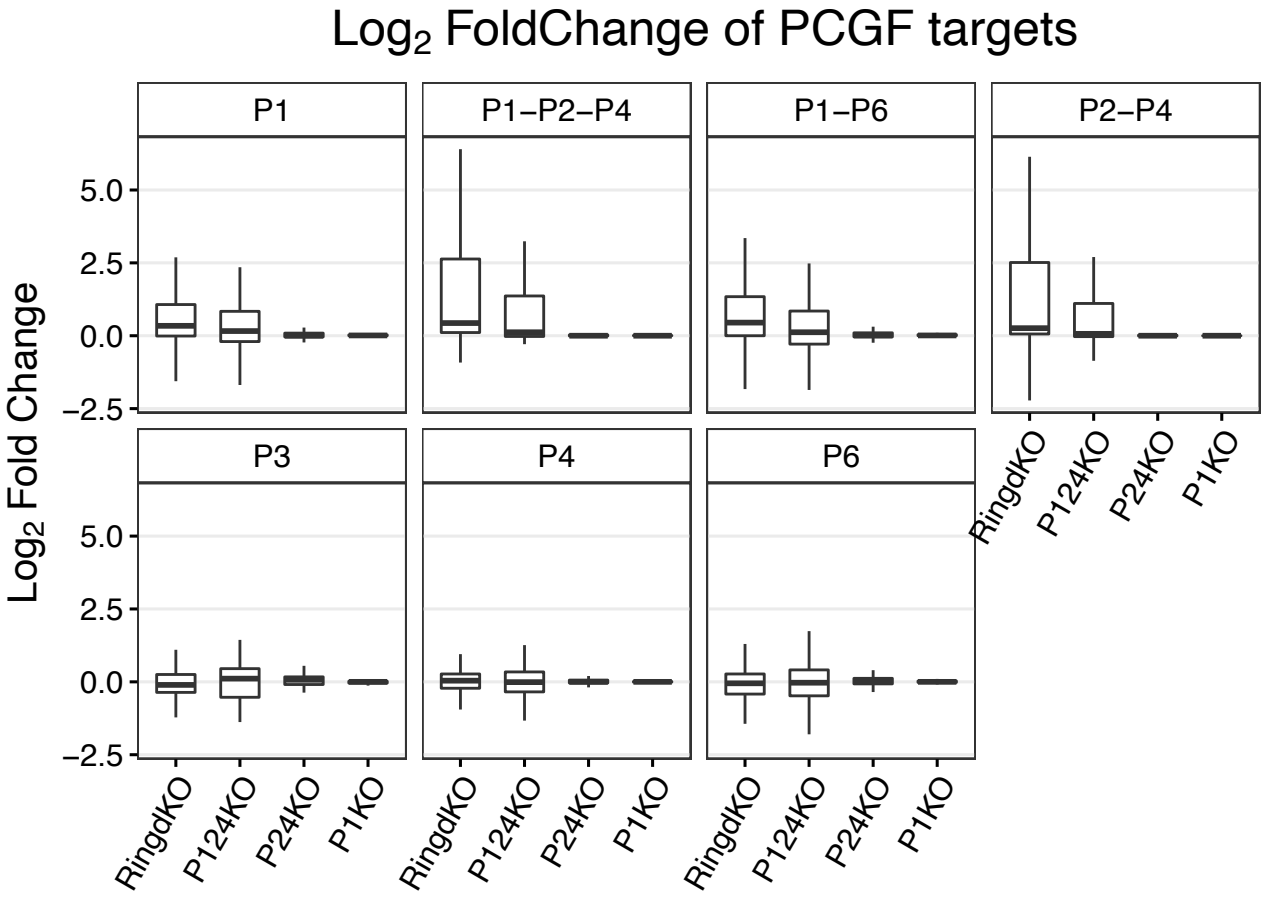

Figure 4.6.8: Boxplot showing the expression of common or unique PCGFs target genes in adult intestinal cells upon depletion of RING1b, PCGF1, PCGF2/4 and PCGF1/2/4

These findings confirmed that PCGF1 and PCGF2 compensate each other in transcriptional repression. Surprisingly, in contrast with what we observed in ESc, combined loss of PCGF1/2/4 lead not only to RING1b displacement, H2AK119ub deposition alteration, but in adult intestinal cell it also induced a significant transcriptional reactivation. These means that PCGF proteins may play different roles in different cell types, depending also on their differentiation state.

Here, we uncovered the activities of PRC1 subcomplexes in adult intestinal cells, providing a first analysis on their functional proprieties in transcriptional repression during intestinal homeostasis. Taken together all the histology and mechanism data, we speculated that single PCGF proteins are

dispensable for intestinal cell self-renewal and differentiation, and that single PCGFs do not control PRC1 globally activity. However, we found that PCGF1, PCGF2 and PCGF4 together are indispensable during intestinal regeneration and maintenance of normal intestinal architecture. PRC1.1, PRC1.2, and PRC1.4 are necessary for PRC1 activity and for transcriptional repression.

In ESc, despite the loss of RING1b binding and the lack of H2Aub, the reactivation of transcription is possible only in absence also of PCGF6. However, in intestinal cell we demonstrated that PCGF6 is dispensable for RING1b bind and for transcriptional reactivation. Moreover, we observed that PCGF6 is not associated with always with RING1b, suggesting an alternative role of PRC1.6 in adult cells.

These funding pushed us to better investigate the interesting role of PCGF6 in intestine.

4.7 PCGF6 display a non-canonical chromatin association in intestinal cells compare to ESC

In ESc, PCGF6 plays an important role in transcriptional control. We have already demonstrated that PCGF6 can exists in complex with RING1a/b defining PRC1.6 subcomplex, or without Ring1a/b, and that RING1a/b activity is dispensable for PCGF6 complex assembly and chromatin recruitment (2). In contrast, RING1b binding and H2Aub1 deposition was very low in PCGF6 unique target sites. Moreover, in ESc, PCGF6 unique target shows a "permissive" transcriptional state (2). In undifferentiated cells, transcriptional activation, and loss of chromatin compaction occurs in absence of PCGF1, PCGF2, PCGF4 and PCGF6 together. However, in this work we speculated that in adult cells, the lack of PCGF1/2/4 is sufficient to Ring1b displacement, H2Aub1 lost and transcriptional reactivation. Indeed, in intestine, PCGF6 seems to play a completely different role form other PCGFs.

Then we decide to investigate the different biological functions for PRC1.6 in undifferentiated and differentiated cells. To do that we are using mouse model carrying Cre recombinase, that allow us the depletion of PCGF6 from the whole intestinal epithelium. In particular, we used AhCRE; PCGF6 flox/flox and VillinCREert2; PCGF6 flox/flox mice.

We have initially analyzed the differences in chromatin association of PRC1.6 in ESc and intestinal cells. We found that in differentiated cells, PCGF6 binds both CpG negative and positive region. Instead in ESc, as we have already reported (2), PCGF6 is mainly associated with CpG rich island (Figure 4.7.1 A). In intestinal cells we have also observed that PCGF6 shown specific binding on chromatin. In fact, on a total amount of 4385 target genes, 3691 were unique for PCGF6, and not for other PCGF proteins, except for a small amount of co-occupancy with PCGF1 (Figure 4.7.1 B). This was different from what we have already reported in ESc, where PCGF6 binds not only unique target gens, but share also, target gens with PCGF1 and PCGF2 (2).

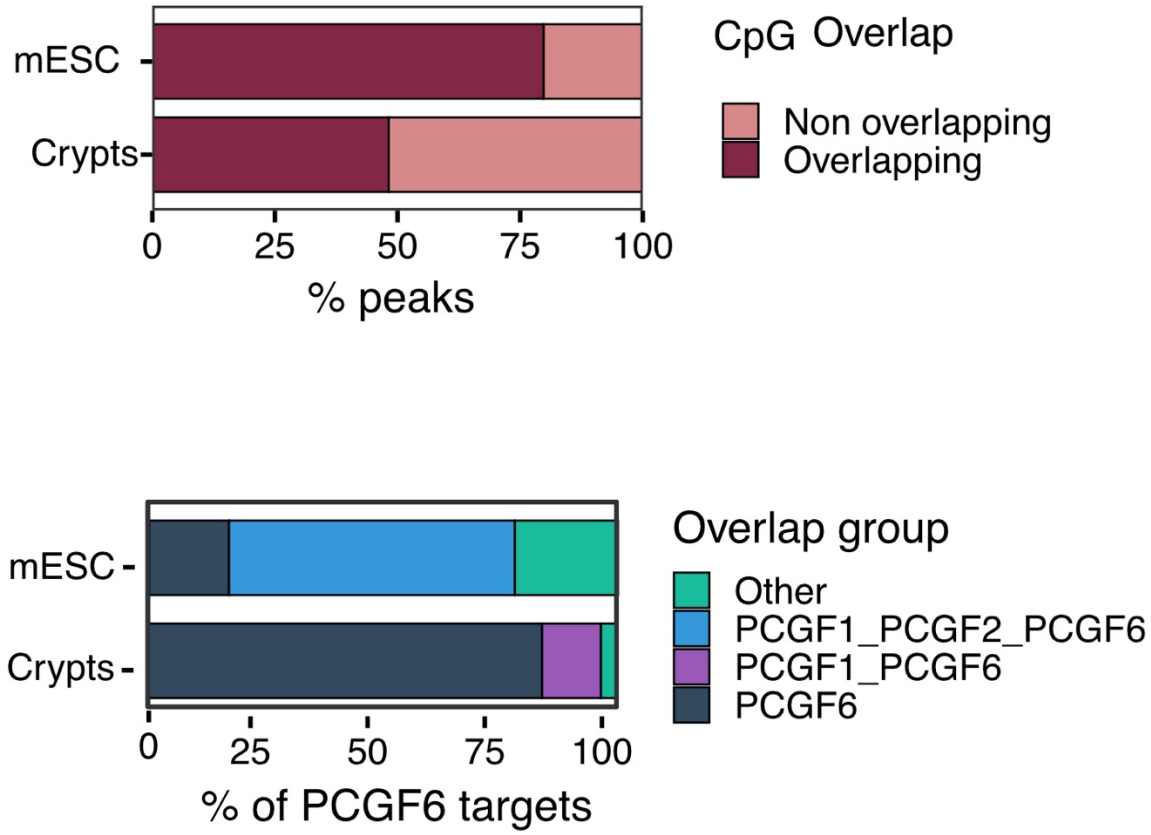

Figure 4.7.1: Differences of PCGF6 distribution in intestinal cells and ESc.

A. Diagram showing the percent of PCGF6 targets at CpG positive and negative chromatin regions.
B. Column graph representing the specificity of PCGF6 and the very low co-occupancy on chromatin with other PCGF proteins.

These first observations confirm our hypothesis of different role for PCGF6 in distinct type of cells. Moreover, in both ESc PCGF6 as well as other `PCGFs is localized principally at promoter region (2). Instead, in intestinal cells PCF6 is surprisingly associated in equal amount at both promoter and distal chromatin regions (Figure 4.7.2 B). Analysis of Motif enrichment at PCGF6 site shows that PRC1.6 in adult cells binds specific E-BOX/bHLH-ZIP region, as was observed also in ESc (Figure 4.7.2 A) (2). The recruitment of PCGF6 on DNA by E-BOX recognition was observed both at promoter and also at intergenic region (Figure 4.7.2 C).

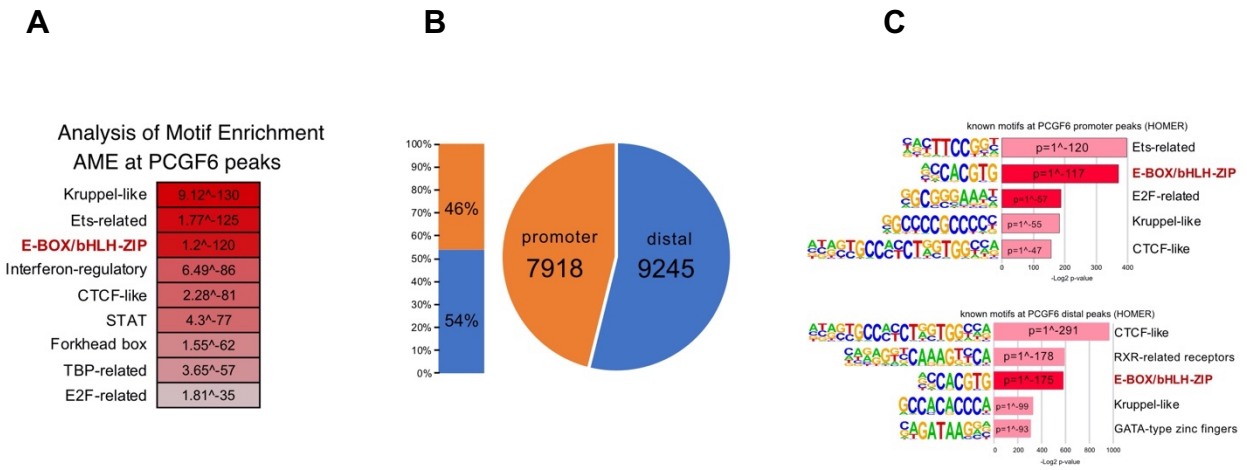

Figure 4.7.2: DNA localization of PRC1.6 in adult intestinal cells

A. Motif discovery analysis discovery performed underneath the summit of PCGF6 peaks globally
B. Column graph representing the specificity of PCGF6 and the very low co-occupancy on chromatin with other PCGF proteins.
C. Motif discovery analysis discovery performed underneath the summit of PCGF6 peaks on promoter and intergenic regions

Then, we performed ChIP sequencing analysis for Ring1b, for H2Aub1 and H3K27me3 histone markers in wild type and also in PCGF6 KO intestinal cells. As previously mentioned, the global binding of Ring1b on chromatin was unaltered in cells lacking PCGF6, as well as H2Aub1 and H3K27me3 deposition (Figure 4.7.3).

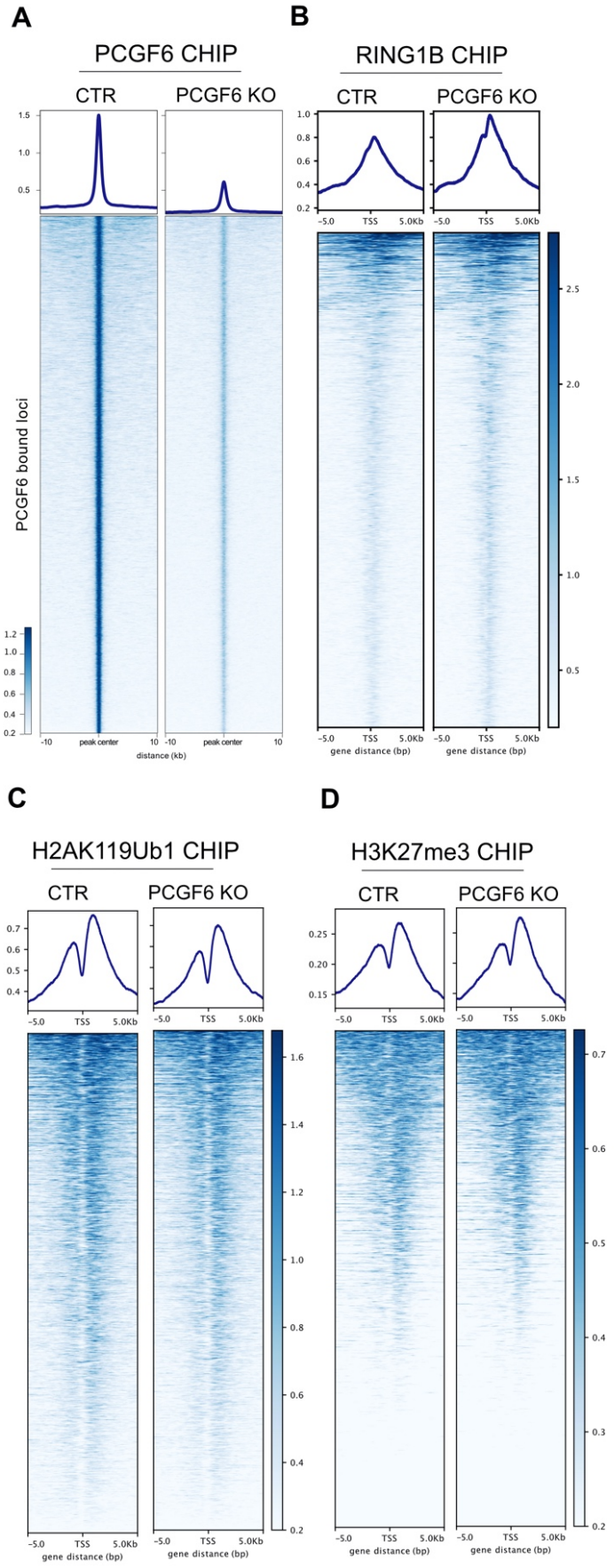

Figure 4.7.3: Heatmaps of ChIp - sequencing analysis on adult intestinal cells.

A. Heatmap representing normalized PCGF6 CHIP-seq intensity of +/- 5Kb from TSS of PCGF6 loci
B. Heatmap representing normalized Ring1b CHIP-seq intensity of +/- 5Kb from TSS of Ring1b target genes in intestinal Crypts
C. Heatmap representing normalized H2AK119ub1 CHIP-seq intensity of +/- 5Kb from TSS of Ring1b target genes in intestinal Crypts
D. Heatmap representing normalized H3K27me3 CHIP-seq intensity of +/- 5Kb from TSS of Ring1b target genes in intestinal Crypts

Then we looked at the presence of Ring1b, and H2Aub1 on PCGF6 binding sites by overlapping the targets of each. As expected at the majority of Ring1b targets, was present H2Aub1 histone mark. However, only 1241 PCGF6 targets were in common with RING1b, and only on 910 of those was also observed H2Aub1 deposition (Figure 4.7.4). Interestingly, we have found that PCGF6 showed 13070 specific and unique targets, in which there was no presence of Ring1b binding nor PRC1 activity (Figure 4.7.4). This data suggested us a novel role of PCGF6 in intestinal cells that was not correlated with PRC1.

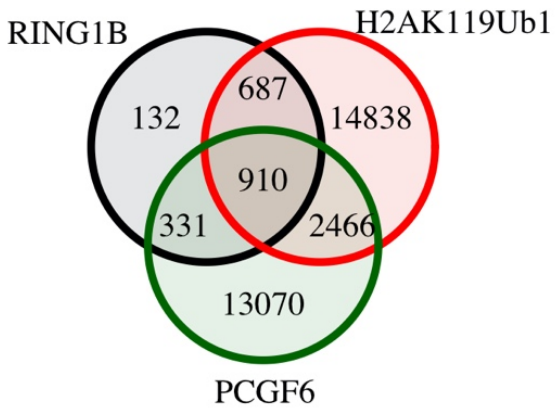

Figure 4.7.4: Vann diagram showing the overlap between Ring1b targets, PCGF6 targets and H2AK119ub1 positive loci in adult intestinal cells

4.8 PCGF6 Knock Out do not show apparent intestinal homeostasis alteration

Given the peculiarity of PRC1.6 role in adult intestinal cells, we decided to investigate the function of PCGF6 in tissue homeostasis. To do that we took advances of the use of *LGR5-GFP-ires-CreERT2/Rosa26Lox-stop-Lox LacZ* to delete PCGF6 in ISC, AhCRE and VillinCREert2 that allow us the deplation of PCGF6 from all intestinal cell types.

First, we performed LacZ staining of intestinal section derived from LGR5+ wild type and LGR5+ PCGF6 KO mice, we did not observe any differences in ISC proliferation and self-renewal, and the number of stained cells where the same in absence of PCGF6 among crypts-villi axis. As previously mentioned, by using AhCre PCGF6 KO mouse model we observed that, intestinal lacking PCGF6 normal architecture and morphology, meaning that the PRC1.6 is dispensable during intestinal homeostasis (Figure 4.8.1).

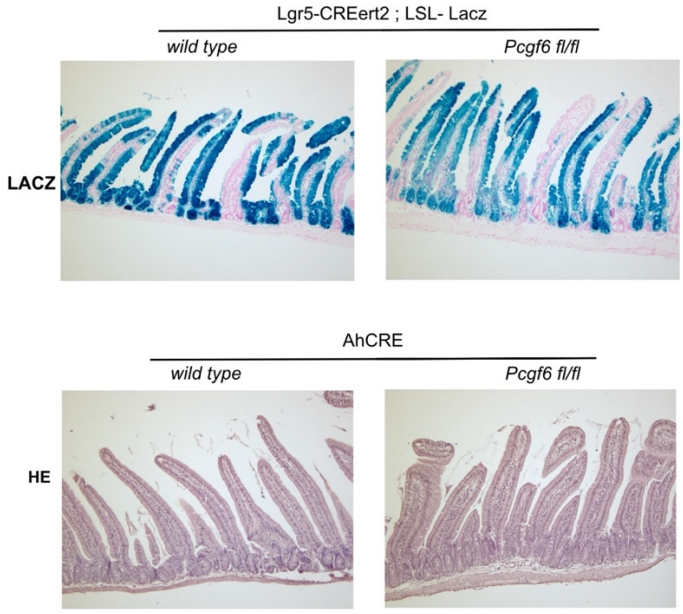

Figure 4.8.1: Histology of Duodenum from wild type and PCGF6 KO mice. Beta-Galactosidase reaction on intestinal sections from LGR5-GFP-ires-CreERT2/Rosa26Lox-stop-Lox LacZ wild type and PCGF6 KOs mice (upper panel). Hematoxylin and Eosin of duodenum sections (bottom panel).

Second, we decided to assess the role of PCGF6 in intestinal cell differentiation, by using VIllinCREert2 mouse model in which the protein is deleted not only in ISC but also from the other intestinal cell types. Wild type and PCGF6 KO mice were sacrificed at 15 days form tamoxifen administration, and intestinal sections were collected. On those, we performed immunohistochemistry against all the different cell population that compose the intestine.

In intestine lacking PCGF6, Paneth, enteroendocrine and Goblet cells were present as in the wild type intestine (Figure 4.8.2).

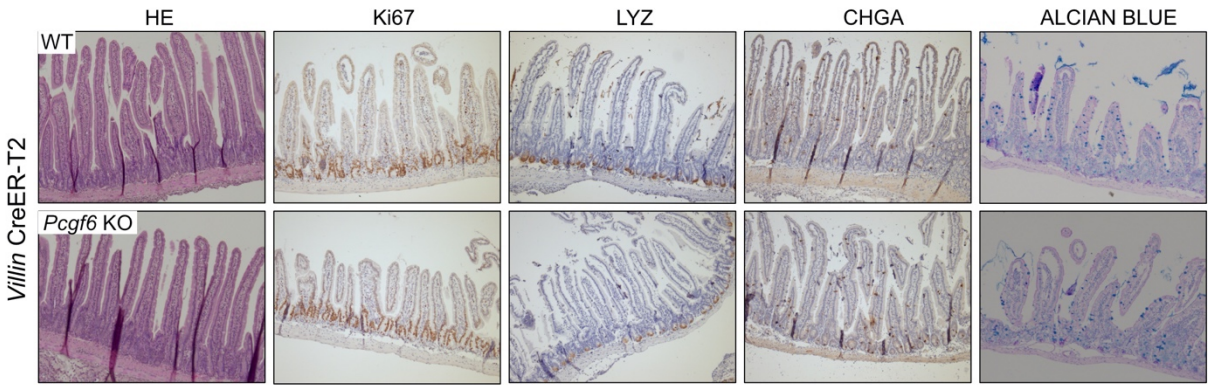

Figure 4.8.2: Immunohistochemistry staining for Ki67 (proliferation marker), LYZ (Paneth cells), CHGA (enteroendocrine cells), Alcian Blue (Goblet cells) in VillinCREert2 and VillinCREert2: PCGF6 KO derived intestinal sections.

4.9 PCGF6 depletion leads accumulation Intestinal Tuft cells

To investigate the role of PCGF6 in intestinal homeostasis we performed also immunohistochemistry analysis for DCLK1, a specific marker for intestinal Tuft cells, in AhCRE and also in VillinCREert2 mouse model (both allows the depletion of PCGF6 in the whole intestine). Tuft cells are a very rare cell population and represent only the 1% of the epithelium. Very interesting, we found that intestine

lacking the expression of PCGF6, accumulated specifically intestinal Tuft cells. We quantified, the differences in Tuft cells number in both the mouse model, by counting the number of DCLK1 positive cells for number of intestinal crypts. In AhCRE PCGF6 KO, DCLK1+ Tuft cell number was increased 5 times more compare to the wild type, and this was even higher in VIllinCREert2 PCGF6 KO (Figure 4.9.1).

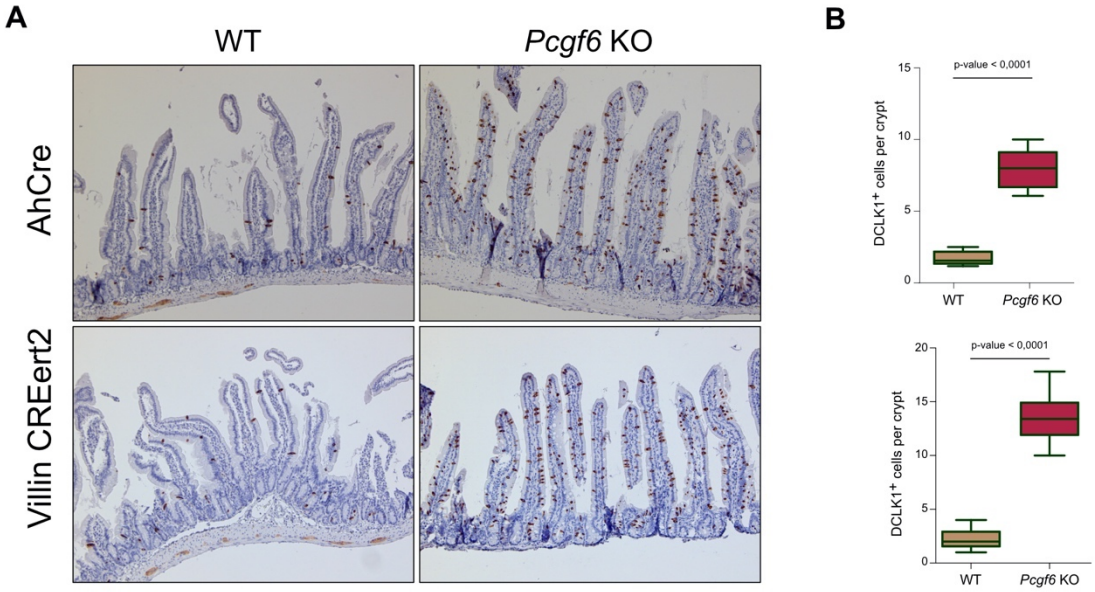

Figure 4.9.1: Immunohistochemistry staining for DCLK1 in intestinal sections.

A. Immunohistochemistry staining for DCLK1 (Tuft cells) in AhCRE wild type and AhCRE PCGF6 KO (upper panel) and VillinCREert2 and VillinCREert2: PCGF6 KO derived intestinal sections.
B. Quantification of DCLK1+ Tuft cell in AhCRE wild type and AhCRE PCGF6 KO (upper panel) and VillinCREert2 and VillinCREert2: PCGF6 KO

The accumulation of Tuft cells was also observed by performing Western blot analysis of total protein extraction from wild type and PCGF6 KO crypts (Figure 4.9.2 A). To confirm the accumulation of Tuft cells, we also checked at mRNA level of others cell markers such Pou2f3, Ptgs1, Gli1b, Gnat3 by performing RT-qPCR (Figure 4.9.2 B). With these results we have hypothesized that PCGF6 controls Tuft cell differentiation during intestinal homeostasis.

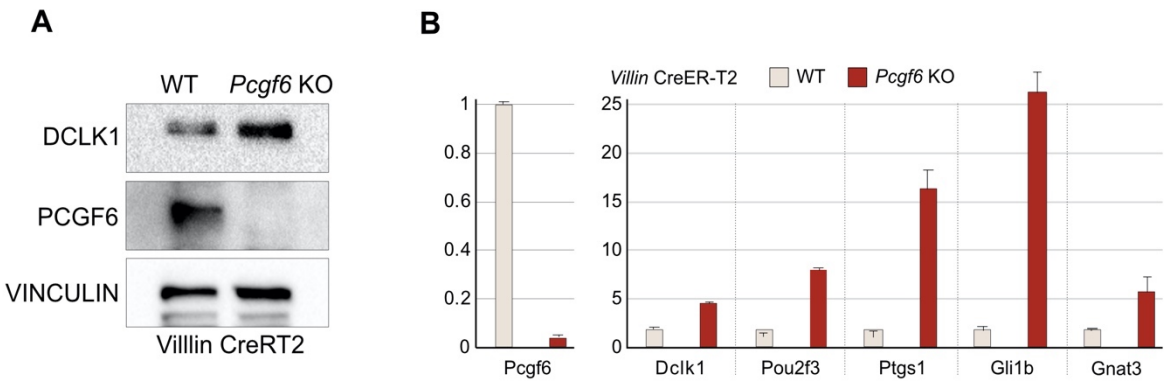

Figure 4.9.2: Tuft cells accumulation in PCGF6 KO intestine.

A. DCLK1 protein levels in VillinCREert2 and VillinCREert2; PCGF6 KO crypts
B. mRNA levels of Tuft cell specific markers in VillinCREert2 and VillinCREert2: PCGF6 KO crypts

4.10 PCGF6 directly controls Tuft cell signature, including master regulator Pou2f3, and predispose for immunogenic response in a cell autonomous mechanism

Then we assessed whether PCGF6 controlled Tuft cell hyperplasia in a cell autonomous event. In order to do this, we grew organoids from intestinal crypts derived from wild type and PCGF6 KO mice. Also in this case, the experiment was performed in both mouse models, in order to strengthen the results. We confirmed the maintenance of PCGF6 depletion, and that the counterselection did not occurs after plating, by performing RT-qPCR on RNA extraction from organoids. Then, we investigated the Tuft cells accumulation in organoids by performing immunofluorescence analysis for DCLK1 positive cells and performing RT-qPCR on RNA extraction from organoids. We have found that organoids growth from intestinal crypts derived from PCGF6 KO mice were rich of Tuft cells compare to wild type, and that DCLK1 genes was upregulated in those organoids (FIGURE

4.10.1). All this data downright that the accumulation of Tuft cells in intestine lacking PCGF6 is a cell autonomous event and suggests that PCGF6 controls directly this process.

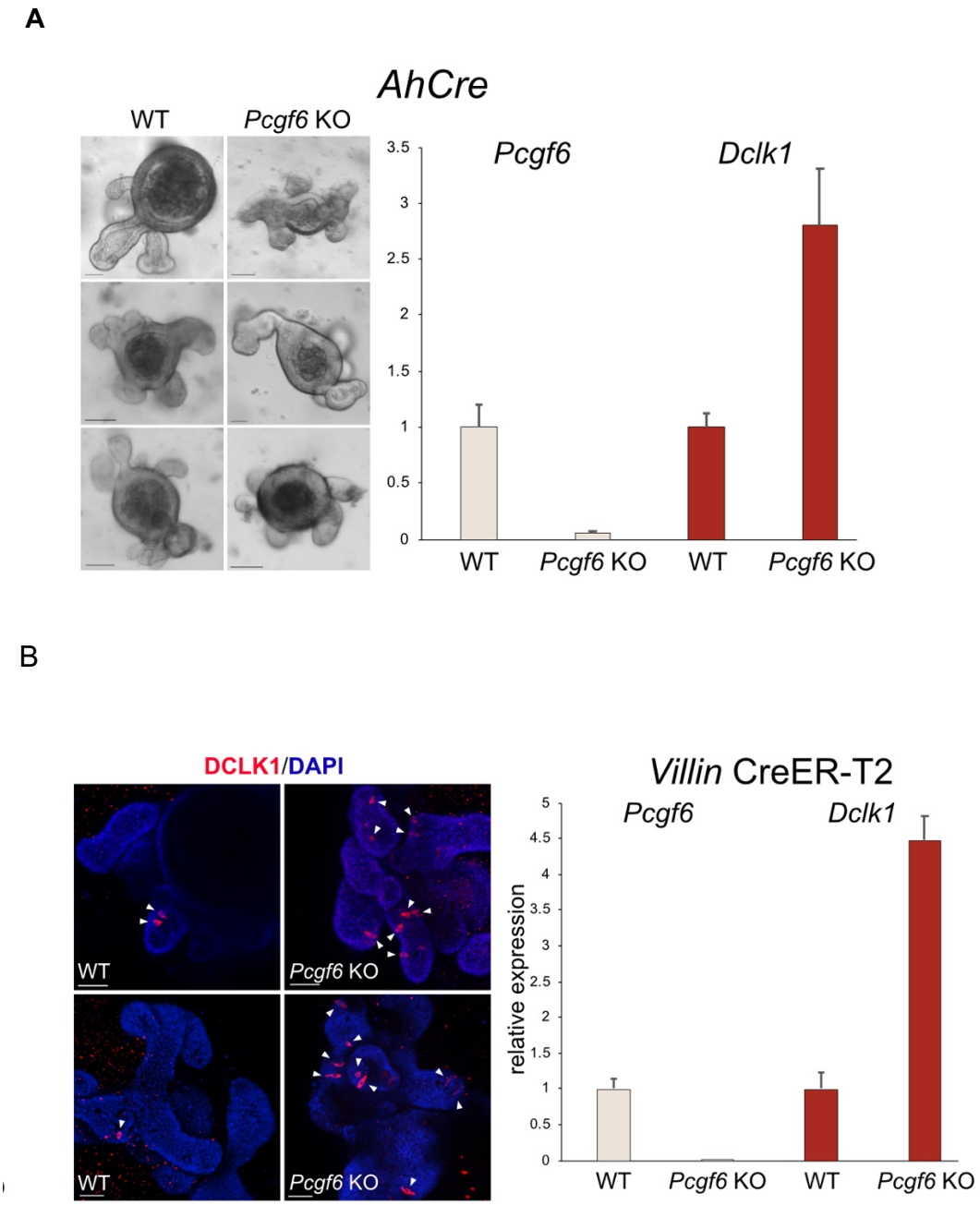

Figure 4.10.1: Mini guts grown from intestinal crypts

A. Pictures of organoids derived from AhCRE and AhCRE PCGF6 KO, after 3 days of culturing (left) and mRNA relative expression of PCGF6 and DCLK1 7 day after plating.
B. Immunofluorescence for DCLK1 of organoids derived from VillinCREert2 and VillinCREert2 PCGF6 KO, after 7 days of culturing (left) and mRNA relative expression of PCGF6 and DCLK1 7 day after plating.

Additionally, we have valuated the Tuft cells hyperplasia through functional studies.

Given their chemosensory activity, intestinal Tuft cell accumulation is associated with an abnormal presence of type 2 innate lymphoid cells (ILC2) in the intestinal Lamina Propria (104). Thus, we decided to examinate the presence of ILC2 in wild type intestine and in PCGF6 KO intestine. By performing FACS analysis of cells that were present in the Lamina propria, we have found the accumulation of ILC2 cells, which presents high level of CD25 and high level of GATA3, but not the accumulation of other ILC cell types, in intestine lacking PCGF6 protein (FIGURE 4.10.2). Thus, we speculate that PCGF6 loss causes also a hyperactivity of Type 2 immune response in intestine, confirming the hyperplasia of Tuft cells.

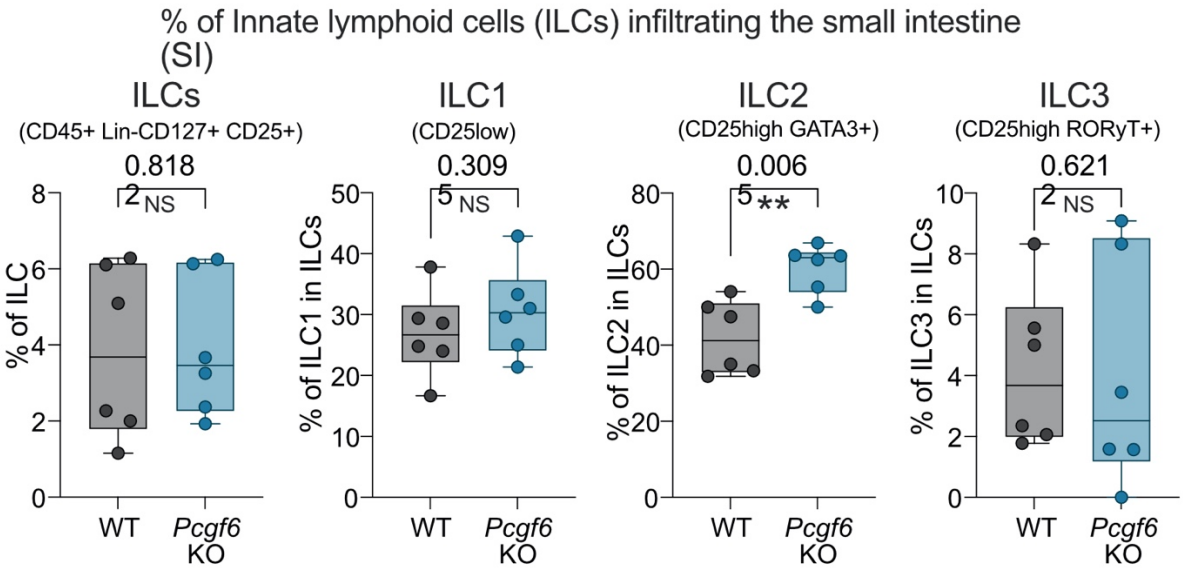

Figure 4.10.2: Flow cytometry analysis of Lamina Propria mononuclear cells isolated from wild type and PCGF6 KO mice show high number of ILC2 infiltrated cells upon depletion of PCGF6

To more accurately investigate the role of PCGF6 in Tuft cells accumulation in intestine, we decided to elucidate the contribution of PCGF6 in transcriptional regulation of intestinal cell signature.

We performed RNA sequencing of mRNA derived from intestinal cells of AhCRE and VillinCREert2, in wild type and PCGF6 KO. The number of deregulated genes was different in the two mouse models, maybe due the different transgene efficiency. However, in both mouse models lacking the expression of PCGF6, we have found that the more significant upregulated genes were related to Tuft cell signature (Figure 4.10.3 A). The transcriptome profile of PCGF6 KO showed more than 50% of the genes upregulated were associate with Tuft signature (Figure 4.10.3 B). In addition, gene set enrichment analysis (GSEA) of transcriptome profile of PCGF6 deficient cells showed a significant enrichment for Tuft cell signature compared to wild type cells (Figure 4.10.4 A).

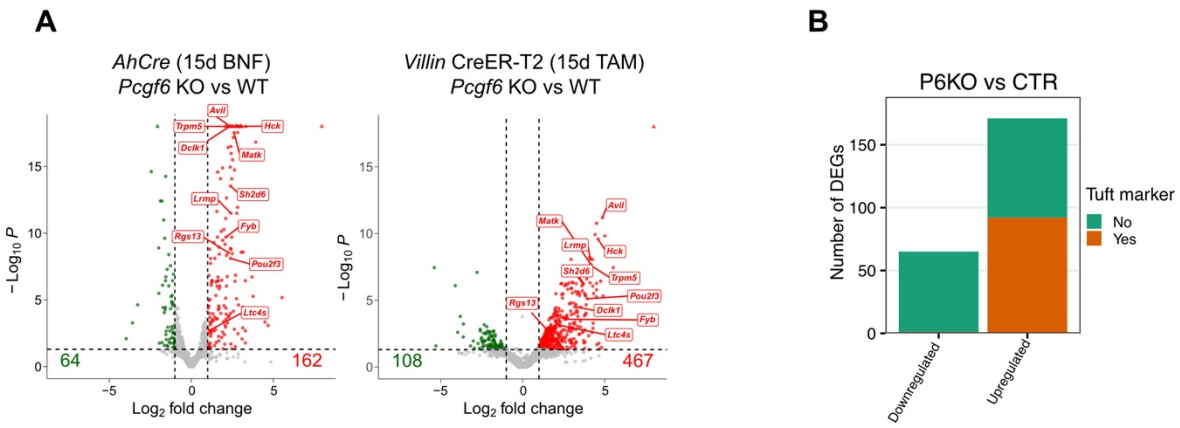

Figure 4.10.3: Transcriptome profile of PCGF6 deficient intestinal cell show upregulation of Tuft cell signature.

A. Volcano blot of deregulated genes in AhCRE PCGF6 KO (left) and VillinCREert2 PCGF6 KO (right). Both mouse models show upregulation of intestinal Tuft cell markers.
B. Column plot representing the number of downregulated genes and upregulated genes associated with Tuft cells signature (orange) upon PCGF6 depletion

Moreover, by performing GSE analysis for signature of other intestinal cell types, we have found that PCGF6 loss specifically upregulated Tuft cell correlated signature and not others, suggesting a very restricted role of PCGF6 in Tuft cell differentiation (Figure 4.10.4 B)

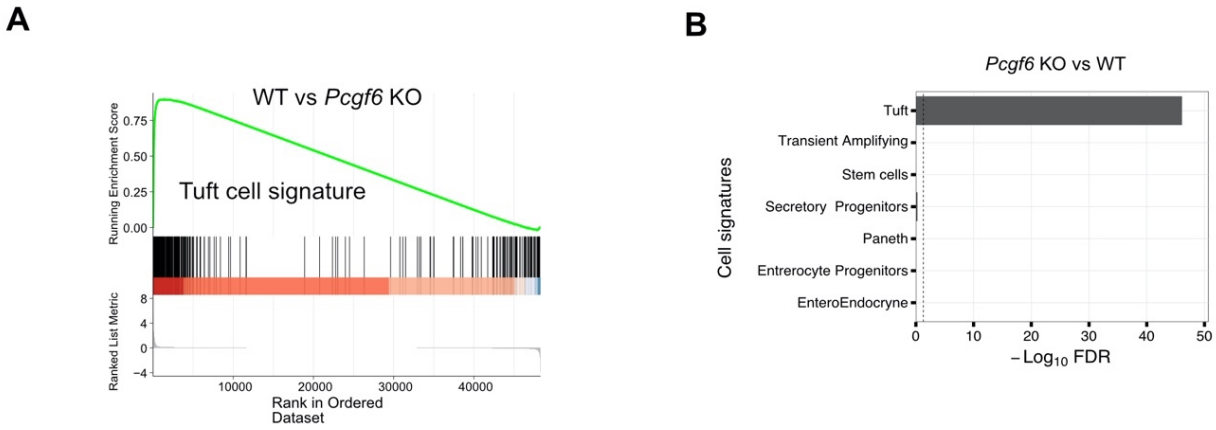

Figure 4.10.4: Transcriptome profile of PCGF6 deficient intestinal cell show upregulation of Tuft cell signature.

A. Gene set enrichment analysis of transcriptome profile of PCGF6 KO compared to wild type show enrichment in Tuft cells signature.
B. Column Graph showing specific upregulation of Tuft cell signature and no other intestinal cell signature in PCGF6 KO

The upregulation of Tuft marker was validated by RT-qPCR on nuclear extract form intestinal cells (Figure 4.10.5)

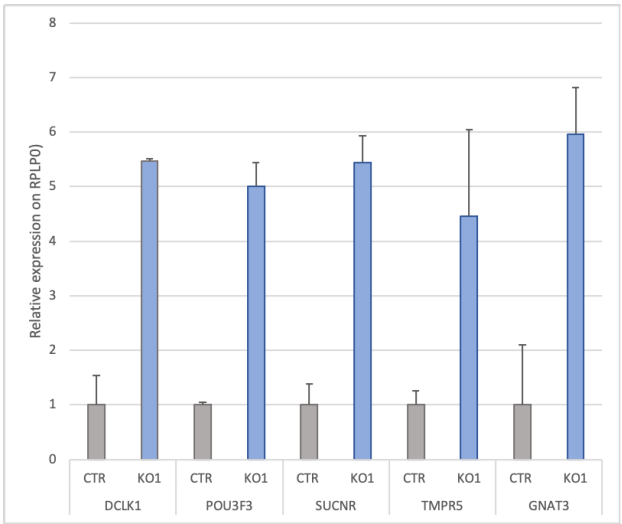

Figure 4.10.5: Relative expression of Tuft cell markers in WT and PCGF6 KO intestinal cell

Very importantly, with RNA sequencing analysis, we have found that one of the gene upregulated in PCGF6 KO cells was Pou2f3, which is known to be a master regulator for Tuft cells differentiation (6). We confirmed the upregulation of Pou2f3 transcription factor by performing immunofluorescence analysis of duodenum section derived from wild type and PCGF6 KO mice (FIGURE 4.10.6 A). The number of Pou2f3 positive cells in intestine lacking PCGF6 was almost 3 times more compared to wild type intestine (FIGURE 4.10.6 B).

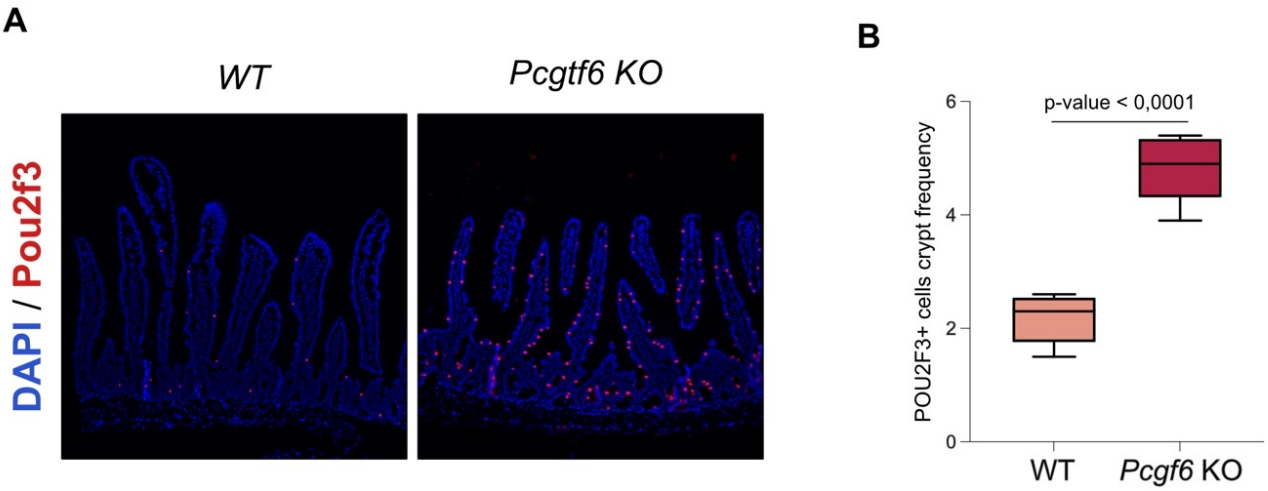

Figure 4.10.6: Upregulation of Taft cells master regulator in absence of PCGF6

A. Immunofluorescence for Pou2f3 transcription factor in wild type and PCGF6 KO intestine.
B. Column Graph showing quantification of Pou2f3 signal among intestinal crypts

Then, we decided to analyze the transcriptional control of PCGF6 in Pou2f3 expression. By ChIP-seq analysis we found that only PCGF6, and no other PCGF protein were present on Pou2f3 promoter, meaning that the repression of TF Pou2f3 in intestinal cell is restrictedly controlled by PCGF6 (Figure 4.10.7).

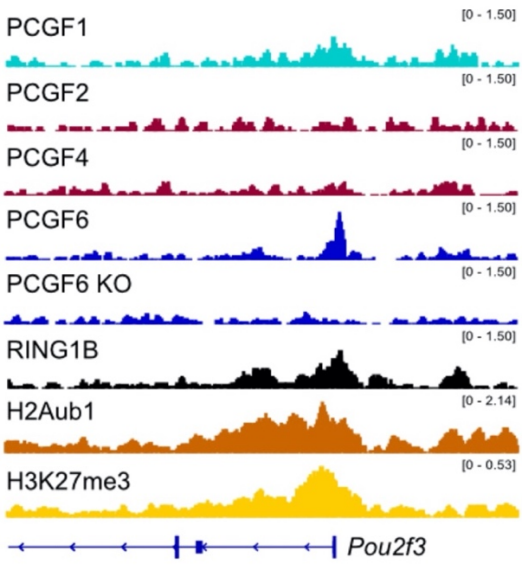

Figure 4.10.7: Genomic snapshots of PCGF1, PCGF2, PCGF6, RING1b, H2Aub1 and H3K27me3 at Pou2f3 promoter region in WT, and PCGF6 KO

Moreover, we found that upon PCGF6 removal from intestinal cells, RING1b binding as well as H2Aub1 deposition on Pou2f3 promoter was reduced but not completely lost (Figure 4.10.8).

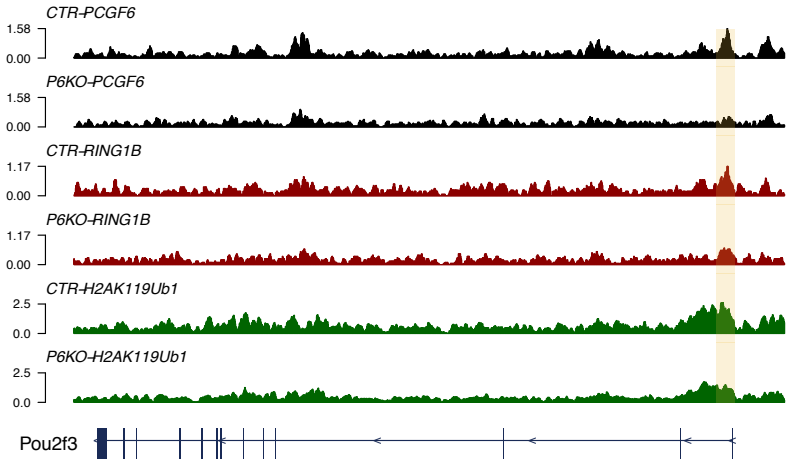

Figure 4.10.8: Genomic snapshots of PCGF6, RING1b, H2Aub1 and H3K27me3 at Pou2f3 promoter region in WT and PCGF6 KO

This data suggests us the hypothetic control of PCGF6 in transcriptional regulation of Tuft cells markers, first at all the master regulator Pou2f3, in a PRC1 independent manner.

4.11 PCGF6 restrict Tuft specification in a Ring1b independent mechanism

Then, we decide to investigate better if PCGF6 controls directly or via PRC1.6 the transcription of Tuft cells markers. This question was extremely necessary to explain the role of PCGF6 in Tuft cell differentiation. In fact, as previously mentioned, we observed that PCGF6 share only partially the binding on chromatin with Ring1b, and with other PCGF proteins. Moreover, intestine in which the expression of PCGF6 was loss, the globally activity of PRC1 and PRC2 was not altered. For all these reasons we decided to investigate if also RING1b or other PCGFs protein were involved in Tuft cell markers transcriptional control and so Tuft cells accumulation. To do so, we needed to compare the transcriptome profile of PCGF6 KO intestinal cells with transcriptome profile of Ring1a/b dKO, and other PCGF KO intestinal cells. We divided the transcriptome profile in gene associated with Tuft cell signature, and other genes. Interestingly, we have found that Tuft markers were upregulated only in PCGF6 KO cells, and not in RING1b KO cells (FIGURE 4.11.1).

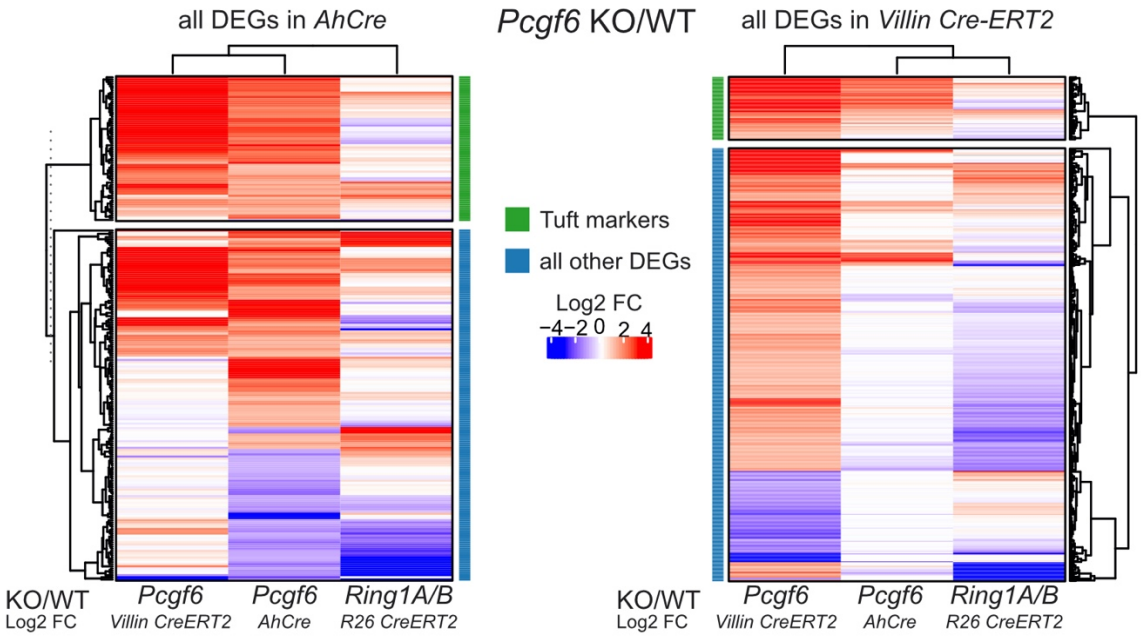

Figure 4.11.1: Heatmaps of deregulated genes in AhCRE PCGF6 (left) and VillinCREert2 PCGF6 (right) on each specific control found in AhCRE PCGF6 KO, VillinCREert2 PCGF6 KO and Ring1a/b KO. Deregulated genes were clustered in Tuft markers and others.

Moreover, when we compared deregulated genes found in PCGF6 KO with PCGF1 KO, PCGF2/4 KO, or PCGF3/5 KO intestinal cells, also in this case, Tuft cell signature was upregulated only in intestine lacking PCGF6 proteins (FIGURE 4.11.2).

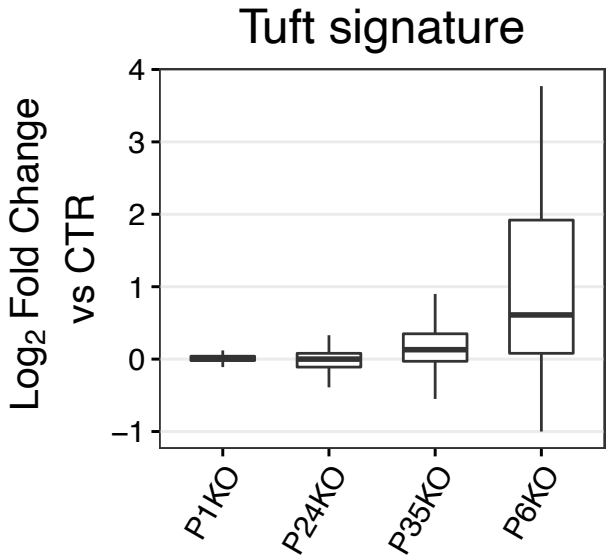

Figure 4.11.3: Column graph showing the expression of Tuft signature in different PCGF KOs intestinal cells.

All these results suggested that PCGF6 restrictively control the expression of Tuft cell signature, probably in a Ring1a/b independent manner.

Then, we decided to look at the occupancy of PCGF6 protein on genes associated with Tuft cells signature. From ChiP sequencing analysis we have found that 35% of upregulated Tuft marker were specifically PCGF6 targets (FIGURE 4.11.3).

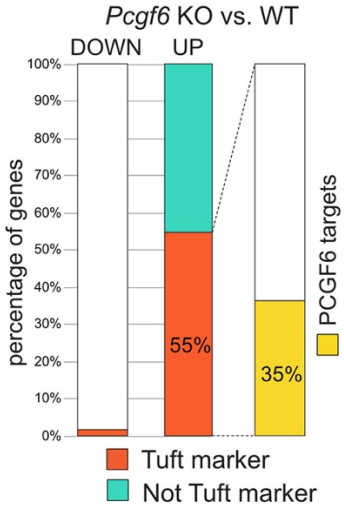

Figure 4.11.3: Percentage of downregulated genes (left) and upregulated genes (middle) in PCGF6 KO compared to control. Percentage of PCGF6 targets of upregulated gene of Tuft signature in PCGF6 KO cells.

Then we decided to assess, if the binding of PCGF6 on genes of Tuft signature was specific for PCGF6. For this purpose, we compared the binding of PCGF6 and other PCGF proteins on genes associated with Tuft cells signature (FIGURE 4.11.4). At this point we demonstrated that only PCGF6 binds specifically Tuft cell genes.

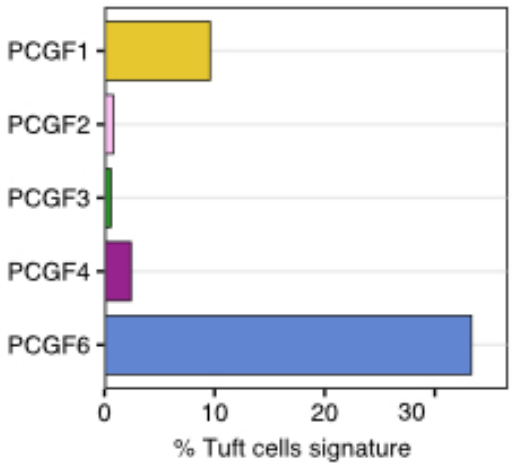

Figure 4.11.4: PCGFs binding on Tuft cell genes

Next, we want to know if the binding of PCGF6 and the control of the expression of Tuft markers, was associated with Ring1b binding and activity. By performing ChIP – sequencing analysis we observed that intensity of Ring1b binding on PCGF6 targets, both Tuft associated and not associated marker, was unchanged between wild type and PCGF6 KO cells. Accordingly, with this, also the H2AK119ub1 deposition by PRC1 was unchanged on PCGF6 Tuft targets and not Tuft targets, between wild type and PCGF6 KO cells (FIGURE 4.11.5).

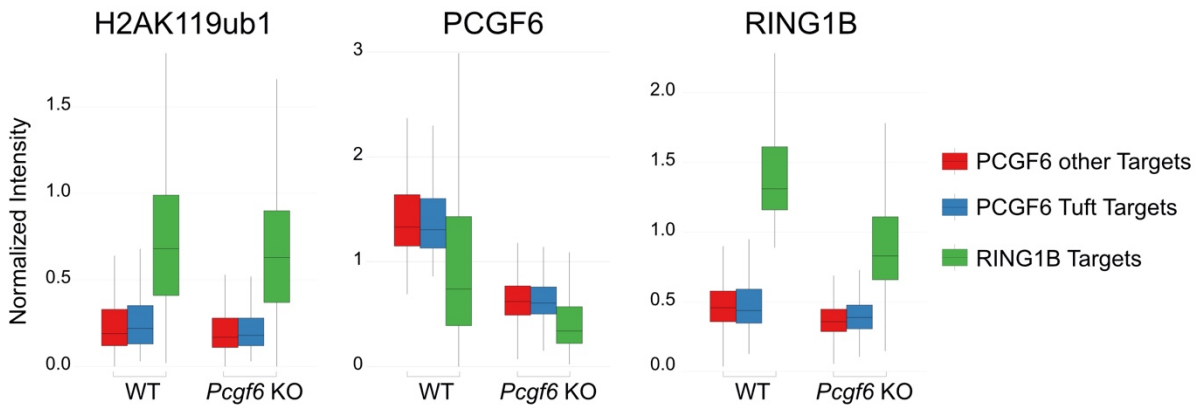

Figure 4.11.5: Percentage of downregulated genes (left) and upregulated genes (middle) in PCGF6 KO compared to control. Percentage of PCGF6 targets of upregulated gene of Tuft signature in PCGF6 KO cells.

This data confirmed that PCGF6 specifically binds Tuft cell genes in a Ring1b independent manner, and that control their expression. We these founding we discovered a new role for PCGF6 protein, which is a part of PRC1 activity, and give to the scientific community new scenery not only in Polycomb related field but also in intestine biology.

However, the mechanism with PCGF6 promotes Tuft cells hyperplasia in intestine is under investigation.

5. DISCUSSION

The PRC1 catalytic unit Ring1a/b is essential during the regulation of intestinal homeostasis. In our previous study, by inactivation of Ring1a/b form ISCs, we have established that PRC1 activity is crucially indispensable for stem cell self-renewal (4). Moreover, different from other scenarios in which CdKn2a de-repression by loss of PRC1 or PRC2 was the major mechanism behind, we have reported that in intestinal PRC1-dependent control of ISCs self-renewal is CdKn2a independent (4). Instead, we previously report that PRC1 activity directly controls the repression of inhibitors factor for Wnt/B-catenin signaling, which is extremely relevant during intestinal development, and regeneration (4). We have demonstrated that important role of PRC1 catalytic units. However, nothing is known about the role of six PRC1 subcomplexes in intestinal homeostasis. For instance, Ring1b can associate with six mutual exclusive PCGF proteins, forming six different subcomplexes.

In this study, we identify the role of PCGF proteins in adult intestine, and we discovered that PCGF1, PCGF2 and PCGF4 are essential for PRC1 global activity during homeostasis.

First, we have demonstrated that single PCGF proteins are dispensable for intestinal homeostasis. By taking advance of the use of LGR5-GFP-ires-CreERT2/ /Rosa26Lox-stop-Lox LacZ mouse strain we had the opportunity to investigate PRC1 role in intestinal cells. Our data revealed that lacking PCGF1, PCGF2/4, PCGF3/5 and PCGF6 do not affect intestinal architecture. In fact, ISC self-renewal and their capacity to regenerate the intestine during homeostasis, was normal in mice deficient of PCGF1, PCGF2/4, PCGF3/5 and PCGF6 expression. By using AhCRE and VillinCREert2 mouse model, we study the molecular mechanism in transcriptional repression and cellular identity maintenance in adult intestine, controlled by single PCGF proteins. We have found that single PCGFs do not affects the binding on Ring1b on chromatin. According with that, global H2AK119ub1 deposition was not altered in intestinal cells in which PCGF1, PCGF2/4, PCGF3/5 and PCGF6 KO cells. However, as in ESCs, also in adult intestinal cells, PCGF3/5 controls H2Aub1 intergenic deposition.

It is well established that PCGF proteins compensate each other in transcriptional repression in embryonic stem cells (1) (2). In adult intestine, deep analysis of chromatin association of single PCGF proteins confirmed the co-occupancy of PCGF2 and PCGF4 on the same targets, and that PCGF1 partially co-occupy PCGF6 target genes. Very interestingly, PCGF6 binds a high number of unique targets, suggesting its independent role from PRC1. Moreover, we found that PCGF1 and PCGF2/4 shares a high number of targets genes, which suggested us the hypothetic cooperation of these proteins in transcriptional repression control.

For this reason, we decided to generate a mouse model lacking this three different PCGFs. LGR5-GFP-ires-CreERT2/ /Rosa26Lox-stop-Lox LacZ ; PCGF1/2/4 tKO mouse model was used for ISC lineage tracing. We observed that loss of these proteins from intestinal stem cells impairs cells proliferation, cellular self-renewal that inhibits a correct homeostasis, and so the formation of normal intestinal epithelium. Using AhCRE and VillinCREert2 mouse models, we observed that the lack of PCGF1/2/4 deeply affected the intestinal homeostasis, and the normal intestinal architecture. At molecular levels, loss of PCGF1/2/5 from adult intestinal cells, induced the displacement of Ring1a/b from the chromatin, which affected H2Aub1 deposition. Therefore, depletion of PCGF1/2/4 together, caused a massive expression of several genes. However, we are still investigating if PRC1-loss-of- activity phenotype is dependent or independent from Ink4a-ARF locus activation.

In summary, our analysis demonstrates that PRC1.2 and PRC1.4 are not sufficient to control transcriptional identity in adult intestinal cells, and that PRC1.1 compensates the absence of PRC1.2 and PRC1.4 in regulating genes expression.

During our studies, we have found a novel role for PCGF6 proteins, differentially from what we observed for PCGF1, PCGF2/4 and PCGF3/5. In adult intestinal cells, PCGF6 displays a biological role independent from PRC1.

Intestinal epithelium lacking the expression of PCGF6, show normal architecture and morphology, with unchanged ISCs self-renewal. However, depletion of PCGF6 from intestine leads to Tuft cell population hyperplasia.

We have found that PCGF6 could binds both promoter and intergenic regions with the same affinity, and that PCGF6 present a high number of unique target genes, which are not in common with Ring1a/b nor with other PCGF proteins. Among unique PCGF6 targets, we found Tuft cell markers, included the master regulator for Tuft differentiation Pou2f3.

Additionally, transcriptome profile analysis of PCGF6 KO intestinal cells, displayed enrichment of Tuft cell signature. As a matter of fact, more than 50% of upregulated genes found in PCGF6 KO intestinal cells were Tuft cell markers. These genes were not upregulated in other PCGF KO or in Ring1b KO, confirming the unique correlation between PCGF6 and Tuft cells differentiation, that is completely independent from PRC1 activity.

In conclusion, we reported a new biological role for PCGF6 protein in intestinal cells, that provides important knowledge in Polycomb protein field.

6. FUTURE PROSPECTIVES AND ON-GOING

Based on these results, we have demonstrated that single PCGF proteins are dispensable for intestinal homeostasis. By taking advance of the use of transgenic mouse model we have demonstrated that ISC self-renewal and intestinal regeneration is unchanged upon depletion of single PCGFs. In fact, Ring1b binding and H2AK119ub deposition, was not mutated in PCGF1, PCGF2/4, PCGF3/5 and PCGF6 KO cells. This was also observed for H3K27me3 deposition,

meaning that the repressive machinery of Polycomb proteins was well established even after depletion of single PCGFs.

In addition, in intestinal cells lacking the expression of PCGF1, PCGF2/4, PCGF3/5 and PCGF6, show a transcriptional profile similar to wild type. In PCGF1, PCGF2/4, PCGF3/5 and PCGF6 KOs the transcriptional repression played by PRC1 is maintained, and not significant reprogramming accurse.

Interestingly, we have found that concomitant depletion of PCGF1, PCGF2 and PCGF4 affects intestinal homeostasis, through impairment of ISC self-renewal, and cellular identity maintenance. Upon depletion of PCGF1, PCGF2 and PCGF4, Ring1b protein was globally displayed from the chromatin, and H2AK119ub1 deposition was completely abrogated. Moreover, transcriptome profile of PCGF1/2/4 tKO was affected. Depletion of PCGF1, PCGF2 and PCGF4 leads to a massive deregulation of gene expression, very similar to what we have already observed in Ring1a/b KO.

However, we are now investigated the mechanism behind the role of PCGF1/2/4 in ISC self-renewal and cellular identity maintenance. It is known, that Polycomb proteins are linked with Cdkn2a locus repression, and we have already demonstrated that Ring1a/b associated phenotype is independent from Cdkn2a de-repression and the consequent senescence that could arise (105) (4). Thus, we want to find out if the phenotype observed upon depletion of PCGF1/2/4 is also independent from Cdkn2a locus activation. For this reason, we are generating a mouse model with the constitutive inactivation of p16 and Arf expression (Cdk2a -/-), with PCGF1/2/4 $^{fl/fl}$ mice. On this mouse model we will perform histology analysis in order to understand if this protein have a role in intestinal homeostasis in a CdK2a independent manner. If with this rescue experiment, we will obtain the same results obtained with PCGF1/2/4 KO alone, it will mean that PRC1.1, PRC1.2 and PRC1.4 together are able to maintain the repression profile of intestinal cells that determinate the cellular identity.

But since, we found upregulation of the Ink4a/Arf locus already in PCGF2/4 dKO but with alteration of cell proliferation rate, we are very confident that the phenotype observed in PCGF1/2/4 tKO is not correlated with activation of p16 and p19, and the senesce process (Figure 5.1).

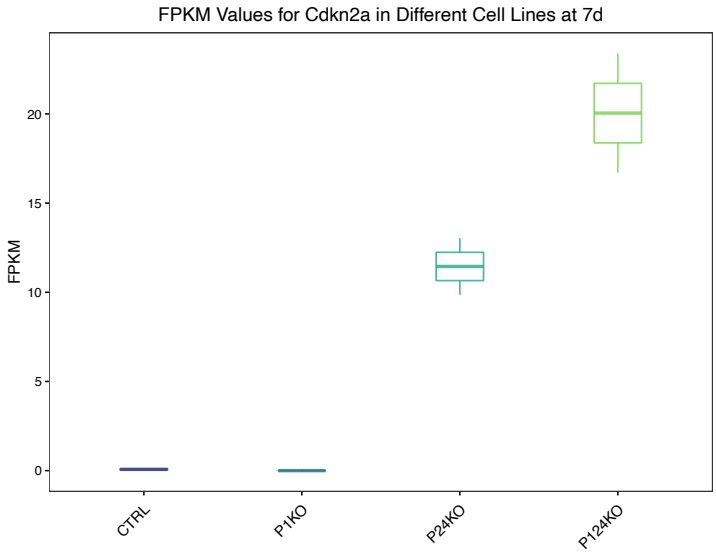

Figure 5.1: FPKM values for CdKN2a in WT, PCGF1 KO, PCGF2/4 KO and PCGF1/2/4 KO

Besides the role of PCGF1, PCGF2 and PCGF4, we are also interested on the cooperation of PCGF1, PCGF3, PCGF5 and PCGF6, namely non-canonical PRC1, in transcriptional repression regulation in adult intestinal cells. We have already obtained results on the role of PCGF1/3/5/6 qKO In ISC self-renewal by using the LGR5-GFP-ires-CreERT2 Rosa26lox-stop-lox LacZ mouse model. The depletion of PCGF1/3/5/6 in ISC seems to not affect the intestinal stem cells proliferation, and their capacity to repopulate the epithelium during homeostasis. However, we did not collect any data on the role of PCGF1/3/5/6 on PRC1 binding or activity, eider on transcriptome profile. To elucidate the cooperation of PCGF1/3/5/6, we are now generating VillinCREert2; PCGF1/3/5/6 qKO. Taking advance of the ChIP sequencing technique, we will investigate if these complexes could control Ring1b binding, and H2AK119ub histone marker deposition, as well as PRC2 activity. Then we will assess if the depletion of PCGF1/3/5/6 qKO in adult intestinal cells, could compromise the transcriptome profile, leading to a deregulation of genes silencing.

We also found a new role for PCGF6 protein in adult intestine. We have demonstrated that different from ESc, PCGF6 show functionality independently from Ring1b. In intestine PCGF6 protein alone is sufficient to repress genes associated with Tuft cell differentiation. In fact, intestine lacking PCGF6 protein show a hyperplasia condition, with significant increased number of Tuft cells. Moreover, we have found that PCGF6 directly binds Tuft cells markers, which leads to upregulation of those genes. We have found that PCGF6 directly bounds and controls the expression of Tuft cell master regulator Pou2f3. Since we have not found Ring1b binding, not either H2AK119 deposition on Pou2f3 promoter, we assumed that Pou2f3 transcription factor expression is regulated from PCGF6 exclusively, in PRC1 independent manner.

However, the mechanism behind this speculation is under investigation. Discussed data motif enrichment analysis we have found that PCGF6 is recruited to DNA by E-box recognition, as well as MYC protein. Given that we have already demonstrate the antagonism mechanism between MYC and PCGF6 in ESc (2), here we are hypothesizing that this could also append in intestinal cells. To confirm that PCGF6 plays the role of ‘‘attenuator’’ of Tuft cell markers transcription though a mechanism independent from Ring1b and H2Aub1 deposition, we will perform ChIP sequencing analysis for MYC protein in adult intestinal cells.

Additionally, from deep analysis of ChIP sequencing data we have found that PCGF6 binds at the same way promoter but also intergenic regions, and its binding is equal distributed on CpG rich positive and negative region (Figure 5.2).

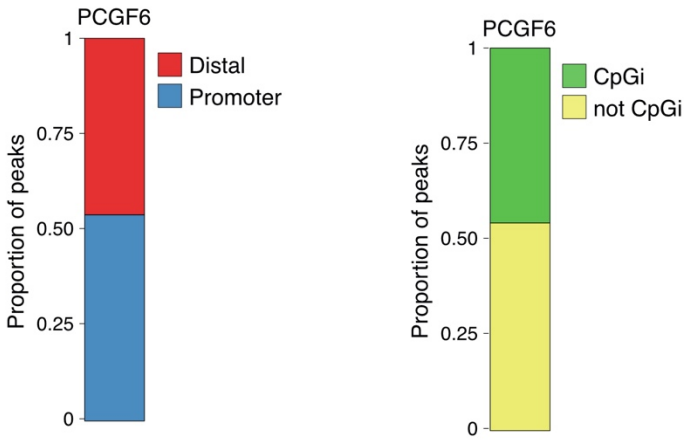

Figure 5.2: Representation of proportion of PCGF6 peaks distribution on distal and promoter (left), and proportion of PCGF6 peaks distribution on CpGi and not CpGi island

Given this data, and the absence of RING1b on Tuft cell marker, we are hypnotizing that PCGF6 could control the expression of those through binding of transcriptional regulatory sequence.

Cohesin and CTCC-binding factor (CTCF) are an important protein that are associated with regulatory function, such transcriptional activation and repression, specially of lineage-specific genes (160) (161). To investigate the possible regulatory implication of PCGF6 in Tuft cell signature in intestinal cells, we decide to observe the presence of PCGF6 on CTCF and RAD21 binding sites. ChIP -seq preliminary data demonstrated, as expected, that CTCF and RAD21 are mostly localized in distal region and on CpGi negative region (Figure 5.3). Contrary to that, RING1b mostly localized at promoter region and CpGi positive region (5.3). Instead, as I mentioned above PCGF6 shown both localizations.

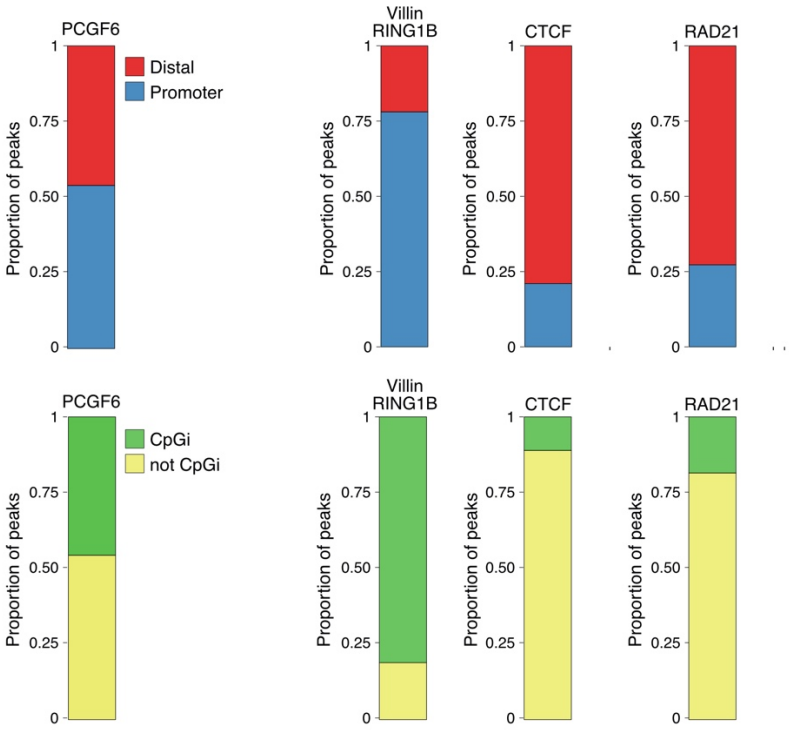

Figure 5.3: Representation of proportion of PCGF6, RING1B, CTCF and RAD21 peaks distribution on distal and promoter (upper), and proportion of PCGF6 peaks distribution on CpGi and not CpGi island.

Then we decided to investigate if PCGF6 binds the same targets genes of CTCF and RAD21. Surprisingly, in wild type intestinal cells PCGF6 co-localize with CTCF, and also with RAD21 for one third.

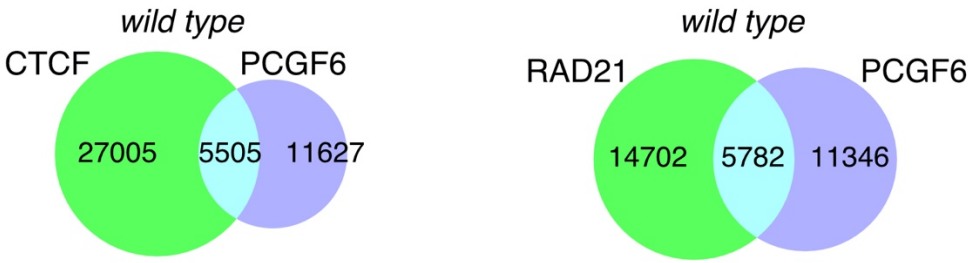

Figure 5.4: Vann diagram showing the overlap between CTCF targets, PCGF6 targets in WT intestinal cells (left). Vann diagram showing the overlap between RAD21 targets, PCGF6 targets in WT intestinal cells (right).

In fact, we found 5505 target genes of PCGF6 were in common with CTCF, and 5782 PCGF6 target genes were in common with RAD21 (Figure 5.4). This preliminary data suggests that PCGF6 effectively binds regulatory regions and contribute to chromatin organization and gene expression regulation. However, by overlapping the CTCF target found in wild type and PCGF6 KO intestinal cells, we observed that the binding of CTCF and RAD21 was not alters (Figure 5.5)

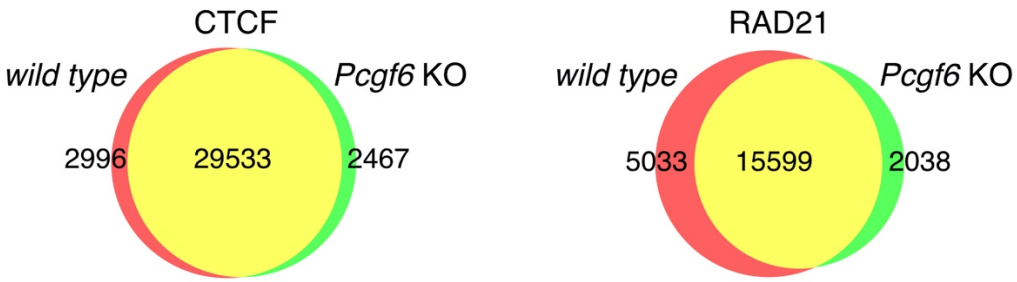

Figure 5.5: Vann diagram showing the overlap between CTCF targets in WT and PCGF6 KO intestinal cells (left). Vann diagram showing the overlap between RAD21 targets in WT and PCGF6 KO intestinal cells (right).

Whit these data we speculated that PCGF6 protein could play important function in gene expression by controlling distal regulatory element, and that the absence of PCGF6 do not destabilize other complexes.

In order to understand the implication of PCGF6 in gene expression regulation, we will perform Mass Spectrometry analysis by using and endogenous PCGF6 antibody. In this way, it will be possible characterize if PCGF6 is a component of specific distal regulatory machinery.

7. **BIBLIOGRAPHY**

1. Gao Z, Zhang J, Bonasio R, et al. PCGF Homologs, CBX Proteins, and RYBP Define Functionally Distinct PRC1 Family Complexes. Mol Cell. 2012;45(3):344-356. doi:10.1016/j.molcel.2012.01.002.

2. Scelfo A., Fernandez-Perez D., Tamburri S., et al. Functional Landscape of PCGF proteins reveals both RING1A/B-dependent and RING1A/B-independent specific activities. Molecular Cell.2019

3. The polycomb group protein PCGF6 mediates germline gene silencing by recruiting histone-modifying proteins totarget gene promoters. J. Biol. Chem.(2020) 295(28) 9712–9724

4. Chiacchiera F, Rossi A, Jammula S, et al. Polycomb Complex PRC1 Preserves Intestinal Stem Cell Identity by Sustaining Wnt/Beta-Catenin Transcriptional Activity. Cell Stem Cell. 2016;18(1):91-103. doi:10.1016/j.stem.2015.09.019.

5. Bjerknes M, Khandanpour C, Moroy T, Fujiyama T, Hoshino M, Klisch TJ, Ding Q, Gan L, Wang J, Martin MG, et al. 2012. Or- igin of the brush cell lineage in the mouse intestinal epitheli- um. Dev Biol 362: 194–218.

6. Yu-Han Huang,1 Olaf Klingbeil,1 Xue-Yan He,1 Xiaoli S. Wu,1,2 Gayatri Arun,1 Bin Lu,1 Tim D.D. Somerville,1 Joseph P. Milazzo,1 John E. Wilkinson,3 Osama E. Demerdash,1 David L. Spector,1 Mikala Egeblad,1 Junwei Shi,4 and Christopher R. Vakoc1 (2018). POU2F3 is a master regulator of a tuft cell-like variant of small cell lung cancer

7. Helin, K. and D. Dhanak (2013). "Chromatin proteins and modifications as drug targets." Nature 502(7472): 480-488.

8. Trojer, P., A. R. Cao, Z. Gao, Y. Li, J. Zhang, X. Xu, G. Li, R. Losson, H. Erdjument- Bromage, P. Tempst, P. J. Farnham and D. Reinberg (2011). “L3MBTL2 protein acts in concert with PcG protein-mediated monoubiquitination of H2A to establish a repressive chromatin structure.” Mol Cell 42(4): 438-450.

9. Kornberg, R. D. (1974). "Chromatin structure: a repeating unit of histones and DNA." Science 184(4139): 868-871.

10. Richmond, T. J. and C. A. Davey (2003). "The structure of DNA in the nucleosome core." Nature 423(6936): 145-150.

11. (Sudarsanam and Winston 2000, Levine and Tjian 2003).

12. Hargreaves, D. C. and G. R. Crabtree (2011). "ATP-dependent chromatin remodeling: genetics, genomics and mechanisms." Cell Res 21(3): 396-420.

13. Dominski, Z. and W. F. Marzluff (2007). "Formation of the 3' end of histone mRNA: getting closer to the end." Gene 396(2): 373-390.

14. Marzluff, W. F. and R. J. Duronio (2002). "Histone mRNA expression: multiple levels of cell cycle regulation and important developmental consequences." Curr Opin Cell Biol 14(6): 692-699.

15. Rothbart, S. B. and B. D. Strahl (2014). "Interpreting the language of histone and DNA modifications." Biochim Biophys Acta 1839(8): 627-643.

16. Illingworth, R. S. and A. P. Bird (2009). "CpG islands--'a rough guide'." FEBS Lett 583(11): 1713-1720.

17. Okano, M., D. W. Bell, D. A. Haber and E. Li (1999). "DNA methyltransferases Dnmt3a and Dnmt3b are essential for de novo methylation and mammalian development." Cell 99(3): 247-257.

18. Okano, M., S. Xie and E. Li (1998). "Dnmt2 is not required for de novo and maintenance methylation of viral DNA in embryonic stem cells." Nucleic Acids Res 26(11): 2536-2540.

19. Arnaudo, A. M. and B. A. Garcia (2013). "Proteomic characterization of novel histone post-translational modifications." Epigenetics Chromatin 6(1): 24.

20. Kouzarides, T. (2007). "Chromatin modifications and their function." Cell 128(4): 693-705.

21. Jenuwein, T. and C. D. Allis (2001). "Translating the histone code." Science 293(5532): 1074-1080.

22. Poynter, S. T. and C. Kadoch (2016). "Polycomb and trithorax opposition in development and disease." Wiley Interdiscip Rev Dev Biol 5(6): 659-688.

23. Lewis, E. B. (1978). "A gene complex controlling segmentation in Drosophila." Nature 276(5688): 565-570.

24. Ingham, P. W. (1983). "Differential expression of bithorax complex genes in the absence of the extra sex combs and trithorax genes." Nature 306(5943): 591-593.

25. Ingham, P. W. (1985). "Genetic control of the spatial pattern of selector gene expression in Drosophila." Cold Spring Harb Symp Quant Biol 50: 201-208.

26. Struhl, G. and M. Akam (1985). "Altered distributions of Ultrabithorax transcripts in extra sex combs mutant embryos of Drosophila." EMBO J 4(12): 3259-3264.

27. Morey, L. and K. Helin (2010). "Polycomb group protein-mediated repression of transcription." Trends Biochem Sci 35(6): 323-332.

28. Aranda, S., G. Mas and L. Di Croce (2015). "Regulation of gene transcription by Polycomb proteins." Sci Adv 1(11): e1500737.

29. Cao, R., L. Wang, H. Wang, L. Xia, H. Erdjument-Bromage, P. Tempst, R. S. Jones and Y. Zhang (2002). "Role of histone H3 lysine 27 methylation in Polycomb-group silencing." Science 298(5595): 1039-1043.

30. Muller, J., C. M. Hart, N. J. Francis, M. L. Vargas, A. Sengupta, B. Wild, E. L. Miller, M. B. O'Connor, R. E. Kingston and J. A. Simon (2002). "Histone methyltransferase activity of a Drosophila Polycomb group repressor complex." Cell 111(2): 197-208.

31. Cao, R., Y. Tsukada and Y. Zhang (2005). "Role of Bmi-1 and Ring1A in H2A ubiquitylation and Hox gene silencing." Mol Cell **20**(6): 845-854.

32. Bracken, A. P., N. Dietrich, D. Pasini, K. H. Hansen and K. Helin (2006). "Genome-wide mapping of Polycomb target genes unravels their roles in cell fate transitions." Genes Dev 20(9): 1123-1136.

33. Poynter, S. T. and C. Kadoch (2016). "Polycomb and trithorax opposition in development and disease." Wiley Interdiscip Rev Dev Biol **5**(6): 659-688.

34. Li, G., R. Margueron, M. Ku, P. Chambon, B. E. Bernstein and D. Reinberg (2010). "Jarid2 and PRC2, partners in regulating gene expression." Genes Dev **24**(4): 368-380.

35. Pasini, D., A. P. Bracken, M. R. Jensen, E. Lazzerini Denchi and K. Helin (2004). "Suz12 is essential for mouse development and for EZH2 histone methyltransferase activity." EMBO J 23(20): 4061-4071.

36. Ketel, C. S., E. F. Andersen, M. L. Vargas, J. Suh, S. Strome and J. A. Simon (2005). "Subunit contributions to histone methyltransferase activities of fly and worm polycomb group complexes." Mol Cell Biol **25**(16): 6857-6868.

37. Pasini, D., P. A. Cloos, J. Walfridsson, L. Olsson, J. P. Bukowski, J. V. Johansen, M. Bak, N. Tommerup, J. Rappsilber and K. Helin (2010). "JARID2 regulates binding of the Polycomb repressive complex 2 to target genes in ES cells." Nature **464**(7286): 306-310.

38. Ballare, C., M. Lange, A. Lapinaite, G. M. Martin, L. Morey, G. Pascual, R. Liefke, B. Simon, Y. Shi, O. Gozani, T. Carlomagno, S. A. Benitah and L. Di Croce (2012). "Phf19 links methylated Lys36 of histone H3 to regulation of Polycomb activity." Nat Struct Mol Biol 19(12): 1257-1265.

39. Mousavi, K., H. Zare, A. H. Wang and V. Sartorelli (2012). "Polycomb protein Ezh1 promotes RNA polymerase II elongation." Mol Cell 45(2): 255-262.

40. Margueron, R., G. Li, K. Sarma, A. Blais, J. Zavadil, C. L. Woodcock, B. D. Dynlacht and D. Reinberg (2008). "Ezh1 and Ezh2 maintain repressive chromatin through different mechanisms." Mol Cell 32(4): 503-518.

41. Margueron, R., N. Justin, K. Ohno, M. L. Sharpe, J. Son, W. J. Drury, 3rd, P. Voigt, S. R. Martin, W. R. Taylor, V. De Marco, V. Pirrotta, D. Reinberg and S. J. Gamblin (2009). "Role of the polycomb protein EED in the propagation of repressive histone marks." Nature **461**(7265): 762-767.

42. Wagner, E. J. and P. B. Carpenter (2012). "Understanding the language of Lys36 methylation at histone H3." Nat Rev Mol Cell Biol 13(2): 115-126.

43. Helin, K. and D. Dhanak (2013). "Chromatin proteins and modifications as drug targets." Nature 502(7472): 480-488.

44. Bannister, A. J. and T. Kouzarides (2011). "Regulation of chromatin by histone modifications." Cell Res 21(3): 381-395.

45. Ferrari, K. J., A. Scelfo, S. Jammula, A. Cuomo, I. Barozzi, A. Stutzer, W. Fischle, T. Bonaldi and D. Pasini (2014). "Polycomb-dependent H3K27me1 and H3K27me2 regulate active transcription and enhancer fidelity." Mol Cell 53(1): 49-62.

46. Shilatifard, A. (2012). "The COMPASS family of histone H3K4 methylases: mechanisms of regulation in development and disease pathogenesis." Annu Rev Biochem **81**: 65-95.

47. Brookes, E., I. de Santiago, D. Hebenstreit, K. J. Morris, T. Carroll, S. Q. Xie, J. K. Stock, M. Heidemann, D. Eick, N. Nozaki, H. Kimura, J. Ragoussis, S. A. Teichmann and A. Pombo (2012). "Polycomb associates genome-wide with a specific RNA polymerase II variant, and regulates metabolic genes in ESCs." Cell Stem Cell 10(2): 157-170.

48. Voigt, P., W. W. Tee and D. Reinberg (2013). "A double take on bivalent promoters." Genes Dev 27(12): 1318-1338.

49. Ku, M., R. P. Koche, E. Rheinbay, E. M. Mendenhall, M. Endoh, T. S. Mikkelsen, A. Presser, C. Nusbaum, X. Xie, A. S. Chi, M. Adli, S. Kasif, L. M. Ptaszek, C. A. Cowan, E. S. Lander, H. Koseki and B. E. Bernstein (2008). "Genomewide analysis of PRC1 and PRC2 occupancy identifies two classes of bivalent domains." PLoS Genet 4(10): e1000242.

50. Morey, L., G. Pascual, L. Cozzuto, G. Roma, A. Wutz, S. A. Benitah and L. Di Croce (2012). "Nonoverlapping functions of the Polycomb group Cbx family of proteins in embryonic stem cells." Cell Stem Cell 10(1): 47-62.

51. O'Loghlen, A., A. M. Munoz-Cabello, A. Gaspar-Maia, H. A. Wu, A. Banito, N. Kunowska, T. Racek, H. N. Pemberton, P. Beolchi, F. Lavial, O. Masui, M. Vermeulen, T. Carroll, J. Graumann, E. Heard, N. Dillon, V. Azuara, A. P. Snijders, G. Peters, E. Bernstein and J. Gil (2012). "MicroRNA regulation of Cbx7 mediates a switch of Polycomb orthologs during ESC differentiation." Cell Stem Cell 10(1): 33-46.

52. Boyer, L. A., K. Plath, J. Zeitlinger, T. Brambrink, L. A. Medeiros, T. I. Lee, S. S. Levine, M. Wernig, A. Tajonar, M. K. Ray, G. W. Bell, A. P. Otte, M. Vidal, D. K. Gifford, R. A. Young and R. Jaenisch (2006). "Polycomb complexes repress developmental regulators in murine embryonic stem cells." Nature 441(7091): 349-353.

53. Pasini, D., A. P. Bracken, J. B. Hansen, M. Capillo and K. Helin (2007). "The polycomb group protein Suz12 is required for embryonic stem cell differentiation." Mol Cell Biol 27(10): 3769-3779.

54. Tavares, L., E. Dimitrova, D. Oxley, J. Webster, R. Poot, J. Demmers, K. Bezstarosti, S. Taylor, H. Ura, H. Koide, A. Wutz, M. Vidal, S. Elderkin and N. Brockdorff (2012). "RYBP- PRC1 complexes mediate H2A ubiquitylation at polycomb target sites independently of PRC2 and H3K27me3." Cell 148(4): 664-678.

55. Blackledge, N. P., J. C. Zhou, M. Y. Tolstorukov, A. M. Farcas, P. J. Park and R. J. Klose (2010). "CpG islands recruit a histone H3 lysine 36 demethylase." Mol Cell 38(2): 179-190.

56. Barrero, M. J. and J. C. Izpisua Belmonte (2013). "Polycomb complex recruitment in pluripotent stem cells." Nat Cell Biol 15(4): 348-350.

57. Scelfo, A., A. Piunti and D. Pasini (2015). "The controversial role of the Polycomb group proteins in transcription and cancer: how much do we not understand Polycomb proteins?" FEBS J 282(9): 1703-1722.

58. Ogawa, H., K. Ishiguro, S. Gaubatz, D. M. Livingston and Y. Nakatani (2002). "A complex with chromatin modifiers that occupies E2F- and Myc-responsive genes in G0 cells." Science 296(5570): 1132-1136.

59. Scheuermann, J. C., A. G. de Ayala Alonso, K. Oktaba, N. Ly-Hartig, R. K. McGinty, S. Fraterman, M. Wilm, T. W. Muir and J. Muller (2010). "Histone H2A deubiquitinase activity of the Polycomb repressive complex PR-DUB." Nature 465(7295): 243-247.

60. Orkin, S. H. and K. Hochedlinger (2011). "Chromatin connections to pluripotency and cellular reprogramming." Cell 145(6): 835-850.

61. Mendenhall, E. M., R. P. Koche, T. Truong, V. W. Zhou, B. Issac, A. S. Chi, M. Ku and B. E. Bernstein (2010). "GC-rich sequence elements recruit PRC2 in mammalian ES cells." PLoS Genet **6**(12): e1001244.

62. lymphomas and collaborates with myc in tumorigenesis." Oncogene 8(11): 3161-3164.

He, J., L. Shen, M. Wan, O. Taranova, H. Wu and Y. Zhang (2013). "Kdm2b maintains murine embryonic stem cell status by recruiting PRC1 complex to CpG islands of developmental genes." Nat Cell Biol 15(4): 373-384.

63. Xu, B., D. M. On, A. Ma, T. Parton, K. D. Konze, S. G. Pattenden, D. F. Allison, L. Cai, S. Rockowitz, S. Liu, Y. Liu, F. Li, M. Vedadi, S. V. Frye, B. A. Garcia, D. Zheng, J. Jin and G. G. Wang (2015). "Selective inhibition of EZH2 and EZH1 enzymatic activity by a small molecule suppresses MLL-rearranged leukemia." Blood 125(2): 346-357.

64. Stielow, B., F. Finkernagel, T. Stiewe, A. Nist and G. Suske (2018). "MGA, L3MBTL2 and E2F6 determine genomic binding of the non-canonical Polycomb repressive complex PRC1.6." PLoS Genet 14(1): e1007193.

65. Cohen, I., D. Zhao, C. Bar, V. J. Valdes, K. L. Dauber-Decker, M. B. Nguyen, M. Nakayama, M. Rendl, W. A. Bickmore, H. Koseki, D. Zheng and E. Ezhkova (2018). "PRC1 Fine-tunes Gene Repression and Activation to Safeguard Skin Development and Stem Cell Specification." Cell Stem Cell 22(5): 726-739 e727.

66. Fursova, N. A., N. P. Blackledge, M. Nakayama, S. Ito, Y. Koseki, A. M. Farcas, H. W. King, H. Koseki and R. J. Klose (2019). "Synergy between Variant PRC1 Complexes Defines Polycomb-Mediated Gene Repression." Mol Cell 74(5): 1020-1036 e1028.

67. Pivetti, S., D. Fernandez-Perez, A. D'Ambrosio, C. M. Barbieri, D. Manganaro, A. Rossi, L. Barnabei, M. Zanotti, A. Scelfo, F. Chiacchiera and D. Pasini (2019). "Loss of PRC1 activity in different stem cell compartments activates a common transcriptional program with cell type-dependent outcomes." Sci Adv 5(5): eaav1594.

68. Faust, C., A. Schumacher, B. Holdener and T. Magnuson (1995). "The eed mutation disrupts anterior mesoderm production in mice." Development 121(2): 273-285.

69. O'Carroll, D., S. Erhardt, M. Pagani, S. C. Barton, M. A. Surani and T. Jenuwein (2001). "The polycomb-group gene Ezh2 is required for early mouse development." Mol Cell Biol 21(13): 4330-4336.

70. Takeuchi, T., Y. Yamazaki, Y. Katoh-Fukui, R. Tsuchiya, S. Kondo, J. Motoyama and T. Higashinakagawa (1995). "Gene trap capture of a novel mouse gene, jumonji, required for neural tube formation." Genes Dev 9(10): 1211-1222.

71. Wang, H., L. Wang, H. Erdjument-Bromage, M. Vidal, P. Tempst, R. S. Jones and Y. Zhang (2004). "Role of histone H2A ubiquitination in Polycomb silencing." Nature 431(7010): 873-878.

72. de Napoles, M., J. E. Mermoud, R. Wakao, Y. A. Tang, M. Endoh, R. Appanah, T. B. Nesterova, J. Silva, A. P. Otte, M. Vidal, H. Koseki and N. Brockdorff (2004). "Polycomb group proteins Ring1A/B link ubiquitylation of histone H2A to heritable gene silencing and X inactivation." Dev Cell 7(5): 663-676.

73. Richly, H., L. Aloia and L. Di Croce (2011). "Roles of the Polycomb group proteins in stem cells and cancer." Cell Death Dis **2**: e204.

74. Endoh, M., T. A. Endo, T. Endoh, Y. Fujimura, O. Ohara, T. Toyoda, A. P. Otte, M. Okano, N. Brockdorff, M. Vidal and H. Koseki (2008). "Polycomb group proteins Ring1A/B are functionally linked to the core transcriptional regulatory circuitry to maintain ES cell identity." Development 135(8): 1513-1524.

75. Yan, Y., W. Zhao, Y. Huang, H. Tong, Y. Xia, Q. Jiang and J. Qin (2017). "Loss of Polycomb Group Protein Pcgf1 Severely Compromises Proper Differentiation of Embryonic Stem Cells." Sci Rep 7: 46276.

76. Ross, K., A. K. Sedello, G. P. Todd, M. Paszkowski-Rogacz, A. W. Bird, L. Ding, T. Grinenko, K. Behrens, N. Hubner, M. Mann, C. Waskow, C. Stocking and F. Buchholz (2012). "Polycomb group ring finger 1 cooperates with Runx1 in regulating differentiation and self-renewal of hematopoietic cells." Blood **119**(18): 4152-4161.

77. van der Lugt, N. M., J. Domen, K. Linders, M. van Roon, E. Robanus-Maandag, H. te Riele, M. van der Valk, J. Deschamps, M. Sofroniew, M. van Lohuizen and et al. (1994). "Posterior transformation, neurological abnormalities, and severe hematopoietic defects in mice with a targeted deletion of the bmi-1 proto-oncogene." Genes Dev **8**(7): 757-769.

78. Alkema, M. J., N. M. van der Lugt, R. C. Bobeldijk, A. Berns and M. van Lohuizen (1995). "Transformation of axial skeleton due to overexpression of bmi-1 in transgenic mice." Nature 374(6524): 724-727.

79. Akasaka, T., M. Kanno, R. Balling, M. A. Mieza, M. Taniguchi and H. Koseki (1996). "A role for mel-18, a Polycomb group-related vertebrate gene, during theanteroposterior specification of the axial skeleton." Development **122**(5): 1513-1522.

80. Park, I. K., D. Qian, M. Kiel, M. W. Becker, M. Pihalja, I. L. Weissman, S. J. Morrison and M. F. Clarke (2003). "Bmi-1 is required for maintenance of adult self-renewing haematopoietic stem cells." Nature 423(6937): 302-305.

81. Wiederschain, D., L. Chen, B. Johnson, K. Bettano, D. Jackson, J. Taraszka, Y. K. Wang, M. D. Jones, M. Morrissey, J. Deeds, R. Mosher, P. Fordjour, C. Lengauer and J. D. Benson (2007). "Contribution of polycomb homologues Bmi-1 and Mel-18 to medulloblastoma pathogenesis." Mol Cell Biol 27(13): 4968-4979.

82. Zhao, W., Y. Huang, J. Zhang, M. Liu, H. Ji, C. Wang, N. Cao, C. Li, Y. Xia, Q. Jiang and J. Qin (2017). "Polycomb group RING finger proteins 3/5 activate transcription via an interaction with the pluripotency factor Tex10 in embryonic stem cells." J Biol Chem **292**(52): 21527-21537.

83. Chiacchiera, F., A. Rossi, S. Jammula, M. Zanotti and D. Pasini (2016). "PRC2 preserves intestinal progenitors and restricts secretory lineage commitment." EMBO J 35(21): 2301- 2314.

84. Cheung, P., C. D. Allis and P. Sassone-Corsi (2000). "Signaling to chromatin through histone modifications." Cell **103**(2): 263-271.

85. Rinaldi, L. and S. A. Benitah (2015). "Epigenetic regulation of adult stem cell function." FEBS J 282(9): 1589-1604.

86. Vogelstein, B., N. Papadopoulos, V. E. Velculescu, S. Zhou, L. A. Diaz, Jr. and K. W. Kinzler (2013). "Cancer genome landscapes." Science 339(6127): 1546-1558.

87. Ireland H et al. Inducible Cre-mediated control of gene expression in the murine gastrointestinal tract: effect of loss of beta-catenin.

88. el Marjou F , et al. 2004. Tissue-specific and inducible Cre-mediated recombination in the gut epithelium.

89. Andras Nagy et al. Genesis 2000. Cre recombinase: The universal reagent for genome tailoring

90. Barker, N., J. H. van Es, J. Kuipers, P. Kujala, M. van den Born, M. Cozijnsen, A. Haegebarth, J. Korving, H. Begthel, P. J. Peters and H. Clevers (2007). "Identification of stem cells in small intestine and colon by marker gene Lgr5." Nature 449(7165): 1003-1007.

91.Tian, H., B. Biehs, S. Warming, K. G. Leong, L. Rangell, O. D. Klein and F. J. de Sauvage (2011). "A reserve stem cell population in small intestine renders Lgr5-positive cells dispensable." Nature 478(7368): 255-259.

92. de Lau, W., W. C. Peng, P. Gros and H. Clevers (2014). "The R-spondin/Lgr5/Rnf43 module: regulator of Wnt signal strength." Genes Dev 28(4): 305-316.

93. Leung, C., S. H. Tan and N. Barker (2018). "Recent Advances in Lgr5(+) Stem Cell Research." Trends Cell Biol 28(5): 380-391.

94. Gehart, H. and H. Clevers (2019). "Tales from the crypt: new insights into intestinal stem cells." Nat Rev Gastroenterol Hepatol 16(1): 19-34.

95. Barker, N. (2014). "Adult intestinal stem cells: critical drivers of epithelial homeostasis and regeneration." Nat Rev Mol Cell Biol 15(1): 19-33.

96. Clevers, H. (2006). Wnt/beta-catenin signaling in development and disease. Cell 127, 469–480.

97. Clevers, H., Loh, K.M., and Nusse, R. (2014). Stem cell signaling. An integral program for tissue renewal and regeneration: Wnt signaling and stem cell con- trol. Science 346, 1248012.

98. van der Flier, L.G., and Clevers, H. (2009). Stem cells, self-renewal, and differ- entiation in the intestinal epithelium. Annu. Rev. Physiol. 71, 241–260.

99. van Es JH, van Gijn ME, Riccio O, van den Born M, Vooijs M, Begthel H, Cozijnsen M, Robine S, Winton DJ, Radtke F, Clevers H (2005) Notch/gamma-secretase inhibition turns proliferative cells in intestinal crypts and adenomas into goblet cells. Nature 435: 959–963

100. Fre S, Huyghe M, Mourikis P, Robine S, Louvard D, Artavanis-Tsakonas S (2005) Notch signals control the fate of immature progenitor cells in the intestine. Nature 435: 964–968

101. VanDussen KL, Carulli AJ, Keeley TM, Patel SR, Puthoff BJ, Magness ST, Tran IT, Maillard I, Siebel C, Kolterud A, Grosse AS, Gumucio DL, Ernst SA, Tsai YH, Dempsey PJ, Samuelson LC (2012) Notch signaling modulates proliferation and differentiation of intestinal crypt base columnar stem cells. Development 139: 488–497

102. Endoh, M., Endo, T.A., Shinga, J., Hayashi, K., Farcas, A., Ma, K.W., Ito, S., Sharif, J., Endoh, T., Onaga, N., et al. (2017). PCGF6-PRC1 suppresses pre- mature differentiation of mouse embryonic stem cells by regulating germ cell-related genes. eLife 6, e21064.

103. Stielow, B., Finkernagel, F., Stiewe, T., Nist, A., and Suske, G. (2018). MGA, L3MBTL2 and E2F6 determine genomic binding of the non-canonical Polycomb repressive complex PRC1.6. PLoS Genet. 14, e1007193.

104. Madison S. Strine et al. Plos pathigens 2022. Tuft cells are key mediators of interkingdom interactions at mucosal barrier surfaces

105. Birchenough, G. M., M. E. Johansson, J. K. Gustafsson, J. H. Bergstrom and G. C. Hansson (2015). "New developments in goblet cell mucus secretion and function." Mucosal Immunol **8**(4): 712-719.

106. Worthington, J. J., F. Reimann and F. M. Gribble (2018). "Enteroendocrine cells-sensory sentinels of the intestinal environment and orchestrators of mucosal immunity." Mucosal Immunol **11**(1): 3-20.

107. Howitt, M. R., S. Lavoie, M. Michaud, A. M. Blum, S. V. Tran, J. V. Weinstock, C. A. Gallini, K. Redding, R. F. Margolskee, L. C. Osborne, D. Artis and W. S. Garrett (2016). "Tuft cells, taste-chemosensory cells, orchestrate parasite type 2 immunity in the gut." Science **351**(6279): 1329-1333.

108. Bevins, C. L. and N. H. Salzman (2011). "Paneth cells, antimicrobial peptides and maintenance of intestinal homeostasis." Nat Rev Microbiol **9**(5): 356-368.

109. Scoville, D. H., T. Sato, X. C. He and L. Li (2008). "Current view: intestinal stem cells and signaling." Gastroenterology **134**(3): 849-864.

110. Barker, N., A. van Oudenaarden and H. Clevers (2012). "Identifying the stem cell of the intestinal crypt: strategies and pitfalls." Cell Stem Cell **11**(4): 452-460.

111. Sato, T., J. H. van Es, H. J. Snippert, D. E. Stange, R. G. Vries, M. van den Born, N. Barker, N. F. Shroyer, M. van de Wetering and H. Clevers (2011). "Paneth cells constitute the niche for Lgr5 stem cells in intestinal crypts." Nature **469**(7330): 415-418.

112. Potten, C. S. (1977). "Extreme sensitivity of some intestinal crypt cells to X and gamma irradiation." Nature **269**(5628): 518-521.

113. Dekaney, C. M., A. S. Gulati, A. P. Garrison, M. A. Helmrath and S. J. Henning (2009). "Regeneration of intestinal stem/progenitor cells following doxorubicin treatment of mice." Am J Physiol Gastrointest Liver Physiol **297**(3): G461-470.

114. Nusse, R. and H. Clevers (2017). "Wnt/beta-Catenin Signaling, Disease, and Emerging Therapeutic Modalities." Cell **169**(6): 985-999.

115. **Jessica Perochon** et al. Genes, 2018 .Wnt Signalling in Intestinal Stem Cells: Lessons from Mice and Flies

116. He, X. C., J. Zhang, W. G. Tong, O. Tawfik, J. Ross, D. H. Scoville, Q. Tian, X. Zeng, X. He, L. M. Wiedemann, Y. Mishina and L. Li (2004). "BMP signaling inhibits intestinal stem cell self-renewal through suppression of Wnt-beta-catenin signaling." Nat Genet **36**(10): 1117-1121.

117. Zhen Qi and Yehua Li et al. Nature communication 2017. BMP restricts stemness of intestinal Lgr5+ stem cells by directly suppressing their signature genes

118. Guruharsha, K. G., M. W. Kankel and S. Artavanis-Tsakonas (2012). "The Notch signalling system: recent insights into the complexity of a conserved pathway." Nat Rev Genet **13**(9): 654-666.

119. Miettinen, P. J., J. E. Berger, J. Meneses, Y. Phung, R. A. Pedersen, Z. Werb and R. Derynck (1995). "Epithelial immaturity and multiorgan failure in mice lacking epidermal growth factor receptor." Nature **376**(6538): 337-341.

120. Kayahara, T., M. Sawada, S. Takaishi, H. Fukui, H. Seno, H. Fukuzawa, K. Suzuki, H. Hiai, R. Kageyama, H. Okano and T. Chiba (2003). "Candidate markers for stem and early progenitor cells,

Musashi-1 and Hes1, are expressed in crypt base columnar cells of mouse small intestine." FEBS Lett 535(1-3): 131-135.

121. Yang, Q., N. A. Bermingham, M. J. Finegold and H. Y. Zoghbi (2001). "Requirement of Math1 for secretory cell lineage commitment in the mouse intestine." Science 294(5549): 2155-2158.

122. Jadhav, U., K. Nalapareddy, M. Saxena, N. K. O'Neill, L. Pinello, G. C. Yuan, S. H. Orkin and R. A. Shivdasani (2016). "Acquired Tissue-Specific Promoter Bivalency Is a Basis for PRC2 Necessity in Adult Cells." Cell **165**(6): 1389-1400.

123. Martijn A.J.Koppens at al. Gastroenterology 2016. Deletion of Polycomb Repressive Complex 2 From Mouse Intestine Causes Loss of Stem Cell

124. Ogawa H., Ishiguro K., Gaubatz S., Livingston D. M., and Nakatani Y. (2002) A complex with chromatin modifiers that occupies E2F- and Myc-responsive genes in G0 cells. Science 296, 1132–1136 10.1126/science.1069861

125. Zhao W., Tong H., Huang Y., Yan Y., Teng H., Xia Y., Jiang Q., and Qin J. (2017) Essential role for polycomb group protein Pcgf6 in embryonic stem cell maintenance and a noncanonical polycomb repressive complex 1 (PRC1) integrity. J. Biol. Chem. 292, 2773–2784 10.1074/jbc.M116.763961

126. Matzuk M. M., and Lamb D. J. (2002) Genetic dissection of mammalian fertility pathways. Nat. Cell Biol. 4, s41–s49 10.1038/ncb-nm-fertilityS41

127. Mengjie Liu, et all. The polycomb group protein PCGF6 mediates germline gene silencing by recruiting histone-modifying proteins to target gene promoters

128. Huang Y., Zhao W., Wang C., Zhu Y., Liu M., Tong H., Xia Y., Jiang Q., and Qin J. (2018) Combinatorial control of recruitment of a variant PRC1.6 complex in embryonic stem cells. Cell Rep. 22, 3032–3043 10.1016/j.celrep.2018.02.072

129. 10. Zhao W., Tong H., Huang Y., Yan Y., Teng H., Xia Y., Jiang Q., and Qin J. (2017) Essential role for polycomb group protein Pcgf6 in embryonic stem cell maintenance and a noncanonical polycomb repressive complex 1 (PRC1) integrity. J. Biol. Chem. 292, 2773–2784 10.1074/jbc.M116.763961

130. Qin J., Whyte W. A., Anderssen E., Apostolou E., Chen H. H., Akbarian S., Bronson R. T., Hochedlinger K., Ramaswamy S., Young R. A., and Hock H. (2012) The polycomb group protein

L3mbtl2 assembles an atypical PRC1-family complex that is essential in pluripotent stem cells and early development. Cell Stem Cell 11, 319–332 10.1016/j.stem.2012.06.002

131. Maeda I., Okamura D., Tokitake Y., Ikeda M., Kawaguchi H., Mise N., Abe K., Noce T., Okuda A., and Matsui Y. (2013) Max is a repressor of germ cell-related gene expression in mouse embryonic stem cells. Nat. Commun. 4, 1754 10.1038/ncomms2780

132. Pohlers M., Truss M., Frede U., Scholz A., Strehle M., Kuban R. J., Hoffmann B., Morkel M., Birchmeier C., and Hagemeier C. (2005) A role for E2F6 in the restriction of male-germ-cell-specific gene expression. Curr. Biol. 15, 1051–1057 10.1016/j.cub.2005.04.060

133. Chao-Shun et al,.Sci Rep 2016. Polycomb Group Protein Pcgf6 Acts as a Master Regulator to Maintain Embryonic Stem Cell Identity

134. Zdzieblo D, Li X, Lin Q, Zenke M, Illich DJ, et al. (2014) Pcgf6, a polycomb group protein, regulates mesodermal lineage differentiation in murine ESCs and functions in iPS reprogramming. Stem Cells 32: 3112–3125.:
135. Zdzieblo D, Li X, Lin Q, Zenke M, Illich DJ, et al. (2014) Pcgf6, a polycomb group protein, regulates mesodermal lineage differentiation in murine ESCs and functions in iPS reprogramming. Stem Cells 32: 3112–3125.

136. Huang, X., Wei, C., Li, F. et al. PCGF6 regulates stem cell pluripotency as a transcription activator via super-enhancer dependent chromatin interactions. Protein Cell 10, 709–725 (2019).

137. Kagey MH, Newman JJ, Bilodeau S, Zhan Y, Orlando DA, van Berkum NL, Ebmeier CC, Goossens J, Rahl PB, Levine SS, et al. Mediator and cohesin connect gene expression and chromatin architecture. Nature. 2010;467(7314):430–435. doi: 10.1038/nature09380.

138. nina

139. Burnichon N, Cascón A, Schiavi F, Morales NP, Comino-Méndez I, Abermil N, Inglada-Pérez L, de Cubas AA, Amar L, Barontini M, et al. (2012) MAX mutations cause hereditary and sporadic pheochromocytoma and paraganglioma. Clin Cancer Res 18: 2828–2837. 10.1158/1078-0432.CCR-12-0160

140. omero OA, Torres-Diz M, Pros E, Savola S, Gomez A, Moran S, Saez C, Iwakawa R, Villanueva A, Montuenga LM, et al. (2014) MAX inactivation in small cell lung cancer disrupts MYC-SWI/SNF

programs and is synthetic lethal with BRG1. Cancer Discov 4: 292–303. 10.1158/2159-8290.CD-13-0799

141. Mathsyaraja H, Catchpole J, Freie B, Eastwood E, Babaeva E, Geuenich M, Cheng PF, Ayers J, Yu M, Wu N, et al. (2021) Loss of MGA repression mediated by an atypical polycomb complex promotes tumor progression and invasiveness. Elife 10: e64212. 10.7554/eLife.64212

142. Zhang Y, Li C, Xue W, Zhang M, Li Z (2018) Frequent mutations in natural killer/T cell lymphoma. Cell Physiol Biochem 49: 1–16. 10.1159/000492835

143. eddy A, Zhang J, Davis NS, Moffitt AB, Love CL, Waldrop A, Leppa S, Pasanen A, Meriranta L, Karjalainen-Lindsberg ML, et al. (2017) Genetic and functional drivers of diffuse large B cell lymphoma. Cell 171: 481–494.e15. 10.1016/j.cell.2017.09.027

144. Di Croce L, Helin K (2013) Transcriptional regulation by Polycomb group proteins. Nat Struct Mol Biol 20: 1147–1155. 10.1038/nsmb.2669

145. Moritz Middelhoff, C. Benedikt Westphalen, [...], and Michael Quante, Dclk1-expressing tuft cells: critical modulators of the intestinal niche?

146. 112. Sato A. Tuft cells. Anat Sci Int 82: 187–199, 2007. doi: 10.1111/j.1447-073X.2007.00188.x

147. Chase CC, Munn EA. Surface binding and uptake of polycationic ferritin by neonatal piglet intestinal epithelium. J Cell Sci 46: 235–252, 1980.

148. Bezençon C, Fürholz A, Raymond F, Mansourian R, Métairon S, Le Coutre J, Damak S. Murine intestinal cells expressing Trpm5 are mostly brush cells and express markers of neuronal and inflammatory cells. J Comp Neurol 509: 514–525, 2008. doi: 10.1002/cne.21768.

149. Bjerknes M, Khandanpour C, Möröy T, Fujiyama T, Hoshino M, Klisch TJ, Ding Q, Gan L, Wang J, Martín MG, Cheng H. Origin of the brush cell lineage in the mouse intestinal epithelium. Dev Biol 362: 194–218, 2012. doi: 10.1016/j.ydbio.2011.12.009.

150. jerknes M, Khandanpour C, Möröy T, Fujiyama T, Hoshino M, Klisch TJ, Ding Q, Gan L, Wang J, Martín MG, Cheng H. Origin of the brush cell lineage in the mouse intestinal epithelium. Dev Biol 362: 194–218, 2012. doi: 10.1016/j.ydbio.2011.12.009.

151. Matsumoto I, Ohmoto M, Narukawa M, Yoshihara Y, Abe K. 2011. Skn-1a (Pou2f3) specifies taste receptor cell lineage. Nat Neurosci 14: 685–687.

152. Junpei Yamashita, Makoto Ohmoto, Tatsuya Yamaguchi, Ichiro Matsumoto. Plos One, 2017 Skn-1a/Pou2f3 functions as a master regulator to generate Trpm5-expressing chemosensory cells in mice

153. Matsumoto I, Ohmoto M, Narukawa M, Yoshihara Y, Abe K. Skn-1a (Pou2f3) specifies taste receptor cell lineage. Nat Neurosci. 2011;14: 685–687. pmid:21572433

154. Howitt MR, Lavoie S, Michaud M, et al. Tuft cells, taste-chemosensory cells, orchestrate parasite type 2 immunity in the gut. Science. 2016;351(6279):1329-1333. doi:10.1126/science.aaf1648

155. Gerbe, F., Sidot, E., Smyth, D. et al. Intestinal epithelial tuft cells initiate type 2 mucosal immunity to helminth parasites. Nature 529, 226–230 (2016). https://doi.org/10.1038/nature16527

156. von Moltke, J., Ji, M., Liang, HE. et al. Tuft-cell-derived IL-25 regulates an intestinal ILC2–epithelial response circuit. Nature 529, 221–225 (2016).

157 Marija S. Nadjsombati et al. Immunology 2018. Detection of Succinate by Intestinal Tuft Cells Triggers a Type 2 Innate Immune Circuit

158. Amrita Banerjee et al., Gatroenterology 2020. Succinate Produced by Intestinal Microbes Promotes Specification of Tuft Cells to Suppress Ileal Inflammation

159. Westphalen CB, Asfaha S, Hayakawa Y, Takemoto Y, Lukin DJ, Nuber AH, Brandtner A, Setlik W, Remotti H, Muley A, Chen X, May R, Houchen CW, Fox JG, Gershon MD, Quante M, Wang TC. Long-lived intestinal tuft cells serve as colon cancer-initiating cells. J Clin Invest 124: 1283–1295, 2014. doi: 10.1172/JCI73434

160. Jennifer E. Phillips et al. Cell 2003. Master Weaver of the Genome

161. Jessica Zuin, et al,. PNAS 2013. Cohesin and CTCF differentially affect chromatin architecture and gene expression in human cells

MATERIALS AND METHODS

MOUSE MODELS

Mice were housed accordingly to the guidelines set out in the European Commission Recommendation 2007/526/EC, 18 June 2007, for the accommodation and care of animals used in experimental and other scientific purposes. All experiments were performed in accordance with the Italian Law (D.L.vo 116/92 and following additions), which enforces the EU 86/609 Directive (Council Directive 86/609/EEC of 24 November 1986 on the approximation of laws, regulations and administrative provisions of the Member States regarding the protection of animals used for experimental and other scientific purposes).

In this study were used different conditional knock out mouse models:

- The LGR5-GFP-ires-CreERT2 Rosa26lox-stop-lox LacZ mice were used for lineage tracing, in which only the LGR5+ ISC expresses the Cre recombinase. (Barker, van Es et al. 2007). Cre recombinase activation in LGR5-CreERT2 strains was induced by performing four intraperitoneal injections of Tamoxifen (Sigma-Aldrich) dissolved at 75mg/kg in corn oil.
- The AhCre mice in which the Cre recombinase is expressed upon CYP1A1 promoter, in whole intestinal epithelium, with the only exception of Paneth cells. Induction of Cre transcription is allow after 4 intraperitoneal injections of beta-naphthoflavone dissolved at 80 mg/kg in corn oil (Ireland, Kemp et al. 2004).
- VillinCREert2 mice in which the Cre recombinase is expressed under the Villin intestinal specific promoter. In this case the nuclear translocation of Cre recombinase is permitted after four intraperitoneal injections of Tamoxifen (Sigma-Aldrich) dissolved at 75mg/kg in corn oil.

We crossed this mouse model with conditional PCGFs KO mice in order to obtain different strains that allow the deplation of single, double and triple PCGFs. In particular, we obtained:

- *LGR5-GFP-ires-CreERT2 Rosa26lox-stop-lox LacZ ; PCGF1* $^{fl/fl}$
- *LGR5-GFP-ires-CreERT2 Rosa26lox-stop-lox LacZ ; PCGF2/4* $^{fl/fl}$

- *LGR5-GFP-ires-CreERT2 Rosa26lox-stop-lox LacZ ; PCGF3/5* $^{fl/fl}$
- *LGR5-GFP-ires-CreERT2 Rosa26lox-stop-lox LacZ ; PCGF6* $^{fl/fl}$
- *LGR5-GFP-ires-CreERT2 Rosa26lox-stop-lox LacZ ; PCGF1/2/4* $^{fl/fl}$
- *LGR5-GFP-ires-CreERT2 Rosa26lox-stop-lox LacZ ; PCGF1/3/5/6* $^{fl/fl}$

- *AhCRE ; PCGF1* $^{fl/fl}$
- *AhCRE ; PCGF3/5* $^{fl/fl}$
- *AhCRE ; PCGF6* $^{fl/fl}$

- *VillinCREert2 ; PCGF1* $^{fl/fl}$
- *VillinCREert2 ; PCGF2/4* $^{fl/fl}$
- *VillinCREert2 ; PCGF1/2/4* $^{fl/fl}$
- *VillinCREert2 ; PCGF6* $^{fl/fl}$

GENOTYPING

Ear biopsies were conserved in 100% Ethanol and washed with 1X PBS before DNA extraction. Samples were digested in 200 ul μL Digestion buffer (TRIS-HCl pH 7,5 10 mM, EDTA pH8 10 mM, NaCl 10 mM, SDS 0,5%) with 0.5 mg/ml Proteinase K at 52°C for at least 5 hours or overnight shaking. Digested tissues were then purified by adding 1 volume of each Guanidine thiocyanate solution (Guanidine Thiocyanate 0,345 g/ml, EDTA pH8 10 mM, TRIS-HCl pH 7,5 10 mM, NaCl 10 mM) and 75% Ethanol. DNA was isolated with conoSpin^{TM} Spin Column for DNA (Epoch Life Science), and eluated with water. 5 μL of this DNA were used for each PCR.

HISTOLOGY ANALYSIS

Intestines were harvest immediately after death. Duodenum, jejenum and ileum of the small intestine were cleaned, flushed with cold PBS, opened longitudinally and fixed for 12h at 4C in 4% formaldehyde. Samples were kept in EtOH at 70% for one day. Then samples were embedded in paraffin and 5um sections were obtained using microtome. Morphology analysis of intestines was performed by hematoxylin and eosin. Immunohistochemistry analyses were done with heat-induced antigen unmasking solution 10mM Sodium Citrate, and blocking with 5% BSA. Anti-lysozyme (Dako, A0099), anti-ChgA (Abcam, ab15160), anti-DCLK1 (Cell Signalling 62257) and anti-KI67 (Abcam, ab16667), were used as primary antibodies in blocking solution overnight at 4C. Periodic acid–Schiff (PAS) and Alcian blue staining were used following manufacturer's instructions. For immunofluorescence analysis fresh tissue where briefly fixed with PFA 4% for 3 hours at 4°C and then placed in 30% sucrose over-night followed by embedding in OCT (Tissue TEK 4583). Samples were sectioned with cryostat at 4um thickness. Anti – Pou2f3 (Sigma) was used as primary antibody in blocking solution overnight at 4C, and nuclei were co-stained with DAPI.

For lineage tracing, intestine was pre fixied for 3 hours at 4°C in a solution containing PBS Gluteraldehyde 0.2%, NP-40 0,02% and PFA 2%. After washing in PBS, tissues were incubated for 1 hour at room temperature with the Equilibration Buffer containing MgCl2 2mM, NP-40 0,02% and Sodium Deoxycholate 0,1% in PBS. Tissues were stained overnight at RT with 5 mM K3Fe(CN)6, 5 mM K4Fe(CN)6 and 1mg/ml X-Gal (5-bromo-4-chloro-3-indolyl- beta-D-galactopyranoside) in equilibration buffer. 24 hours later, intestine was washed with PBS and fixed over-night in 4% PFA. The embedded as described in the Histology section. All images were acquired using an Olympus BX51 bright field microscopy and Leica Sp8 confocal microscope.

INTESTINAL CRYPTS PURIFICATION

Small intestine was harvested, flashed with cold PBS, and opened longitudinally. Villi were removed with glass coverslip by scraping the tissue. Organ was then chopped in small pieces and incubated in PBS with 2mM for 10 minutes, and then with 5mM for 45 minutes. Intestine was resuspended in 20 ml cold PBS (+ 1% FBS) and shacked to isolate crypts mechanically. Supernatant was passed through a 70 μM cell strainer. Obtained crypts were used for other techniques.

CHROMATIN IMMUNOPRECIPITATION PREPARATION FOR NGS

Intestines were harvested and intestinal crypts were isolated by digestion with 2mM EDTA in PBS. Samples were fixed in 1% formaldehyde for 15 minutes at room temperature. Fixation reaction was quenched using Glycin at 2M and samples were resuspended in SDS 0,5%. Chromatin was resuspended in IP buffer (2 volume of SDS buffer 0,5% + 1 volume Triton solution) and sonicated in order to obtain bulk DNA fragment of 300-500 bp. Immunoprecipitation of transcription factor was performed by using 500ug of chromatin and 8ug of antibody, and immunoprecipitation of histone modifications were performed by using 250ug of chromatin and 5ug antibody. Anti - Ring1b (homemade), anti – PCGF6 (homemade), anti- H2AK119ub1 (cell signaling D27C4) were used as primary antibody overnight at 4°C. Protein-antibody complexes were pulled down with Sepharose Protein A beads. DNA was isolated with decrosslinking solution (NaHCO3 0.1 M and SDS 1% at 65°C shacking) and purified with PCR purification Kit (Qiagen). Enrichment was verified with qPCR checking specific targets. For Ring1b and H2AK119ub1 were used as targets: HOXA11) HOXD9, WNT5A. For PCGF6 were used as target for enrichment verification PCED1 (, MICU2. (Primers sequences are available upon request). DNA was sequenced with Illumina HiSeq2000.

ChIP SEQUENCING AND ANALYSIS

Paired-end reads were aligned to the mouse reference genome mm10, or mm10 and dm6 for histone ChIP-Rx, using Bowtie v1.2.2 (Langmead et al., 2009) without allowing for multi-mapping (–m 1) and parameters -l 10 -X 1000. PCR duplicates were removed using samblaster . Ambiguous reads mapping to both mm10 and dm6 were discarded. Peaks were called using MACS2 v2.1.1 (Zhang et al., 2008) with parameters -f BAMPE --keep-dup all -m 10 30 -p 1e-10. Genomic peak annotation was performed with the R package ChIPpeakAnno v3.15 (Zhu et al., 2010), considering the region+/– 2.5 kb around the TSS as the promoter. Overlaps were performed using the R package VennDiagram v1.6.20 (Chen and Boutros, 2011). Gene ontology analyses of ChIP-seq targets were performed using the Bioconductor package clusterProfiler (Yu et al., 2012) setting as threshold an adjusted p-value and q-value of 0.01.

For heatmap and intensity plot representation of ChIP-seq signal, BigWig files with input signal subtracted were generated using the function bamCompare from deepTools 2.0 (Ramirez et al., 2016) with parameters --ratio subtract –bs 50 --extendReads. To normalize for differences in sample library size, a scaling factor for each sample was calculated as (1/total mapped reads)*1000000 and was applied during BigWig file generation with the parameter --scaleFactors from bamCompare. For ChIP-Rx samples the scaling factor was calculated as described in (Orlando et al., 2014). Heatmaps were performed using the functions computeMatrix with settings reference-point --referencePoint center/TSS -b 8000 -a 8000 -bs 50, followed by plotHeatmap from deepTools excluding blacklisted regions by ENCODE (Consortium, 2012). For boxplot representation the function multiBigwigSummary (using BED-file and --outRawCounts options) from deeptools was used to calculate the number of reads under peaks, which was further normalized by peak size (kb).

RNA PREPARATION

Total RNA extraction was performed by using RNasy Plus KIT (Qiagen) on crypts isolated pellets. RNA was eluted with Nuclease free water (Ambion) and stored at – 80. 2ng of extracted RNA was

processes following Smart-seq2 protocol (Switching Mechanism at the 5' end of the RNA Transcript) (Picelli, Faridani et al. 2014) with minor modification, for NGS. For RT-qPCR were used 500-1000ng of purified RNA. RT was performed with ImProm-IITM Reverse Transcriptase reagents, following Promega standard transcription protocol. Retrotranscribed cDNA was analyzed by RT-qPCR with SYBER green Qpcr Master Mix (Applied bioscience) with the primers list described in Table.

RNA SEQUENCING AND ANALYSIS

RNA quality control was performed with Bionalyzer. Reads were aligned to the mouse reference genome mm10 using STAR v2.7 (REF) without allowing multimapping reads (--outFilterMultimapNmax 1). PCR duplicates were removed using samblaster (REF). Gene counts were calculated using featureCounts (REF) with parameters -s 0 -t exon -g gene_name using Gencode (REF) M21 (GRCm38) annotation downloaded from (https://www.gencodegenes.org/mouse/). Differential expression analyses were performed using the R package DESeq2 v1.20 (Love et al., 2014) using default parameters. Genes with an absolute log2 fold change of 1.5 and FDR < 0.05 were considered as differentially expressed. Gene ontology analysis of differentially expressed genes was performed using the Bioconductor package clusterProfiler (Yu et al., 2012) with default parameters.

PROTEIN EXTRACTION AND WESTERN BLOT

To obtained proteins, Intestinal crypts pellets were lysed with S300 buffer (TRIS- HCl pH 8 20 mM, NaCl 300 mM, Glycerol 10%, Igepal 0.2%) with protease inhibitors. Lysates were then diltuted with LEAMMLY buffer 1x at concentration of 2ug/ul. Lysate were separated on SDS-PAGE and transferred on nitrocellulose membrane. Blocking was performed with 5% low fat dried milk in TBS 0,05% Tween 20. First antibodies were diluted in blocking solution at the dilution reported in Table.

Secondary antibodies were also diluted in blocking solution. Signal revelation was perfomed with ClarityTM Western ECL Substrate (Bio Rad) and acquired using ChemiDoc XRS+ (Bio Rad).

MURINE LAMINA PROPRIA MONONUCLEAR CELL AND EPITHELIAL CELL ISOLATION FROM SMALL INTESTINE.

For LPMC isolation, small intestine was collected, Peyer's Patches removed, and tissues were cleared of faces in ice cold PBS. Tissues were cut in small pieces (approx. 0.5 cm) and incubated on shaking for 30 min in RPMI 2% FBS, DTT 1mM, EDTA 0.5M. The step was repeated twice without the use of DTT the second time. Epithelial cells were collected from these steps and used for further analysis. Tissues were then mechanically homogenized in 4 ml of RPMI 2% FBS using the GentleMACS protocol "mouse-intestine" three times. The homogenized was filtered sequentially through a 100 µm and a 70 µm filter. LPMC were isolated with a Percoll gradient, by layering cells, in 5 ml of 40% Percoll, on top of 5 ml 100% Percoll. Cells were centrifuged for 20 min at 400 g with no acceleration and no break. LPMC were collected from the white ring formed between the two Percoll phases. Cells were then used for staining and flow cytometry.

FLOW CYTOMETRY

Cells were stained extracellularly using ice cold PBS for 15 min at 4C. Unspecific antibody binding was blocked by using CD16/32. Cell fixation, permeabilization and intracellular staining was performed using the FOXP3/Transcription factor staining buffer set (Thermofisher) as described by the vendor. Samples were acquired using a FACSCelesta flow cytometer (BD Biosciences, Franklin Lakes NJ, USA). Data were analyzed using the FlowJo software (Version 10.7, TreeStar, Ashland, OR, USA).

MINI-GUT CULTURE PREPARATION

Mini-Gut cultures were prepared as previously described (Sato et al, 2009). Briefly, 800 intestinal crypt were embedded in Matrigel (BD Biosciences) and plated in a single well of 24-wells plate. Mini-gut were cultured in Advanced DMEM/ F12 supplemented with HEPES, Glutammine, antibiotics, N2, B27, EGF (all from GE Healthcare), Noggin (Peprotech), and mRSPO1 (homemade). First two days all mini-gut cultures were growth also with WNT5a supplements. For RNA extraction, first minigut was isolated by descrap Matrigel with Corning solution (sigma). Then RNA was estracted with RNasy micro KIT (Qiagen).

Table of Antibodies

Marker	Reactivity	Clone	Vendor	Cat.no	Dilution	Color
CD16/32	Mouse	2.4G2	TONBO	70-0161-U500	1:50	-
CD127	Mouse	A7R34	Biolegend	135039	1:200	APC.Cy7
CD11b	Mouse	M1/70	TONBO	35-0112-U100	1:200	FITC
CD11c	Mouse	N418	TONBO	35-0114-U100	1:200	FITC
CD3	Mouse	17A2	TONBO	35-0032-U100	1:200	FITC

CD19	Mouse	1D3	TONBO	35-0193-U100	1:200	FITC
CD45.2	Mouse	104	Biolegend	109838	1:200	BV510
CD25	Mouse	P61	Biolegend	102029	1:200	PerCP.Cy5.5
IL25R	Mouse	MUNC33	Thermofisher	12-7361-82	1:200	PE
GATA3	Human/Mouse	L50-823	BD	563349	1:100	BV421
RORγT	Human/Mouse	AFKJS-9	eBioscience	17-6988-80	1:100	APC

9. FIGURE TABLE

2.3 EPIGENETIC AND POLYCOMB GROUP PROTEIN

4.1 SINGLE PCGFS ARE DISPENSABLE FOR INTESTINAL HOMEOSTASIS

E. HE of intestinal sections from AhCRE Ctrl and AhCRE PCGF1, PCGF3/5, PCGF6 KOs

F. HE of intestinal sections from VillinCREert2 Ctrl and VillinCREert2 PCG2/4 KO.

Figure 4.1.3: immunohistochemistry of intestinal section derived from wild type and KO mice at 15 days

A. IHC for Lysozyme, Chromogranin A and Alcian Blue in AhCre wild type and AhCre PCGF1, PCGF3/5 and PCGF6 KOs

B. IHC for Lysozyme, and Alcian Blue in VillinCREert2 wild type and VillinCREert2 PCGF2/4 KO

Figure 4.1.4: immunohistochemistry of intestinal section derived from wild type and KO mice at 15 days

C. IHC for Ki67 of AhCre wild type and AhCre PCGF1, PCGF3/5 and PCGF6 KOs sections

D. IHC for Ki67 VillinCREert2 wild type and VillinCREert2 PCGF2/4 KO

Figure 4.1.5: Beta-Galactosidase reaction on intestinal sections from LGR5-GFP-ires-CreERT2/Rosa26Lox-stop-Lox LacZ wild type and KOs mice. Panel of LacZ staining at 7 days (top) and 15 days (bottom) in LGR5-GFP-ires-CreERT2/Rosa26Lox-stop-Lox LacZ and LGR5-GFP-ires-CreERT2/Rosa26Lox-stop-Lox LacZ PCGF1, PCGF3/5, PCGF6 and PCGF2/4 KOs

4.2 Single PCGFs are dispensable PRC1 activity in intestinal cells

Figure 4.2.1: Chromatin immunoprecipitation following by sequencing for H2Ak119ub1 across Ring1b peaks for wild type intestinal cells and PCGF single KOs.

C. Heatmaps of H2AK119ub1 ChIP levels on Ring1b targets

D. Boxplot of quantitative H2AK119ub1 ChIP levels on Ring1b targets

Figure 4.2.2: Chromatin immunoprecipitation following by sequencing for H2Ak119ub1 genome-wide for wild type intestinal cells and PCGF single KOs.

C. Boxplot of H2AK119ub1 genome-wide signal at promoter (left) and intergenic (right) regions

D. Intergenic H2Ak119ub signal

Figure 4.2.3: Chromatin immunoprecipitation following by sequencing for H2Ak119ub1 genome-wide for wild type intestinal cells and PCGF single KOs.

C. Boxplot of H2AK119ub1 genome-wide signal at promoter (left) and intergenic (right) regions
D. Intergenic H2Ak119ub signal

Figure 4.2.4: Chromatin immunoprecipitation following by sequencing for H2Ak119ub1 across Ring1b targets for wild type intestinal cells and PCGF single KOs.

C. Heatmap representing normalized Ring1b CHIP-seq intensity of +/- 5Kb from TSS of Ring1b target genes in intestinal Crypts
D. Boxplot of quantification Ring1b ChIp-seq intensity of Ring1b target genes

Figure 4.2.5: Chromatin immunoprecipitation following by sequencing for H3K27me3 genome-wide for wild type intestinal cells and PCGF single KOs.

A. Heatmap representing normalized H3K27me3 CHIP-seq intensity of +/- 5Kb from TSS of Ring1b target genes in intestinal Crypts
B. Boxplot of quantification H3K27me3 ChIp-seq intensity of Ring1b target genes

4.3 PCGF loss does not affect PRC1 associated transcriptional repression

Figure 4.3.1: Transcriptome profile of adult intestinal cells derived from single Knock out mice

C. Volcano blot of de-regulated genes in Ring1a/b dKO, PCGF1 KO, PCFF2/4 KO, PCGF3/5 KO and PCGF6 compared to wild type
D. Gene ontology enrichment analysis of upregulated genes (top) and downregulated genes (battom)

Figure 4.3.2: Transcriptome profile of adult intestinal cells derived from single Knock out mice show different overlap

C. Column graph showing percentage of de-regulated genes in single PCGF KO and Ring1b KO in dult intestinal cells
D. Overlap of downregulated genes found in different PCGF single KOs (left) and upregulated gene (right)

4.4 PRC1 subcomplexes regulates specific clusters of targets genes

Figure 4.4.1: Boxplot showing peaks length and number for different PCGFs chromatin binding

D. Peaks length for PCGF2 and PCGF4
E. Peaks length for PCGF1, PCGF3, PCGF5 and PCGF5
F. Total Number of single PCGFs target genes

Figure 4.4.2: PCGFs chromatin localization in wild type intestinal cells / cluster targets genes

Figure 4.4.3: PCGFs association on promoter/intergenic region and on CpG rich island

Figure 4.4.4: Heatmaps representing ChIP-seq normalized PCGF1, PCGF2, PCGF3, PCGF4, PCGF6 Ring1b, SUZ12, H2AKI19ub1 and H3K27me3 ChIP-seq intensity of +/- 5Kb from TSS of specific and common PCGFs target genes

Figure 4.4.5: PCGFs bindings unique and common target genes on chromatin in adult intestinal cells.

A.Column graph representing overlap among PCGFs target genes
B. Motif enrichment analysis of PCGFs target genes

Figure 4.4.6: PCGF proteins show different binding with PRC1 and PRC2 target genes

E. Column graph representing overlap between PCGF targets genes and Ring1b target genes
F. Column graph representing overlap between PCGF targets genes and H2Aub1 target genes
G. Column graph representing overlap between PCGF targets genes and SUZ12 target genes
H. Column graph representing overlap between PCGF targets genes and H3K27me3 target gene

Figure 4.4.7: Gene ontology enrichment analysis of PCGFs unique and common targets genes

Figure 4.4.8: column graph representing mRNA expression of PCGFs unique and common target genes

4.5 PCGF1, PCGF2, PCGF4 are indispensable for intestinal cell self-renewal and cellular identity

Figure 4.5.1 Lineage tracing analyses of LGR5-GFP-ires-CreERT2 /Rosa26Lox-stop-Lox LacZ at 7, 15 and 30 dpi

Lineage tracing analyses of Ring1a/b dKO, PCGF1/2/4 tKO and PCGF1/3/5/6 qKO, showing the effects of depletion of these subcomplexes on ISC self-renewal and differentiation.

Figure 4.5.2 Lineage tracing analyses of LGR5-GFP-ires-CreERT2 /Rosa26Lox-stop-Lox LacZ at 30 dpi.
Lineage tracing analyses of Ring1a/b dKO, PCGF1/2/4 tKO and PCGF1/3/5/6 qKO, showing the effects of depletion of these subcomplexes on ISC self-renewal and differentiation.

Figure 4.5.3 GFP signal in LGR5-GFP-ires-CreERT2 /Rosa26Lox-stop-Lox LacZ at 30 dpi.

C. Intestinal section stained for DAPI (nuclei) and GFP (LGR5 + ISC)
D. Quantification of percentage of LGR5-GFP+ ISC wild type, Ring1a/b KO, PCGF1/2/4 KO and PCGF1/3/5/6 KO mice

Figure 4.5.4: VillinCREert2 mouse model. PCGF1/2/4 depletion alters intestinal architecture

C. Pictures of intestine of wild type and KO mice
D. Histology analysis of wild type and PCGF1/2/4 KO intestinal section. Hematoxylin and Eosin (up) and Immunoistochemystry for Ki67 (battom)

Figure 4.5.5 Immunofluorescence staining for H2AK119Ub1 level (green) and Ki67 (red) in VillinCREert2 wild type and PCGF1/2/4 KO at different time points.

Figure 4.5.6 immunoistochemistry staining for CHGA (enteroendocrine), DCLK1 (Tuft), Lyzozyme (Paneth) and Alcian Blue (Goblet) in
VillinCREert2 wild type and PCGF1/2/4 KO.

Figure 4.5.7: Alkaline phosphatase staining for enterocytes in VillinCREert2 and VillinCREert2 PCGF1/2/4 KO at 15 and 21 days.

4.6 Loss of PRC1.1, PRC1.2 and PRC1.4 resulted in total RING1b chromatin displacement, loss of H2AK119ub1 and strong transcriptional reactivation

Figure 4.6.1: Heatmap representing normalized H2AK119ub1 CHIP-seq intensity of +/- 5Kb from TSS of Ring1b target genes in intestinal Crypts from PCGF1, PCGF2/4 and PCGF1/2/4 KO.

Figure 4.6.2: Heatmap representing normalized H2AK119ub1 CHIP-seq intensity of +/- 5Kb from TSS of Ring1b target genes in intestinal Crypts from PCGF1, PCGF2/4 and PCGF1/2/4 KO.

Figure 4.6.3: Heatmap representing normalized H3K27me3 CHIP-seq intensity of +/- 5Kb from TSS of Ring1b target genes in intestinal Crypts from PCGF1, PCGF2/4 and PCGF1/2/4 KO.

Figure 4.6.4: Principal component analysis of transcriptome profiles of Ring1a/b KO, PCGF1 KO, PCGF2/4 KO and PCGF1/2/4 KO intestinal cells at 15 days prost tamoxifen administration

Figure 4.6.5: Volcano blot of deregulated genes In VillinCREert2 PCGF1/2/4 tKO derived intestinal cells. In green downregulated genes, in red upregulated genes.

Figure 4.6.6: Gene ontology analysis of deregulated genes in PCGF 1/2/4 KO adult intestinal cells.

Figure 4.6.7: Column plot of percentage expression of RING1b associated genes in RING1b KO, PCGF1 KO, PCGF2/4 KO and PCGF1/2/4 KO

Figure 4.6.8: Boxplot showing the expression of common or unique PCGFs target genes in adult intestinal cells upon depletion of RING1b, PCGF1, PCGF2/4 and PCGF1/2/4

4.7 PCGF6 displays different role in Intestinal cells compare to ESc

Figure 4.7.1: Differences of PCGF6 distribution in intestinal cells and ESc.

C. Diagram showing the percent of PCGF6 targets at CpG positive and negative chromatin regions.
D. Column graph representing the specificity of PCGF6 and the very low co-occupancy on chromatin with other PCGF proteins.

Figure 4.7.2: DNA localization of PRC1.6 in adult intestinal cells

D. Motif discovery analysis discovery performed underneath the summit of PCGF6 peaks globally
E. Column graph representing the specificity of PCGF6 and the very low co-occupancy on chromatin with other PCGF proteins.

F. Motif discovery analysis discovery performed underneath the summit of PCGF6 peaks on promoter and intergenic regions

Figure 4.7.3: Heatmaps of ChIp - sequencing analysis on adult intestinal cells.

E. Heatmap representing normalized PCGF6 CHIP-seq intensity of +/- 5Kb from TSS of PCGF6 loci
F. Heatmap representing normalized Ring1b CHIP-seq intensity of +/- 5Kb from TSS of Ring1b target genes in intestinal Crypts
G. Heatmap representing normalized H2AK119ub1 CHIP-seq intensity of +/- 5Kb from TSS of Ring1b target genes in intestinal Crypts
H. Heatmap representing normalized H3K27me3 CHIP-seq intensity of +/- 5Kb from TSS of Ring1b target genes in intestinal Crypts

Figure 4.7.4: Vann diagram showing the overlap between Ring1b targets, PCGF6 targets and H2AK119ub1 positive loci in adult intestinal cells

4.8 PCGF6 Knock Out do not show apparent intestinal homeostasis alteration

Figure 4.8.1: Histology of Duodenum from wild type and PCGF6 KO mice. Beta-Galactosidase reaction on intestinal sections from LGR5-GFP-ires-CreERT2/Rosa26Lox-stop-Lox LacZ wild type and PCGF6 KOs mice (upper panel). Hematoxylin and Eosin of duodenum sections (bottom panel).

Figure 4.8.2: Immunohistochemistry staining for Ki67 (proliferation marker), LYZ (Paneth cells), CHGA (enteroendocrine cells), Alcian Blue (Goblet cells) in VillinCREert2 and VillinCREert2: PCGF6 KO derived intestinal sections.

4.9 PCGF6 Knock Out do not show apparent intestinal homeostasis alteration

Figure 4.9.1: Immunohistochemistry staining for DCLK1 in intestinal sections.

C. Immunohistochemistry staining for DCLK1 (Tuft cells) in AhCRE wild type and AhCRE PCGF6 KO (upper panel) and VillinCREert2 and VillinCREert2: PCGF6 KO derived intestinal sections.
D. Quantification of DCLK1+ Tuft cell in AhCRE wild type and AhCRE PCGF6 KO (upper panel) and VillinCREert2 and VillinCREert2: PCGF6 KO

Figure 4.9.2: Tuft cells accumulation in PCGF6 KO intestine.

C. DCLK1 protein levels in VillinCREert2 and VillinCREert2; PCGF6 KO crypts
D. mRNA levels of Tuft cell specific markers in VillinCREert2 and VillinCREert2: PCGF6 KO crypts

4.10 PCGF6 directly controls Tuft cell signature including master regulator Pou2f3

Figure 4.10.1: Mini guts grown from intestinal crypts

C. Pictures of organoids derived from AhCRE and AhCRE PCGF6 KO, after 3 days of culturing (left) and mRNA relative expression of PCGF6 and DCLK1 7 day after plating.
D. Immunofluorescence for DCLK1 of organoids derived from VillinCREert2 and VillinCREert2 PCGF6 KO, after 7 days of culturing (left) and mRNA relative expression of PCGF6 and DCLK1 7 day after plating.

Figure 4.10.1: Transcriptome profile of PCGF6 deficient intestinal cell show upregulation of Tuft cell signature.

C. Volcano blot of deregulated genes in AhCRE PCGF6 KO (left) and VillinCREert2 PCGF6 KO (right). Both mouse models show upregulation of intestinal Tuft cell markers.
D. Column plot representing the number of downregulated genes and upregulated genes associated with Tuft cells signature (orange) upon PCGF6 depletion

Figure 4.10.2: Flow cytometry analysis of Lamina Propria mononuclear cells isolated from wild type and PCGF6 KO mice show high number of ILC2 infiltrated cells upon depletion of PCGF6

Figure 4.10.3: Transcriptome profile of PCGF6 deficient intestinal cell show upregulation of Tuft cell signature.

A. Volcano blot of deregulated genes in AhCRE PCGF6 KO (left) and VillinCREert2 PCGF6 KO (right). Both mouse models show upregulation of intestinal Tuft cell markers.
B. Column plot representing the number of downregulated genes and upregulated genes associated with Tuft cells signature (orange) upon PCGF6 depletion

Figure 4.10.4: Transcriptome profile of PCGF6 deficient intestinal cell show upregulation of Tuft cell signature.

C. Gene set enrichment analysis of transcriptome profile of PCGF6 KO compared to wild type show enrichment in Tuft cells signature.
D. Column Graph showing specific upregulation of Tuft cell signature and no other intestinal cell signature in PCGF6 KO

Figure 4.10.5: Relative expression of Tuft cell markers in WT and PCGF6 KO intestinal cell

Figure 4.10.6: Upregulation of Taft cells master regulator in absence of PCGF6

C. Immunofluorescence for Pou2f3 transcription factor in wild type and PCGF6 KO intestine.
D. Column Graph showing quantification of Pou2f3 signal among intestinal crypts

Figure 4.10.7: Genomic snapshots of PCGF1, PCGF2, PCGF6, RING1b, H2Aub1 and H3K27me3 at Pou2f3 promoter region in WT, and PCGF6 KO

Figure 4.10.8: Genomic snapshots of PCGF6, RING1b, H2Aub1 and H3K27me3 at Pou2f3 promoter region in WT and PCGF6 KO

4.11 PCGF6 restrict Tuft specification in a Ring1b independent mechanism

Figure 4.11.1: Heatmaps of deregulated genes in AhCRE PCGF6 (left) and VillinCREert2 PCGF6 (right) on each specific control found in AhCRE PCGF6 KO, VillinCREert2 PCGF6 KO and Ring1a/b KO. Deregulated genes were clustered in Tuft markers and others.

Figure 4.11.3: Column graph showing the expression of Tuft signature in different PCGF KOs intestinal cells.

Figure 4.11.3: Percentage of downregulated genes (left) and upregulated genes (middle) in PCGF6 KO compared to control. Percentage of PCGF6 targets of upregulated gene of Tuft signature in PCGF6 KO cells.

Figure 4.11.4: PCGFs binding on Tuft cell genes

5. FUTURE PROSPECTIVES AND ON-GOING

Figure 5.1 : FPKM values for CdKN2a in WT, PCGF1 KO, PCGF2/4 KO and PCGF1/2/4 KO

Figure 5.2: Representation of proportion of PCGF6 peaks distribution on distal and promoter (left), and proportion of PCGF6 peaks distribution on CpGi and not CpGi island

Figure 5.3: Representation of proportion of PCGF6, RING1B, CTCF and RAD21 peaks distribution on distal and promoter (upper), and proportion of PCGF6 peaks distribution on CpGi and not CpGi island.

Figure 5.4: Vann diagram showing the overlap between CTCF targets, PCGF6 targets in WT intestinal cells (left). Vann diagram showing the overlap between RAD21 targets, PCGF6 targets in WT intestinal cells (right).

Figure 5.5: Vann diagram showing the overlap between CTCF targets in WT and PCGF6 KO intestinal cells (left). Vann diagram showing the overlap between RAD21 targets in WT and PCGF6 KO intestinal cells (right).

10. ACKNOWLEDGEMENTS

Vorrei innanzitutto ringraziare Diego per avermi dato l'opportunità di lavorare su questi entusiasmanti progetti, e per aver posto in me la sua fiducia dal primo momento, e anche quando non lo meritavo. Ringrazio i miei due advisor, Stefano Casola e Francisco Real, per i consigli che mi hanno dato durante il dottorato.

Ringrazio tutti i membri del gruppo Pasini, per avermi dato, ognuno a modo proprio e peculiare, la forza e la grinta di portare a termine questo percorso. In particolar modo, ringrazio Daniel per l'enorme contributo che ha dato per lo svolgimento di questo lavoro. Ringrazio Silvia, per avermi insegnato a fronteggiare le difficoltà senza mai mostrarmi vulnerabile.

Ringrazio Julia e Marta, da poco tempo nella mia vita, ma abbastanza per farmi capire quanto io sia stata fortunata ad averle incontrate. Per il loro supporto, per avermi ascoltata e compresa, senza giudicarmi; per avermi stretto la mano, per avermi scossa quando avevo bisogno di una spinta, e per avermi lasciata fissare il vuoto quando ne avevo bisogno.

Ringrazio Andrea per esserci stato sempre, e per aver creduto in me dal primo momento. Per essere stato la mano dolce che mi ha stretto e amata, per essere la luce nel mio sentiero.

Ringrazio il ricordo di me bambina. Alla caparbietà, alla determinazione e al desiderio di voler cambiare la mia vita. Ai sogni tramutati in realtà.